DEACCLIMATION IN THREE DIMENSIONS: KINETICS, GENETICS AND MORPHOMETRICS OF COLD HARDINESS LOSS IN GRAPEVINES

A Dissertation

Presented to the Faculty of the Graduate School

of Cornell University

In Partial Fulfillment of the Requirements for the Degree of

Doctor of Philosophy

by

Alisson Pacheco Kovaleski

August 2018

DEACCLIMATION IN THREE DIMENSIONS: KINETICS, GENETICS AND MORPHOMETRICS OF COLD HARDINESS LOSS IN GRAPEVINES

Alisson Pacheco Kovaleski, Ph. D.

Cornell University 2018

Bud dormancy and cold hardiness are critical adaptations for surviving winter cold stress for temperate perennial plant species. Grapevines (*Vitis* spp.) resist cold through supercooling of water in their buds, and the level of cold hardiness is largely controlled by air temperature. Deacclimation during the spring is a determinant of timing of budbreak, and is one of the most critical periods for cold hardiness damage. The objective was to characterize the process of cold hardiness loss, or deacclimation, in grapevine buds. Several experiments were conducted to provide insights on deacclimation rates and effects on budbreak; location, distribution, propagation, and damage due to intracellular ice formation; and genes involved in the aforementioned processes. Cold hardiness of buds was determined using differential thermal analysis; genetic regulation was studied using RNA-Seq; and freezing imaging and microtomography was performed using synchrotron X-ray phase contrast imaging. Deacclimation rates (k_{deacc}) in several genotypes demonstrated a dependency on chill accumulation (dubbed deacclimation potential; Ψ_{deacc}) that followed a logistic behavior. The curve describing the response of k_{deacc} to temperature followed an exponential at low (<12 °C) and logarithmic behavior at high (≥12 °C) temperatures. Budbreak phenotype appears tightly linked to k_{deacc} responses, and therefore Ψ_{deacc} is a good quantitative parameter to determine

dormancy transitions. Abscisic acid (ABA) synthesis and signaling appear to be upstream of cold hardiness loss, and ABA-induced aquaporins may be directly related to cold hardiness levels. CBF homologs were not differentially expressed during deacclimation, although other DREB homologs were. The roles of phospholipase D and stilbene synthase should be further explored in the deacclimation process. X-ray phase contrast imaging was not able to resolve ice within grapevine buds. However, movement of tissues due to changes in water density associated with a thermocouple for temperature measurement provided information to identify the center of the bud (primary shoot) as the first portion to freeze. Microtomography using x-ray phase contrast imaging demonstrated that an increase in bud volume is correlated to the loss of hardiness, but major tissue expansions occur after cold hardiness is lost.

BIOGRAPHICAL SKETCH

Alisson Pacheco Kovaleski was born in Vacaria, Brazil, in 1989. He grew up in an agricultural setting, helping his family in their farm, and had his first contact with research helping his father, an entomologist at Embrapa. With great interest in agriculture, he was admitted into Universidade Federal do Rio Grande do Sul in 2006, from where he would later receive his Agronomic Engineer degree. From 2007 until the end of his undergraduate studies, Al worked in a citrus breeding program through a scientific initiation program. In 2009, Al attended University of Florida as an exchange student for a semester, during which period he began working with blueberries. Upon graduation, he decided to enroll at University of Florida to pursue a Master's degree in Horticultural Sciences starting in the Fall of 2011, working with Dr. Jeffrey Williamson and Dr. Rebecca Darnell in blueberry summer pruning.

Once graduated from his Master's, Al went on to pursue his Ph.D. in Horticultural Biology at Cornell University, with minors in Breeding of Horticultural Crops and Physics. At Cornell University, Al was under guidance of Dr. Bruce Reisch and Dr. Jason Londo. During his graduate studies at Cornell, Al actively participated in the executive boards of the *Society for Horticulture* and the *Student Association of the Geneva Experiment Station*. As part of his extracurricular activities, Al also joined the *Friends of Parrott Hall* towards the end of his studies in efforts to save a historical building at Cornell AgriTech in Geneva, NY.

To my family, by blood and by friendship

ACKNOWLEDGMENTS

First and most importantly, I am thankful for my family, for the unconditional love, for being always present, for supporting and believing in my dreams, and for celebrating my accomplishments.

I especially want to thank my advisors Dr. Jason Londo and Dr. Bruce Reisch for providing me with the opportunity to obtain my Ph.D. at Cornell University, for their involvement with my projects, their support for my ideas, and guidance beyond academia. I would also like to thank Dr. Robert Thorne, member of my committee, for advice on my work and help on "physical matters", and special thanks to Dr. Ken Finkelstein, for his collaboration and willingness to contribute for imaging projects.

I would like to thank all the members of the Reisch and Londo groups who helped me with sample and data collection and providing insights during lab meetings to further my research. I am thankful for the help of the "A team" for help with sample collection and preparation, and for taking care of plants used in my research, and for everyone at USDA-ARS-GGRU and Cornell AgriTech who somehow contributed to these projects, and provided a fun environment to work at. I thank Carol Grove and Bridget Cristelli for making their best possible to help me with requirements and legal obstacles of graduate school.

I am thankful for the friendship of my fellow graduate students at Cornell: those in the Field of Horticulture, those randomly met through statistics, those met at the Big Red Barn, and those met through the simple fact of being an international/Brazilian student. They made life fun and much more bearable throughout these years. Thanks to everyone at WCF for their friendship and the shared sweat sessions. Thanks to my roommate Poliana Francescatto, for help in research and in life. To the many groups of friends made throughout the years that stuck together: the

Gainesville Shore, the UF Wolfpack, the “Salinha”, the “Legais”, and others. Thanks to those from Galerinha, my “framily”, for the daily conversations: Bruna Forcelini, Fernanda Guimarães, Bruno Casamali, and Matheus Baseggio. Special thanks to Bruno for the friendship that has lasted over a decade, and for his advice in life and science decisions. I am especially thankful for Matheus Baseggio, for his companionship and help with science and non-science affairs.

I would like to thank my undergraduate advisor, Dr. Sergio Schwarz, and my Masters advisors, Dr. Rebecca Darnell and Dr. Jeff Williamson, for the continued support, and all other mentors who helped me become who I am today.

I would like to thank Anthony Road Wine Co. and Ravines Wine Cellars for access to plant material, and the funding sources for the projects undertaken here: CAPES, Coordenação de Aperfeiçoamento de Pessoal de Nível Superior, Brazil; the National Institute of Food and Agriculture, U.S. Department of Agriculture, through the Northeast Sustainable Agriculture Research and Education program under subaward number GNE16-130; National Science Foundation award DMR-1332208 which supports the Cornell High Energy Synchrotron Source (CHESS).

TABLE OF CONTENTS

page

LIST OF TABLES

LIST OF FIGURES

LIST OF OBJECTS

LIST OF ABBREVIATIONS

AA	Amino Acid
ABA	Abscisic Acid
AFP	Anti-freeze Protein
DEG	Differentially Expressed Gene
DTA	Differential Thermal Analysis
FR-EM	Freeze-fracture replica electron microscopy
GA	Giberellic Acid (Gibberellin)
GDD	Growing Degree-Day
HTE	High Temperature Exotherm
JA	Jasmonic Acid
LTE	Low Temperature Exotherm
NMR	Nuclear Magnetic Resonance
SEM	Scanning Electron Microscopy
TEM	Thermoelectric Module

LIST OF SYMBOLS

Chill	Chill accumulation
ΔV	Change in volume
k_{deacc}	Rate of deacclimation
Ψ_{deacc}	Deacclimation potential
T	Temperature
t	Time

CHAPTER 1
LITERATURE REVIEW

Grapevines (*Vitis* spp.) are native to temperate and subtropical climate zones in the Northern Hemisphere (Mullins *et al.*, 1992). The genus *Vitis* is divided into two broad clades representing Eurasian and North American species. Within the Eurasian species clade lies the domesticated grapevine species, *V. vinifera*, which has generally good fruit quality but lacks many traits associated with abiotic and biotic stress. The opposite is true for wild Eurasian and North American species (such as *V. riparia*). Many important adaptive traits can be found in wild grapevine, and these species are routinely used in breeding programs targeting resistance to pests and pathogens, changing climate, and soil parameters. Perhaps the most important trait in North American species is their tolerance to phylloxera (*Daktulosphaira vitifoliae*; Riley, 1872), although cold hardiness is also increased in some compared to cultivated grapevines (Londo & Kovaleski, 2017).

Perennial plants such as grapevines developed dormancy mechanisms in order to survive unsuitable growth conditions (e.g., low winter temperatures; Lang *et al.*, 1987). In *Vitis* species, the growing vines produce latent buds in leaf axils, which are dormant due to inhibition by the growing shoot tip (paradormancy), preventing growth of lateral vines. Depending on environmental cues, these latent buds may "break" and resume growth, generating new growing vines. During the fall, reduction in photoperiod signals growth to cease in actively growing shoots, and along with decreasing temperatures, initiate necessary changes to induce endodormancy in the buds that remained paradormant (Fennell & Hoover, 1991). Endodormant buds are unable to break and resume growth before exposure to low temperatures, when they fulfill their chill requirement (Lang *et al*. 1987). Chill accumulation can be calculated by a variety of methods, in which accumulation typically occurs as a result of exposure to low, above

freezing temperatures (Shaltout & Unrath, 1983). This mechanism allows the buds to remain dormant even during warm spells and false spring events, which could result in bud mortality if budbreak occurred and seasonal freezing temperatures return. Once the chill requirement is fulfilled, buds transition into ecodormancy through a currently unknown series of physiological changes. During ecodormancy, buds remain in a dormant state while environmental conditions are not conducive for growth (Lang *et al.*, 1987), yet are primed for budbreak should temperatures rise.

Axillary grapevine buds can be vegetative or mixed buds, and therefore may contain inflorescence primordia (anlage) which will give rise to fruit during the following season (Srinivasan & Mullins, 1976). From a biological standpoint, the survival of these structures during the winter is important for reproduction of the plants, while agriculturally this results in the yield of the following growing season. The lateral buds can be compound buds depending on the grapevine species (Morrison, 1991), in which primary, secondary, and tertiary buds are present. The shoot within the primary bud is organized in a monopodium (Srinivasan & Mullins, 1976). Six to 10 basal nodes are preformed in overwintering primary buds (Morrison, 1991). The leaf primordia are formed in a distichous phyllotaxy, and after ~5 nodes, the first anlage forms opposite to the leaf primordia in each node (Srinivasan & Mullins, 1976). Environmental conditions will result in the differentiation of the anlage into inflorescence, tendril, or shoot primordia (Srinivasan & Mullins, 1976).

According to FAO, in 2016 almost 7.1 million ha worldwide were cultivated with grapevines. The top producers are China, Italy, United States, Spain, France, and Turkey (FAO, 2018). In 2017 in the United States, nearly 405,000 ha are cultivated (USDA, 2018). From those, California was responsible for 335,000 ha, followed by Washington (29,500 ha), and New York

is in third with 14,000 ha. Plantings in more northern latitudes, such as in New York and Washington States, can experience winter temperatures that are challenging for grape production. These temperatures may require genotypes that can resist low below-freezing temperatures after acclimation as well as delayed deacclimation through processes discussed further in this review.

Freezing

Climate is generally agreed to be the major factor influencing organism distribution on Earth. More importantly, low temperatures are the most limiting factor governing plant distribution and perennial plants located in higher latitudes experience below freezing temperatures and may be subject to freezing of their tissues (Parker, 1963). In early studies of cold injury, it was postulated that plant death was caused by ice expansion that crushed the living cells, or sap coagulation due to freezing (Parker, 1963). However, more modern studies have shown alternative forms of damage caused by the freezing process.

Ice may form separately extra- and intracellularly (Molisch, 1897; Parker, 1963; Steponkus, 1984), while the location of ice formation is strongly influenced by cooling rate (Steponkus, 1984). Due to the selective permeability of the plasma membrane, cells suspended in partially frozen solutions must come to a water potential equilibrium with the solution. This equilibrium is reached by intracellular ice formation or cell dehydration (Steponkus, 1984). Intracellular ice formation can damage the plasma membrane by rupture or due to loss of the selective permeability (Steponkus, 1984). Ice can also form preferably in different tissues. Within a bud, ice can form predominantly in bud scales and other non-essential portions, then called extraorgan freezing (Steponkus, 1984; Quamme *et al.*, 1995).

Plants have developed different strategies to withstand challenging low temperatures (Burke *et al.*, 1976). One form of survival mechanism is freeze avoidance, which itself can be

separated in two different types: geographical avoidance, with species that are not cold hardy remaining in areas that do not have below freezing temperatures; and plant cycle avoidance, when annual plants overwinter as cold hardy dehydrated seeds (Burke *et al.*, 1976). Perennial plants must, however, overwinter in areas where temperatures drop below freezing temperatures, and thus developed freezing tolerance mechanisms. Some of these plants show a supercooling ability, in which water freezes extracellularly (apoplast) at high below-freezing temperatures and dehydrates the intracellular space (symplast). The little free water that remains in the cells then supercools, resisting ice formation to temperatures that may reach ~−40 °C (Quamme, 1995). These plants are typical of temperate climates, in which minimum temperatures during winter are often above −40 °C. Plants native to climates with harsher winters, such as those in boreal forests, do not supercool. Instead, the strategy used by these plants is to have extracellular ice form at high below-freezing temperatures and then dehydrate intracellular spaces, removing all but bound water from the symplast (Burke *et al.*, 1976). Grapevines belong to the group of plants that deep supercool.

Supercooling

Freezing is the change of state from liquid to solid that involves crystal formation. Freezing of water can occur in two different ways: when foreign substances act as nucleators for ice formation it is denoted as heterogeneous freezing; and when water molecules form aggregates of an ice-like structure, homogenous freezing (Bigg, 1953). Water can, however, remain in the liquid state at temperatures below that of the melting point. This process is named supercooling and occurs when water molecules fail to form aggregates with an ice-like structure (Zachariassen *et al.*, 2004), which would result in ice formation. This state is not thermodynamically stable, and continued decreasing temperature leads to a higher probability of aggregate formation as a result of the decreased thermal movement of molecules. Supercooling

prevents ice formation in a different manner than that of increasing the concentration of the solution. The addition of solutes decreases both melting and freezing points by 1.86 °C/Osm (Zachariassen *et al.*, 2004). Supercooling differs from this, as supercooling is the inequilibrium between freezing and melting points (thermal hysteresis). However, the potential for an effect of solute concentration on homogenous and heterogeneous ice nucleation temperature is a source of controversy (Zachariassen *et al.*, 2004).

Supercooling ability varies with volume of water and rate of cooling (Bigg, 1953). Larger volumes of water freeze at higher temperatures, and the temperature of freezing has a linear relation with the log of volume. Water is also able to supercool to a lower temperature when the cooling rate is greater (Bigg, 1953). However, the variance of nucleation temperature is independent of volume (Wilson & Haymet, 2012). Wilson & Haymet (2012) found that the spread of the nucleation temperature in supercooled water samples between <0.1 nL to 200 µL is on the order of 0.7 °C, using both collected and historical data. The authors speculated that this range is also unrelated to the number of runs to which a sample was subjected (maximum of 37,000 runs in their experiments), or the average temperature of supercooling.

Heterogeneous freezing requires the presence of an ice-nucleating particle, which will aid in the water molecule orientation for ice nucleation, and all nucleation of supercooled biological solutions is heterogeneous (Wilson *et al.*, 2003). Kishimoto *et al.* (2014a) found a high ice nucleation activity in the stems of blueberry (*Vaccinium corymbosum*), localized in the cell wall fraction. This would allow ice nucleation in the extracellular space and supercooling of the intracellular fraction. Kishimoto *et al.* (2014b) also demonstrated that the ice nucleation activity changed over the year, with ice nucleation occurring at lower temperatures during the months of the winter.

Nucleation agents can be both inorganic and organic in nature. Hiranuma *et al.* (2015) evaluated microcrystalline cellulose as an ice nucleator for ice formation in clouds. The authors found that these types of particle, before and after grinding induced ice nucleation below –20 °C. Cellulose is therefore not likely an ice nucleator in the extracellular space in grapes, considering that extracellular ice forms around –5 °C (Mills *et al.*, 2006). In *Zea mays*, sensitivity to frost increased when *Pseudomonas syringae* was applied to leaf surfaces, demonstrating that bacteria may act as ice nucleators (Arny *et al.*, 1976). *P. syringae* produces a protein that serves as template for ice crystal formation, thus promoting nucleation of ice (Wolber *et al.*, 1986). Ice-nucleating bacteria have the ability to cold-condition and increase the threshold nucleation temperature from –8 to –3 °C (Burke & Lindow, 1990). Parody-Morreale *et al.* (1988) found that antifreeze proteins can bind to ice-nucleating sites in bacteria, disrupting the ordered array of water molecules that leads to ice nucleation and propagation.

In insects that are able to supercool, nucleation agents are present in the extracellular space. Zachariassen & Hammel (1976) demonstrated the existence of ice-nucleating agents in the haemolymph of freeze-tolerant bettles. These would ensure the extracellular ice formation at high subzero temperatures which promotes supercooling of the intracellular fluid (Zachariassen & Hammel, 1976), as the membrane prevents seeding of the intracellular space by the extracellular ice (Duman, 1982). The supercooling ability of insects also varies during the year, possibly due to variations in nucleating factors (Duman, 1982). Zebrafish (*Dania rerio*) embryos are not able to supercool and intracellular ice forms as soon as the ice front in the media reaches the cell membrane (Hagedorn *et al.*, 2004). It is possible that inner surface of cells become an ice nucleating agent due to changes in the membrane structure upon contact with ice (Hagedorn *et al.*, 2004).

Supercooling in plants

Perennial plants that supercool compartmentalize the ice formation in the extracellular space, dehydrating the adjacent cells, which then supercool (Burke *et al.*, 1976). Cold hardiness varies between species, but also among varieties within a given species (Parker, 1963). Cells with thick walls have a greater ability to dehydrate as compared to those with thinner walls, which may be one of the factors influencing supercooling temperature, although the mechanism is unclear (Endoh *et al.*, 2009).

There is a correlation between water content in buds and the temperature of intracellular ice formation when artificially cooled (Johnston, 1923; Richards & Bliss, 1986), and differences have been speculated to be a result of differential water uptake by roots in the fall (Johnston, 1923). However, reciprocal grafting of *Vitis* hybrids 'Marechal Foch' and 'Vidal Blanc', which have different hardiness levels, did not find an influence of rootstock on the hardiness level of buds (Sabbatini & Howell, 2013). Therefore, such genetically complex and environmentally influenced characteristics are likely mostly under control of the scion (Sabbatini & Howell, 2013).

Cold hardiness level through supercooling in grapevines is typically measured using differential thermal analysis (DTA; Andrews *et al.*, 1984; Mills *et al.*, 2006). In single buds, a high temperature exotherm (HTE) is observed around −7 °C, followed by one to three low temperature exotherms (LTEs). The three LTEs are typically of different sizes, and the smallest tends to occur at lower temperatures. The largest, medium and small sized LTEs were assumed to be a result of freezing of primary, secondary, and tertiary buds, respectively (Andrews *et al.*, 1984). Buds removed from the freezer immediately following the LTE present injury in the primary bud, while buds removed prior to the LTE have no injury (Andrews *et al.*, 1984; Mills *et al.*, 2006). This demonstrated that the LTE coincides with the freezing injury.

Differential thermal analysis can be very useful for studying cold hardiness. However, DTA alone can make it difficult to conclude that cells are surviving through extracellular freezing and deep supercooling under conditions of slow cooling (Endoh *et al.*, 2009).

Acclimation and Deacclimation to Cold

Although some structures are able to supercool, this ability shifts throughout the year (Ferguson *et al.*, 2011, 2014; Londo & Kovaleski, 2017). These shifts can be split into three separate periods: acclimation, maintenance, and deacclimation. These periods are somewhat connected to dormancy mechanisms, as the period of acclimation matches that of the onset of endodormancy, and the deacclimation is the release of ecodormancy. The maintenance period can therefore be separated in two, depending on whether chill requirement has been fulfilled or not: initially endodormancy and then ecodormancy.

The onset of endodormancy in buds appears to be triggered in some grapevines by the decrease in daylength during late summer and fall (Fennell & Hoover, 1991; Wake & Fennell, 2000). Acclimation to cold starts after the onset of endodormancy, and is mainly induced by decreasing temperatures (Stergios & Howell, 1977; Xin & Browse, 2000; Ferguson *et al.*, 2011, 2014; Londo & Kovaleski, 2017). While short days alone may decrease the killing temperature of buds compared to long days, the changes are very slight (Fennell & Hoover, 1991). However, there is a synergistic effect when short days are associated with low temperatures, promoting deep acclimation (Schnabel & Wample, 1987).

The transition from endo- to ecodormancy in grapevines is enhanced by exposure to low temperatures through chill accumulation (Lang *et al.*, 1987). Although chilling accumulation results in faster and more synchronous budbreak, plants can also resume growth without proper chilling (Schnabel & Wample, 1987; Londo & Johnson, 2014). The chilling requirement for transition is usually found through linear regression as the number of chill hours or units for 50%

budbreak within 21-30 days (Lloyd & Firth, 1990; Ben Mohamed *et al.*, 2010; Londo & Johnson, 2014).

Some plant metabolites appear to be associated with different periods of dormancy. Buds have increased sucrose and proline concentration between 0 and 300 chill hours. After 300h, an increase in the activity of acid invertases leads to the accumulation of soluble sugars (Ben Mohamed *et al.*, 2010). When hydrogen cyanamide is applied to promote budbreak, there is a rapid reduction in starch concentrations probably being turned into soluble sugars (Ben Mohamed *et al.*, 2012). Therefore, higher starch levels are associated with endodormancy, while starch transitions to soluble sugars during chill accumulation and dormancy release (Ben Mohamed *et al.*, 2012). Catalases are also associated with dormancy state. Or *et al.* (2002) found no changes in the expression of catalases in *V. vinifera* 'Perlette' in field conditions from onset to release of dormancy. However, Pérez & Lira (2005) found that activity of catalases was higher in the early periods of endodormancy, and was later inhibited by H_2O_2 accumulation in bud tissues, possibly in response to chilling (Nir *et al.*, 1986). Noriega *et al.* (2007) reported that peroxidase expression in *V. vinifera* 'Thompson seedless' was triggered by the same environmental cues as those that induce endodormancy and acclimation (short days and low temperatures), and therefore quantitative analysis of peroxidase expression or peroxidase isoenzyme activity could be a measure of endodormancy extent in grapevines.

Once plants have met their chilling requirement and become ecodormant, buds are able to deacclimate much faster than during endodormancy. Deacclimation happens in response to exposure to higher temperatures in the field during spring (Andrews *et al.*, 1984). The temperature experienced by plants impacts the rate of deacclimation in buds (Ferguson *et al.*,

2011, 2014; Londo & Kovaleski, 2017), and even within vineyard differences can affect deacclimation and timing of budbreak (Stergios & Howell, 1977).

Some chemicals, such as hydrogen cyanamide, can be used to partially fulfill chilling requirements and promote the transition from endo- to ecodormancy. This is a common practice for areas where insufficient chilling occurs, and leads to growth if plants are exposed to proper growth conditions. Treatment with hydrogen cyanamide results in the return of metabolic activity, and increases the mitotic activity of meristems in previously dormant buds (Carolus & Pouget, 1971; Trejo-Martínez *et al.*, 2009). Hydrogen cyanamide application also enhances respiration and leads to an increase in water content of buds (Shulman *et al.*, 1983; Trejo-Martínez *et al.*, 2009). Once growth initiates, plants cease to supercool and cold damage can occur at temperatures close to 0 °C. Gardea *et al.* (1993) found that application of Frostgard, a commercial antifreeze/cryoprotectant was not effective on leaf tissue of *V. vinifera* 'Pinot noir'. Frostgard had a cryoprotectant effect limited to −2 °C, which has no practical significance according to the authors.

Genetic Regulation of Dormancy and Cold Hardiness

Recent studies have looked for genes associated with acclimation, deacclimation, and dormancy. Kühn *et al.* (2009) evaluated depth of dormancy in late summer and early fall field conditions by using number of days required for 50% budbreak to find the critical daylength for establishment of endodormancy in 'Thompson Seedless'. They found that time to 50% budbreak increased from ~15 days to ~40 days from mid January to early February. They then proceeded to compare the expression levels of *V. vinifera PHYA* and *PHYB* (*VvPHYA* and *VvPHYB*, respectively) between long day and short day. The authors found that the expression of *VvPHYA* and *VvPHYA* changed from an oscillating pattern, with maximum levels before down and minimum levels after dusk, under long day photoperiod to continuous high levels under short

day. Pérez *et al.* (2011) looked at the expression levels of *PHYA*, *PHYB*, and floral integrator genes *CONSTANS* (*CO*), *FLOWERING LOCUS T* (*FT*) and *MADS8* in entry and exit of endodormancy in 'Thompson Seedless'. *VvPHYA*, *VvPHYB*, *VvCO*, *VvFT*, and *VvMADS8* were expressed in grape buds prior to leaves, but were all silenced in mid-summer with the exception of *VvPHYB*. *VvCO*, *VvFT*, and *VvMADS8* were expressed again once buds were endodormant, but *VvPHYA* remained silenced. When endodormancy was over, floral promoters *VvFT* and *VvCO* expression was increased by conducive growing conditions, while the expression of negative regulators *VvFLC* and *VvEBS* decreased. The use of hydrogen cyanamide increased the earlier expression of *VvFT* and *VvCO*, as well as decreased the expression of the negative regulators.

Vergara & Pérez (2010) used canes from 'Thompson Seedless' to study the similarities in gene expression between natural and chemically induced bud break. Treatments with dormancy-breaking compounds (e.g., hydrogen cyanamide and sodium azide) resulted in upregulation of genes related with carbohydrate metabolism and energy, necessary for growth resumption. The genes for two 1,3-β-glucanases (VvβGLU78 and VvβGLU78) were highly expressed through the beginning of dormancy, were transiently down-regulated, then up-regulated during the release of dormancy period in buds in the field. These glucanases are likely involved in developmental processes such as the release of buds from dormancy. *VvβGLU78* was expressed in buds treated with hydrogen cyanamide and sodium azide 2 d after treatment and under forcing conditions, while it took 14 d for the control buds.

During cold exposure, some genes appear to be directly associated with the resistance to cold resulting in increased expression during and after cold exposure. Acclimation by exposure to low temperatures increased the tolerance to extracellular freezing in spinach (*Spinacia*

oleracea), which was correlated to an increase in levels of mRNA (Guy *et al.*, 1985). In *Arabidopsis thaliana*, *COLD-REGULATED* (*COR*) genes are upregulated in response to low temperatures, denoting their role in enhancing freeze tolerance (Hajela *et al.*, 1990; Thomashow, 1994). Jaglo-Ottosen *et al.* (1998) used overexpression of *Arabidopsis CBF1* mutants to induce expression of *COR* genes. CBF1 binds to a DNA regulatory element present in the promoter of multiple *COR* genes (Yamaguchi-Shinozaki & Shinozaki, 1994). Overexpression of *CBF1* led to increased freeze resistance in non-cold-acclimated plants, showing similar survival to below freezing temperatures as cold-acclimated plants from the resulting upregulation of *COR* genes. In grapevines, however, cold acclimation of leaves did not lead to a decrease in freeze damage, and genetic regulation during acclimation and freeze responses appears to be different (Londo *et al.*, 2018).

Some genes associated with cold exposure are shared between other stress response pathways. *COR* genes are also upregulated during drought stress (Hajela *et al.*, 1990). Shinozaki & Yamaguchi-Shinozaki (2000) proposed a model for activation of TATA genes through low temperature and dehydration stresses that intersect at a dehydration responsive element (DRE) gene, also reported C-repeat (CRT). This demonstrates a linkage at the transcriptional level between dehydration and cold stresses. The DRE/CRT gene is activated by the DREB/CBF transcription factors, which contain EREBP/AP2 binding domains (Liu *et al.*, 1998; Wang *et al.*, 2010). Genes with the AP2 domain have been implicated in many stress-induced pathways (Kizis *et al.*, 2001).

In grapes, Fernandez-Caballero *et al.* (2009) evaluated the cryoprotective activity of VcCHIT1b, a chitinase from *V. vinifera* ‘Cardinal’. *Vcchit1b* mRNA levels increased after exposure to low temperatures. VcCHIT1b has antifungal activity, inhibiting hyphal growth of

Botrytis cinerea in agar plates. Although the protein was able to cryoprotect another enzyme against freeze/thaw inactivation, it did not present an antifreeze activity. Wu *et al.* (2014) demonstrated that plant-pathogen interaction pathway genes were upregulated in cold acclimated *V. amurensis* 'Zuoshan-1', demonstrating a linkage between the two pathways. These were, however, studied from leaves exposed to 4 °C for 48h. Many genes related to cold response were found to be upregulated: an ATP-binding cassette transporter gene (GSVIVT01037789001; likely related cold sensing); gibberellins, auxins, and abscisic acid-related signaling genes (with no clear relation under cold stress); transcription factors (e.g., AP2/ERFs); and plant pathogen interaction pathway genes (*CDPKs*, *NOS*, *MEKK*, *JAZ*, *MYC2*, and *WRKY*).

Anti-freeze proteins (AFPs) are also mechanisms to prevent damage resultant from cold exposure and are present in many organisms, such as insects (Duman, 1982; Zachariassen *et al.*, 2004), fish (Kristiansen & Zachariassen, 2005), and plants. Transgenic tobacco (*Nicotiana tabacum*) plants with an AFP gene from carrot (*Daucus carota* var. *sativa*) were able to withstand and recover from temperatures close to 0 °C, and had much lower ion leakage compared to wild type (Fan *et al.*, 2002). Therefore, plant transformation may be a practical and effective way to enhance cold resistance of crop plants.

Observation of Ice Formation

The visualization of the freezing process results in simple answers to questions of how and where freezing occurs (Molisch, 1897). For the purpose of observation of ice, different techniques, such as stereo-light microscopy (Molisch, 1897; Endoh *et al.*, 2009), cryo-scanning electron microscopy (Cryo-SEM; (Endoh *et al.*, 2009), and X-ray phase contrast imaging (Sinclair *et al.*, 2009) can be used, each one yielding different data for the types of structure being studied.

The size and opacity of the structure is also a determinant of the type of technique to use. Using a stereo-light microscope, small extracellular ice crystals, as well as large masses were visible in buds of larch (Endoh *et al.*, 2009). *Xenopus laevis* stage I and II oocytes (Guenther *et al.*, 2006), and three species of unicellular algae (Morris *et al.*, 1986) freezing behavior have been studied using a cryostage in a bright-field microscope. The oocytes have a diameter of about 150 μm, which allowed for the observation of flashing of the intracellular solution when freezing under the microscope (Guenther *et al.*, 2006). The algae presented a graining of the cells followed by darkening when freezing occurred (Morris *et al.*, 1986).

Cryomicroscopy associated with high-speed imaging allows for visualization of patterns of ice spread. The observation of freezing can help modeling the spread of ice within a substrate (Bauerecker *et al.*, 2008), and help identifying gaps in our phenotyping: darkening of cells, which is usually assumed to be the primary sign of intracellular ice formation, actually occurs after ice formation (Stott & Karlsson, 2009). Yang *et al.* (2009) performed similar recordings in human umbilical vein endothelial cells, cooling the cells at different rates (from 15 to 100 °C/min). They observed a different morphology of the ice, depending on the cooling rate, and the intracellular ice initiated preferentially near the membrane closer to the nucleus. Yang *et al.* (2009) also noted that the ice spread within the cell was heterogeneous in speed, with a faster growth rate of the ice in the nucleus compared to the cytoplasm. The same authors used this technique to compare human umbilical vein endothelial cells with MCF-7 breast cancer cells (Yang *et al.*, 2011). They observed that the process of intracellular ice formation was similar, but the occurring rates were found to be different. This suggested that cell-to-cell interactions, membrane properties, and salt and ion distributions in the cells are key factors impacting the process.

Identification of ice location can also be done using indirect methods. Freeze substitution is a method that has been used for frozen beef (Bevilacqua *et al.*, 1979) and salmon (Zhu *et al.*, 2003). Through their method, frozen samples are fixed using Carnoy fluid, which diffuses rapidly through frozen tissue due to its low freezing point. The holes left by the ice formation in the tissue were then measured to determine ice crystal size using light microscopy. To measure volume of ice crystals, freeze substitution can be associated with a fluorescent dye, and thus volume of ice crystals can be measured by slicing the sample under a fluorescent microscope (Do *et al.*, 2004). Another method of freeze substitution uses 1% OsO_4 in acetone (w/v) for fixation of samples (Hong & Rubinsky, 1994). Briefly, the samples were cooled to the desired temperature and then immersed in liquid nitrogen (LN). The samples are then placed in a vial with the osmium tetroxide solution at –196 °C and then put into a freeze substitution apparatus (Padrón *et al.*, 1988), warming up slowly to room temperature over 2 days. The OsO_4 fixes the structures of the cells by stabilizing membranes and proteins, while the acetone replaces the ice in the sample. The samples can then follow a dehydration series and be resin embedded for microtome slicing for light microscopy. To identify the location of ice nucleation, a series of temperatures pre-LN immersion is used (Hong & Rubinsky, 1994).

Endoh *et al.* (2009) also used cryo-scanning electron microscopy (Cryo-SEM) to study freezing behavior of larch buds. The authors used cooling rates of 0.1 and 0.2 °C/min, and 5 °C/day. When the buds reached the desired temperature, they were cryofixed using Freon 22 (–160 °C). The cryofixed buds were put on a cold stage at –95 °C and freeze-fractured after equilibration. Observation of the fracture faces allowed the identification of cells containing intracellular ice in the form of large crystals. Endoh *et al.* (2014) used freeze-fracture replica electron microscopy (FR-EM) to observe damage of membranes due to freezing of cells. FR-EM

consisted of freeze-fracturing samples, such as in Cryo-SEM, followed by etching of surfaces, which were further shadowed by evaporation with platinum-carbon and reinforced by evaporation with carbon. Samples were then removed from the freeze-etching apparatus, and dissolution of the samples was used to obtain the replicas. Pearce & Willison (1985) used similar techniques to observe ice distribution in several tissues of wheat (*Triticum aestivum* L.).

Ishikawa *et al.* (1997) used Nuclear Magnetic Resonance (NMR) Microscopy to visualize freezing behavior of leaf and buds of full-moon maple (*Acer japonicum* Thunb.). The highest resolution used resulted in a pixel size of 39 μm × 39 μm. The contrast between liquid water and ice was obtained by a long recycle delay and a short echo time, with the intensity then reflecting predominantly the density of mobile protons. One of the problems mentioned by the authors, however, was that the asymmetrical morphology of the buds made it difficult to obtain the correct angle for slice selection, which could be overcome with 3-dimensional imaging. Kerr *et al.* (1998) also used NMR to visualize the formation of ice in potatoes, peas, corn, chicken, and carrots. The samples were placed in a freezer at –30 °C, and imaged every 2 minutes until frozen. Similarly to Ishikawa *et al.* (1997), the authors were able to visualize ice formation as a loss of NMR signal intensity, but with much lower resolution (~350 μm). McCarthy & Kauten (1990) also described the use of NMR for food research in the observation of fats, hydrogen, and other characteristics.

While most of the methods required a transparent sample (e.g., microscopy), had low image resolution (e.g., NMR), or had problems resolving the timing of freezing (e.g., Cryo-SEM), X-ray phase contrast imaging appears to be a good alternative method (Socha *et al.*, 2007). In freeze dried samples, the voids created by ice have been imaged using X-ray tomography (Mousavi *et al.*, 2007). However, Sinclair *et al.* (2009) used real time x-ray phase-

contrast imaging to visualize ice formation in insects. The ice crystals deflect the path of parallel x-ray beams, which can be seen as a signal in the images. The authors were able to observe ice forming in diapausing larvae of *Chymomyza amoena* and non-diapausing larvae of *C. amoena* and *Drosophila melanogaster*.

Objectives

Cold resistance and freezing behavior have been studied in various species leading to a large collection of data points highlighting the many different ways that plants survive winter damage. Few of the studies examine the complete complexity of the field, examining physiological, genetic, and morphometric responses within a single species. Much of the impactful science has also occurred in plant species with little economic or horticultural value. Grapevine, with its wide geographic production and phenotypic variation between species represents an excellent model system to bridge the gap between natural adaptation and horticultural utility. In addition, a comprehensive, multiple spectrum characterization of cold resistance for *Vitis* species is lacking. Therefore, a study of cold resistance and freezing behavior of buds of several *Vitis* species, with special attention to cultivated varieties of *Vitis vinifera* was conducted. The objective of the present study was to obtain information on: deacclimation rates; location, distribution, propagation, and damage due to intracellular ice formation; and genes involved in the aforementioned processes.

References

Andrews PK, Sandidge CR III, Toyama TK. **1984**. Deep supercooling of dormant and deacclimating *Vitis* buds. *American Journal of Enology and Viticulture* **35**: 175–177.

Arny DC, Lindow SE, Upper CD. **1976**. Frost sensitivity of *Zea mays* increased by application of *Pseudomonas syringae*. *Nature* **262**: 282.

Bauerecker S, Ulbig P, Buch V, Vrbka L, Jungwirth P. **2008**. Monitoring ice nucleation in pure and salty water via high-speed imaging and computer simulations. *Journal of Physical Chemistry C* **112**: 7631–7636.

Ben Mohamed H, Vadel AM, Geuns JMC, Khemira H. **2010**. Biochemical changes in dormant grapevine shoot tissues in response to chilling: Possible role in dormancy release. *Scientia horticulturae* **124**: 440–447.

Ben Mohamed H, Vadel AM, Geuns JMC, Khemira H. **2012**. Carbohydrate changes during dormancy release in Superior Seedless grapevine cuttings following hydrogen cyanamide treatment. *Scientia horticulturae* **140**: 19–25.

Bevilacqua A, Zaritzky NE, Calvelo A. **1979**. Histological measurements of ice in frozen beef. *International Journal of Food Science & Technology*. **14**: 237–251.

Bigg EK. **1953**. The supercooling of water. *Proceedings of the Physical Society. Section B* **66**: 688.

Burke MJ, Gusta LV, Quamme HA, Weiser CJ, Li PH. **1976**. Freezing and injury in plants. *Annual review of plant physiology* **27**: 507–528.

Burke MJ, Lindow SE. **1990**. Surface properties and size of the ice nucleation site in ice nucleation active bacteria: Theoretical considerations. *Cryobiology* **27**: 80–84.

Carolus M, Pouget R. **1971**. Evolution morphologique et croissance de bourgeons latents de vigne (Vitis vinifera L.) apres un traitement artificiel de levee de dormance. *Acad Sci Paris C R Ser D*.

Do G-S, Sagara Y, Tabata M, Kudoh K-I, Higuchi T. **2004**. Three-dimensional measurement of ice crystals in frozen beef with a micro-slicer image processing system. *International Journal of Refrigeration* **27**: 184–190.

Duman JG. **1982**. Insect antifreezes and ice-nucleating agents. *Cryobiology* **19**: 613–627.

Endoh K, Kasuga J, Arakawa K, Ito T, Fujikawa S. **2009**. Cryo-scanning electron microscopic study on freezing behaviors of tissue cells in dormant buds of larch (*Larix kaempferi*). *Cryobiology* **59**: 214–222.

Endoh K, Kuwabara C, Arakawa K, Fujikawa S. **2014**. Consideration of the reasons why dormant buds of trees have evolved extraorgan freezing as an adaptation for winter survival. *Environmental and experimental botany* **106**: 52–59.

Fan Y, Liu B, Wang H, Wang S, Wang J. **2002**. Cloning of an antifreeze protein gene from carrot and its influence on cold tolerance in transgenic tobacco plants. *Plant cell reports* **21**: 296–301.

FAO. 2015. FAOSTAT. Food and Agriculture Organization of the United Nations, Statistics Division. < http://faostat3.fao.org/> (Accessed 22 July 2018)

Fennell A, Hoover E. **1991**. Photoperiod influences growth, bud dormancy, and cold acclimation in *Vitis labruscana* and *V. riparia*. *Journal of the American Society for Horticultural Science. American Society for Horticultural Science* **116**: 270–273.

Ferguson JC, Moyer MM, Mills LJ, Hoogenboom G, Keller M. **2014**. Modeling dormant bud cold hardiness and budbreak in twenty-three *Vitis* genotypes reveals variation by region of origin. *American Journal of Enology and Viticulture* **65**: 59–71.

Ferguson JC, Tarara JM, Mills LJ, Grove GG, Keller M. **2011**. Dynamic thermal time model of cold hardiness for dormant grapevine buds. *Annals of botany* **107**: 389–396.

Fernandez-Caballero C, Romero I, Goñi O, Escribano MI, Merodio C, Sanchez-Ballesta MT. **2009**. Characterization of an antifungal and cryoprotective class I chitinase from table grape berries (*Vitis vinifera* cv. Cardinal). *Journal of agricultural and food chemistry* **57**: 8893–8900.

Gardea AA, Lombard PB, Crisosto CH, Moore LW, Fuchigami LH, Gusta LV. **1993**. Evaluation of Frostgard as an antifreeze, inhibitor of ice nucleators, and cryoprotectant on Pinot noir leaf tissue. *American Journal of Enology and Viticulture* **44**: 232–235.

Guenther JF, Seki S, Kleinhans FW, Edashige K, Roberts DM, Mazur P. **2006**. Extra- and intra-cellular ice formation in stage I and II *Xenopus laevis* oocytes. *Cryobiology* **52**: 401–416.

Guy CL, Niemi KJ, Brambl R. **1985**. Altered gene expression during cold acclimation of spinach. *Proceedings of the National Academy of Sciences of the United States of America* **82**: 3673–3677.

Hagedorn M, Peterson A, Mazur P, Kleinhans FW. **2004**. High ice nucleation temperature of zebrafish embryos: slow-freezing is not an option. *Cryobiology* **49**: 181–189.

Hajela RK, Horvath DP, Gilmour SJ, Thomashow MF. **1990**. Molecular cloning and expression of COR (Cold-Regulated) genes in *Arabidopsis thaliana*. *Plant Physiology* **93**: 1246–1252.

Hiranuma N, Möhler O, Yamashita K, Tajiri T, Saito A, Kiselev A, Hoffmann N, Hoose C, Jantsch E, Koop T, *et al.* 2015. Ice nucleation by cellulose and its potential contribution to ice formation in clouds. *Nature Geoscience* **8**: 273.

Hong JS, Rubinsky B. **1994**. Patterns of ice formation in normal and malignant breast tissue. *Cryobiology* **31**: 109–120.

Ishikawa M, Price WS, Ide H, Arata Y. **1997**. Visualization of freezing behaviors in leaf and flower buds of full-moon maple by nuclear magnetic resonance microscopy. *Plant Physiology* **115**: 1515–1524.

Jaglo-Ottosen KR, Gilmour SJ, Zarka DG, Schabenberger O, Thomashow MF. **1998**. Arabidopsis CBF1 overexpression induces COR genes and enhances freezing tolerance. *Science* **280**: 104–106.

Johnston ES. **1923**. Moisture relations of peach buds during winter and spring. *Monthly Weather Review* **51**: 591–591.

Kerr WL, Kauten RJ, McCarthy MJ, Reid DS. **1998**. Monitoring the formation of ice during food freezing by magnetic resonance imaging. *LWT - Food Science and Technology* **31**: 215–220.

Kishimoto T, Sekozawa Y, Yamazaki H, Murakawa H, Kuchitsu K, Ishikawa M. **2014a**. Seasonal changes in ice nucleation activity in blueberry stems and effects of cold treatments in vitro. *Environmental and experimental botany* **106**: 13–23.

Kishimoto T, Yamazaki H, Saruwatari A, Murakawa H, Sekozawa Y, Kuchitsu K, Price WS, Ishikawa M. **2014b**. High ice nucleation activity located in blueberry stem bark is linked to primary freeze initiation and adaptive freezing behaviour of the bark. *AoB plants* **6**.

Kizis D, Lumbreras V, Pagès M. **2001**. Role of AP2/EREBP transcription factors in gene regulation during abiotic stress. *FEBS letters* **498**: 187–189.

Kristiansen E, Zachariassen KE. **2005**. The mechanism by which fish antifreeze proteins cause thermal hysteresis. *Cryobiology* **51**: 262–280.

Kühn N, Ormeño-Núñez J, Jaque-Zamora G, Pérez FJ. **2009**. Photoperiod modifies the diurnal expression profile of VvPHYA and VvPHYB transcripts in field-grown grapevine leaves. *Journal of Plant Physiology* **166**: 1172–1180.

Lang GA, Early JD, Martin GC, Darnell RL. **1987**. Endo-, Para-, and Ecodormancy: Physiological terminology and classification for dormancy research. *HortScience* **22**: 371–377.

Liu Q, Kasuga M, Sakuma Y, Abe H, Miura S, Yamaguchi-Shinozaki K, Shinozaki K. **1998**. Two transcription factors, DREB1 and DREB2, with an EREBP/AP2 DNA binding domain separate two cellular signal transduction pathways in drought-and low-

temperature-responsive gene expression, respectively, in Arabidopsis. *The Plant Cell* **10**: 1391–1406.

Lloyd J, Firth D. **1990**. Effect of defoliation time on depth of dormancy and bloom time for low-chill Peaches. *HortScience* **25**: 1575–1578.

Londo JP, Johnson LM. **2014**. Variation in the chilling requirement and budburst rate of wild Vitis species. *Environmental and Experimental Botany* **106**: 138–147.

Londo JP, Kovaleski AP. 2017. Characterization of wild North American grapevine cold hardiness using differential thermal analysis. *American Journal of Enology and Viticulture* **68** : 203-212.

Londo JP, Kovaleski AP, Lillis JA. **2018**. Divergence in the transcriptional landscape between low temperature and freeze shock in cultivated grapevine (Vitis vinifera). *Horticulture Research* **5**: 10.

McCarthy MJ, Kauten RJ. **1990**. Magnetic resonance imaging applications in food research. *Trends in Food Science & Technology* **1**: 134–139.

Mills LJ, Ferguson JC, Keller M. **2006**. Cold-hardiness evaluation of grapevine buds and cane tissues. *American Journal of Enology and Viticulture* **57**: 194–200.

Molisch H. 1897. Untersuchungen über das Erfrieren der Pflanzen. Reprinted in English. 1982 in *Cryo-Letters* **3**:332-390.

Morris GJ, Coulson GE, Engels M. **1986**. A cryomicroscopic study of *Cylindrocystis brebissonii* De Bary and two species of *Micrasterias Ralfs* (Conjugatophyceae, Chiorophyta) during freezing and thawing. *Journal of Experimental Botany* **37**: 842–856.

Morrison JC. **1991**. Bud development in *Vitis vinifera* L. *Botanical gazette* **152**: 304–315.

Mousavi R, Miri T, Cox PW, Fryer PJ. **2007**. Imaging food freezing using X-ray microtomography. *International journal of food science & technology* **42**: 714–727.

Mullins MG, Bouquet A, Williams LE. **1992**. *Biology of the grapevine*. Cambridge University Press.

Nir G, Shulman Y, Fanberstein L, Lavee S. **1986**. Changes in the activity of catalase (EC 1.11. 1.6) in relation to the dormancy of grapevine (*Vitis vinifera* L.) buds. *Plant Physiology* **81**: 1140–1142.

Noriega X, Burgos B, Pérez FJ. **2007**. Short day-photoperiod triggers and low temperatures increase expression of peroxidase RNA transcripts and basic peroxidase isoenzyme activity in grapevine buds. *Phytochemistry* **68**: 1376–1383.

Or E, Vilozny I, Fennell A, Eyal Y, Ogrodovitch A. **2002**. Dormancy in grape buds: isolation and characterization of catalase cDNA and analysis of its expression following chemical

induction of bud dormancy release. *Plant science: an international journal of experimental plant biology* **162**: 121–130.

Padrón R, Alamo L, Craig R, Caputo C. **1988**. A method for quick-freezing live muscles at known instants during contraction with simultaneous recording of mechanical tension. *Journal of Microscopy* **151**: 81–102.

Parker J. **1963**. Cold Resistance in Woody Plants. *The Botanical Review* **29**: 123–201.

Parody-Morreale A, Murphy KP, Di Cera E, Fall R, DeVries AL, Gill SJ. **1988**. Inhibition of bacterial ice nucleators by fish antifreeze glycoproteins. *Nature* **333**: 782–783.

Pearce RS, Willison JH. **1985**. Wheat tissues freeze-etched during exposure to extracellular freezing: distribution of ice. *Planta* **163**: 295–303.

Pérez FJ, Kühn N, Vergara R. **2011**. Expression analysis of phytochromes A, B and floral integrator genes during the entry and exit of grapevine-buds from endodormancy. *Journal of Plant Physiology* **168**: 1659–1666.

Pérez FJ, Lira W. **2005**. Possible role of catalase in post-dormancy bud break in grapevines. *Journal of Plant Physiology* **162**: 301–308.

Quamme HA. **1995**. Deep supercooling in buds of woody plants. In: Biological ice nucleation and its applications. 183–199.

Quamme HA, Su WA, Veto LJ. **1995**. Anatomical Features Facilitating Supercooling of the Flower within the Dormant Peach Flower Bud. *Journal of the American Society for Horticultural Science* **120**: 814–822.

Richards JH, Bliss LC. **1986**. Winter water relations of a deciduous timberline conifer, *Larix lyalii* Parl. *Oecologia* **69**: 16–24.

Riley CV. **1872**. On the cause of deterioration in some of our native grapevines, and one of the probable reasons why European vines have so generally failed with us. *The American naturalist* **6**: 532–544.

Sabbatini P, Howell GS. **2013**. Rootstock scion interaction and effects on vine vigor, phenology, and cold hardiness of interspecific hybrid grape cultivars (*Vitis* spp.). *International Journal of Fruit Science* **13**: 466–477.

Schnabel BJ, Wample RL. **1987**. dormancy and cold hardiness in *Vitis vinifera* L. cv. White Riesling as influenced by photoperiod and temperature. *American journal of enology and viticulture* **38**: 265–272.

Shaltout AD, Unrath CR. **1983**. Rest completion prediction model for 'Starkrimson Delicious' apples. *Journal of the American Society for Horticultural Science* **108**: 957–961.

Shinozaki K, Yamaguchi-Shinozaki K. **2000**. Molecular responses to dehydration and low temperature: differences and cross-talk between two stress signaling pathways. *Current Opinion in Plant Biology* **3**: 217–223.

Shulman Y, Nir G, Fanberstein L, Lavee S. **1983**. The effect of cyanamide on the release from dormancy of grapevine buds. *Scientia Horticulturae* **19**: 97–104.

Sinclair BJ, Gibbs AG, Lee W-K, Rajamohan A, Roberts SP, Socha JJ. **2009**. Synchrotron x-ray visualisation of ice formation in insects during lethal and non-lethal freezing. *PLOS ONE* **4**: e8259.

Socha JJ, Westneat MW, Harrison JF, Waters JS, Lee W-K. **2007**. Real-time phase-contrast x-ray imaging: a new technique for the study of animal form and function. *BMC Biology* **5**: 6.

Srinivasan C, Mullins MG. **1976**. Reproductive anatomy of the grapevine (*Vitis vinifera* L.): origin and development of the anlage and its derivatives. *Annals of Botany* **40**: 1079–1084.

Steponkus PL. **1984**. Role of the plasma membrane in freezing injury and cold acclimation. *Annual Review of Plant Physiology* **35**: 543–584.

Stergios BG, Howell GS. **1977**. Effect of site on cold acclimation and deacclimation of Concord grapevines. *American Journal of Enology and Viticulture* **28**: 43–48.

Stott SL, Karlsson JOM. **2009**. Visualization of intracellular ice formation using high-speed video cryomicroscopy. *Cryobiology* **58**: 84–95.

Thomashow FM. **1994**. *Arabidopsis thaliana* as a model for studying mechanisms of plant cold tolerance. In: Arabidopsis. Cold Spring Harbor Laboratory Press, 807–834.

Trejo-Martínez MA, Orozco JA, Almaguer-Vargas G, Carvajal-Millán E, Gardea AA. **2009**. Metabolic activity of low chilling grapevine buds forced to break. *Thermochimica acta* **481**: 28–31.

USDA National Agricultural Statistics Service. 2018. Noncitrus fruits and nuts 2017 summary. U.S. Dept. Agr., Washington, D.C.

Vergara R, Pérez FJ. **2010**. Similarities between natural and chemically induced bud-endodormancy release in grapevine *Vitis vinifera* L. *Scientia Horticulturae* **125**: 648–653.

Wake CMF, Fennell A. **2000**. Morphological, physiological and dormancy responses of three Vitis genotypes to short photoperiod. *Physiologia Plantarum* **109**: 203–210.

Wang Z-B, Feng L-R, Wang J-J, Wang Z-Y. **2010**. Vitis amuerensis CBF3 Gene Isolation, Sequence Analysis and Expression. *Agricultural sciences in China* **9**: 1127–1132.

Wilson PW, Haymet ADJ. **2012**. The spread of nucleation temperatures of a sample of supercooled liquid is independent of the average nucleation temperature. *The Journal of Physical Chemistry. B* **116**: 13472–13475.

Wilson PW, Heneghan AF, Haymet ADJ. **2003**. Ice nucleation in nature: supercooling point (SCP) measurements and the role of heterogeneous nucleation. *Cryobiology* **46**: 88–98.

Wolber PK, Deininger CA, Southworth MW, Vandekerckhove J, van Montagu M, Warren GJ. **1986**. Identification and purification of a bacterial ice-nucleation protein. *Proceedings of the National Academy of Sciences of the United States of America* **83**: 7256–7260.

Wu J, Zhang Y, Yin L, Qu J, Lu J. **2014**. Linkage of cold acclimation and disease resistance through plant–pathogen interaction pathway in Vitis amurensis grapevine. *Functional & integrative genomics* **14**: 741–755.

Xin Z, Browse J. **2000**. Cold comfort farm: the acclimation of plants to freezing temperatures. *Plant, Cell & Environment* **23**: 893–902.

Yamaguchi-Shinozaki K, Shinozaki K. **1994**. A novel cis-acting element in an Arabidopsis gene is involved in responsiveness to drought, low-temperature, or high-salt stress. *The Plant Cell* **6**: 251–264.

Yang G, Zhang A, Xu LX. **2009**. Experimental study of intracellular ice growth in human umbilical vein endothelial cells. *Cryobiology* **58**: 96–102.

Yang G, Zhang A, Xu LX. **2011**. Intracellular ice formation and growth in MCF-7 cancer cells. *Cryobiology* **63**: 38–45.

Zachariassen KE, Hammel HT. **1976**. Nucleating agents in the haemolymph of insects tolerant to freezing. *Nature* **262**: 285–287.

Zachariassen KE, Kristiansen E, Pedersen SA, Hammel HT. **2004**. Ice nucleation in solutions and freeze-avoiding insects—homogeneous or heterogeneous? *Cryobiology* **48**: 309–321.

Zhu S, Bail ALE, Ramaswamy HS. **2003**. Ice crystal formation in pressure shift freezing of atlantic salmon (*Salmo salar*) as compared to classical freezing methods. *Journal of Food Processing and Preservation* **27**: 427–444.

CHAPTER 2
DEACCLIMATION KINETICS AS A QUANTITATIVE PHENOTYPE FOR DELINEATING THE DORMANCY TRANSITION AND THERMAL EFFICIENCY FOR BUDBREAK IN *Vitis* SPECIES

Introduction

Due to their general stationary habit, plants have evolved many different coping mechanisms to survive stressful conditions in their environment, such as drought and temperature. With regard to winter in temperate climates, annual plants typically survive as dehydrated seeds while perennial plants develop dormancy and cold hardiness. Dormancy is the temporary cessation of visible growth in meristem containing structures, such as buds, and is divided in three types: para-, endo-, and ecodormancy (Lang *et al.*, 1987). Paradormancy is the suspension due to physiological factors within the plant but outside of the dormant structure, such as the suppression of lateral growth by the apical meristem (i.e. apical dominance). Paradormant buds transition into endodormancy as daylength and temperatures decrease, a state suspension of growth due to unknown endogenous factors within the dormant structure, preventing growth during times when environmental conditions fluctuate between conducive and inhibitory (Horvath *et al.*, 2003). During endodormancy, it is generally understood that exposure to low, non-freezing temperatures is necessary (chilling requirement) to transition to the third dormancy state, ecodormancy (Campoy *et al.*, 2011). Tissues maintain a dormant state during ecodormancy due to unsuitable environmental conditions (Lang *et al.*, 1987).

Concomitantly with the onset of dormancy, plants from areas where temperatures drop below freezing develop cold hardiness through different mechanisms. Some plants, or plant tissues, tolerate intracellular ice formation, in which cells are extremely dehydrated by the formation of extracellular ice, and the remaining water is bound (Burke *et al.*, 1976) likely solidifying in a glass-like state. Other plants present a freezing resistance mechanism where

water supercools in the intracellular spaces (Burke *et al.*, 1976). Supercooling is a process through which water can remain in liquid state below its equilibrium freezing point, down to a maximum of ~ −42 °C (Bigg, 1953). These species are typical of mid-latitude temperate climates, where temperatures do not drop below −42 °C during the winter. In buds that present supercooling ability, such as those of grapevines (*Vitis* spp.), cold hardiness may be measured through differential thermal analysis (DTA). This method uses thermoelectric modules that record voltage changes associated with the release of heat due to phase change of water into ice (Mills *et al.*, 2006). Two peaks can be identified in grapevine buds using DTA: a high temperature exotherm (HTE), typically around −5 °C; and a low temperature exotherm (LTE), which varies depending on the environmental conditions experienced by the bud. The HTE represents the freezing of extracellular water (Andrews *et al.*, 1984), which is normal to the process of resisting cold. The LTE, however, is the freezing of intracellular water, and it happens when the supercooling point has been exceeded (Mills *et al.*, 2006). The LTE represents the lethal temperature for a given bud, and is correlated with manual assessments of bud death (Wolf and Cook, 1994). Mean LTE has since been adopted as a consistent and routine measurement of bud cold hardiness (Mills *et al*., 2006, Ferguson *et al*., 2011).

Cold hardiness follows a general U-shaped pattern during the winter, with three different stages: acclimation, maintenance, and deacclimation. This pattern is thought to be primarily driven by air temperature (Ferguson *et al.*, 2011, 2014; Londo and Kovaleski, 2017), although other climatic aspects may also be important, such as relative humidity and daily thermal amplitude (Antivilo *et al.*, 2017). Acclimation appears to occur primarily during endodormancy, while deacclimation is enhanced during ecodormancy (Ferguson *et al.*, 2011, 2014; Londo and Kovaleski, 2017). The transition between endo- and ecodormancy may occur toward the end of

the acclimation stage depending on the climate and genotype, or during the maintenance stage of cold hardiness. This transition is typically evaluated by collecting dormant buds from the field and placing them in growth permissive conditions, followed by monitoring the time needed to reach budbreak (Weinbaum *et al.*, 1989; Lloyd and Firth, 1990; Cook and Jacobs, 2000; Fan *et al.*, 2010; Zhang and Taylor, 2011). The chilling requirement has been considered to be met when 50% budbreak occurs within a time threshold {e.g. 3 weeks for peaches [*Prunus persica* (L.) Batsch; Lloyd and Firth, 1990]; 4 weeks for grapevines (Londo and Johnson, 2014)}. This method represents a subjective threshold for the transition from endo- to ecodormancy. As a result, determining the molecular and metabolic cues and the consequences of this transition, such as budbreak, are very difficult to determine and poorly understood (Penfield, 2008).

As the dynamics of acclimation and deacclimation change with dormancy state (Ferguson *et al.*, 2011, 2014), and dormancy state is determined by accumulation of chilling hours, a future climate may create issues for both cold hardiness and budbreak phenology. Average global temperatures are increasing (Walsh *et al.*, 2014), although episodes of acute cold weather in the northern hemisphere are likely to increase as well through more frequent arctic oscillations (Kolstad *et al.*, 2010). In addition to direct effects to cold hardiness, increasing temperatures will enhance chill accumulation in higher latitudes, while lower latitudes will experience a decrease (Luedeling *et al.*, 2011). Changes in chill accumulation may modify the dynamics of dormancy transitions both in deciduous tree crops and other woody perennials, causing excessive responsiveness to warm spells or erratic budbreak and growth. This will ultimately require a shift towards higher latitudes and elevations of tree crops and assisted migration of forest species as they lag behind their optimal climate niche (Gray and Hamann, 2013). Therefore, it is important to understand how both temperature and dormancy status affect the loss of cold hardiness. The

objective of this study was to understand the relationship between chill accumulation, the dormancy transition, and temperature effects on the loss of cold hardiness and budbreak in wild and cultivated grapevines.

Materials and Methods

Plant material and data collection

Buds of four different species were collected multiple times during the dormant seasons of 2014/15, 2015/16, and 2016/17. *V. vinifera* L. 'Cabernet Franc', 'Cabernet Sauvignon', 'Riesling', and 'Sauvignon blanc' were collected from local vineyards (42.705N, 76.973W; and 42.845N, 77.004W), while *V. aestivalis* Michx. (two clones: PI483138, PI483143), *V. amurensis* Rupr. (three clones: PI588632, PI588635, PI588641), and *V. riparia* Michx. (four clones: PI588275, PI588562, PI588653, PI588711) were collected from the USDA Plant Genetic Resources Unit in Geneva, New York. Buds from nodes 3 to 20 from the base of *V. vinifera* canes were used, while for the other species, buds beyond position 20 were used due to constraints regarding the number of clones, as in Londo and Kovaleski (2017).

Hourly weather data from the closest Network for Environment and Weather Applications station (NEWA; http://www.newa.cornell.edu/) was used to compute chill accumulation using the "North Carolina" model (Shaltout and Unrath, 1983). The start date for each season was chosen based on when chill started to consistently accumulate instead of being negated, as determined by the NC model. These dates were 11 Sept. 2014, 19 Sept. 2015, and 24 Sept. 2016.

Upon collection, canes were cut into single- or two-node cuttings and placed submerging the basipetal cut surface in cups of water. The cups were placed into growth chambers at 2, 4, 7, 8, 10, 11, 22, or 30 °C. Not every genotype or temperature was used at all collection points. This information is available in Supplementary Table A-1. Differential thermal analysis (DTA) was

used to estimate the cold hardiness of individual buds as represented by their low temperature exotherm [LTE; see Mills *et al.* (2006) for details]. Briefly, buds were excised from the cane and placed on thermoelectric modules in plates. The plates were placed in a programmable freezer and subjected to a cooling rate of −4 °C hour^{-1}. Changes in voltage due to heat release in the freezing of water were measured by the thermoelectric module and recorded using a Keithley data logger (Tektronix, Beaverton, OR) attached to a computer. Between 4 and 8 buds were sampled at any time point per treatment to determine mean LTE, and the intervals between measurement days varied between chill accumulation level and temperature treatment, with details provided in Supplementary Table S1. Because lower rates of deacclimation were expected in buds placed at lower temperatures and lower chill accumulations, lower temperature treatments were typically assessed with wider separation between time points compared to high temperature treatments (Supplementary Table A-1).

An experiment was also designed to compare temperature effects on fully chilled grapevines (1440 chill accumulation). Buds held at constant temperatures (2, 4, 7, 11, 22 °C) had their budbreak recorded following the modified E-L scale (Coombe & Iland, 2005) for all *V. vinifera* and *V. riparia*. Five buds were randomly selected and E-L number recorded in the same sampling interval as for LTE (Supplementary Table A-1) until buds were past stage 3 or bud material was exhausted.

Data analysis

Based on sample size across temperatures and across sampled years, data sets for *V. vinifera* were analysed separately for each cultivar, while data for accessions of *V. aestivalis*, *V. amurensis* and *V. riparia* were combined at the species level. Analyses were separated into the effect of chill accumulation and the effect of temperature on rate of deacclimation. The datasets used for each analysis are specified in Supplementary Table A-1.

Effect of Chill Accumulation. In order to assess the effect of chill accumulation on the rate of deacclimation (k_{deacc}), hereafter referred to as deacclimation potential (Ψ_{deacc}), individual rates were calculated using linear regression in R (ver. 3.3.0, R Foundation for Statistical Computing) for each temperature and chill accumulation as factors. Although every temperature within a chill accumulation had the same data for day 0 (field collection), temperatures were still allowed to have different intercepts in order to reduce the effect of day 0 on k_{deacc}. From this regression model, data points that had a studentized residual ≥2.5 were considered outliers and removed from the dataset, and the model was re-fit. The k_{deacc} at each chill accumulation were then transformed to percentage for 4, 7, 10, 11, and 22 °C, standardizing to their k_{deacc} at highest chill accumulation (either 1440 – 7 and 11 °C – or 1580 chill units – 4, 10, and 22 °C). The Ψ_{deacc} was estimated as a logistic regression. Initial estimation used the drc library, but final estimation used the nls() function with the port algorithm, following the equation: Ψ_{deacc} (%)= $1/_{1+ e^{[b \times (\ln Chill - c)]}}$, where b and c are the estimated parameters, and *Chill* is the chill accumulation at the time of sample collection. The parameter c is the inflection point of the logistic and b is the slope associated with the logistic regression.

Effect of Temperature. Instead of using the initially calculated rates derived from the above linear models, the complete data sets were used with the effect of temperature as a continuous variable. The values for the different chill accumulation points were normalized to that of full chill by multiplying the Ψ_{deacc} at any given chill accumulation. Data were divided into two data sets to study the effect of temperature: "low" (2 – 11 °C) and "high" temperature deacclimation (10 – 30 °C). The temperature effect for low temperatures was assumed to be an exponential, and therefore the rates were calculated as $k_{deacc} = m \times e^{(n \times T)}$, where m and n are the parameters estimated, and T is the temperature in °C. For high temperatures, a logarithmic curve

was used: $k_{deacc} = q \times \ln(T - r)$, where q and r are the parameters estimated, and T is the temperature in °C. For both low and high temperatures, parameters were estimated using nls(), with the port algorithm.

Fitness of Effects of Chill and Temperature. The fits of all non-linear curves (effect of chill accumulation, low and high temperatures) were tested using Effron's pseudo-R^2 with the Rsq function in the soilphysics library. The final model for loss of cold hardiness is then $\Delta_{LTE}(T, Chill) = k_{deacc} \times \Psi_{deacc} \times t$, where the change in LTE (Δ_{LTE}) is a function of the temperature (T) it was exposed to, how much chill accumulation ($Chill$) had passed before exposed to deacclimation temperatures, and the time (t) of exposure. A linear model was used to evaluate the accuracy of the predictions using the complete data set, where instead of temperature, $k_{deacc} = \begin{cases} m \times e^{(n \times T)}, & T < 12\ ^{\circ}C \\ q \times ln(T - r), & T \geq 12\ ^{\circ}C \end{cases}$ was used, and instead of accumulated chill, the Ψ_{deacc} was used. The β associated with the estimated k_{deacc} and Ψ_{deacc} was expected to be 1 in this model ($\Delta_{LTE} = \beta \times k_{deacc} \times \Psi_{deacc} \times t$), considering estimations were appropriate.

Budbreak. In order to evaluate whether the same temperature effects governing deacclimation and loss of cold hardiness (measured as LTE) also controlled differences in the temporal rate of budbreak, a linear model was used. For this, forward selection was conducted with a reduced model containing an intercept only, and a full model containing all possible interactions of growing degree-days [GDD = $k_{deacc} \times t$ (day)], temperature, species, and genotype as explanatory variables for bud growth stage. The forward selection was corrected based on the Bayesian information criterion (BIC).

Results

After removing outliers using multiple linear regression, data sets kept ≥ 90% of the observations for all genotypes, with the exception of *V. amurensis*, which had 19.5% of

observations removed (Table 2-1). Linear behaviour appears to describe well the effects of temperature and chill accumulation in the deacclimation of grapevine buds (Fig. 2-1). A logistic regression appeared to be a good fit for the Ψ_{deacc} (Fig. 2-2), with pseudo-R^2 values greater than 0.87 for all genotypes except for 'Cabernet Sauvignon' and *V. amurensis* (0.65 and 0.79, respectively; Table 2-1). The parameter *c* is the natural logarithm of the inflection point, and there was little difference in this parameter for the genotypes tested (e.g., extremes were 6.77 and 6.88, for 'Sauvignon blanc' and 'Riesling', respectively, which is equivalent to 872 to 972 chill units).

The normalized k_{deacc} based on Ψ_{deacc} obtained from multiple linear regression (temperature and chill accumulation as factors; Supplementary Table A-1) and corresponding Arrhenius plot (Fig. 2-3) demonstrated a clear discontinuity between low and high temperatures. A deceleration of the increase of k_{deacc} as temperature increased was observed, which justifies the different behaviors used (exponential and logarithmic for low and high temperatures, respectively). The estimation of temperature effects for low and high temperature intersect between 10 and 11 °C due to uncertainty in the exact temperature where there is a change in behaviors. This is primarily due to the lack of data points between 11 and 22 °C. All the *V. vinifera* cultivars had similar deacclimation rates at low temperatures, but 'Riesling' and 'Cabernet Franc' had higher deacclimation rates at high temperatures than 'Cabernet Sauvignon' and 'Sauvignon blanc' (Table 2-1, Fig. 2-4). *V. riparia* and *V. aestivalis* had similar rates to those of *V. vinifera* at low temperatures, but *V. riparia* had estimated rates similar to *V. amurensis* in higher temperatures. *V. aestivalis* was similar to the faster *V. vinifera* ('Cabernet Franc' and 'Riesling'). *V. amurensis* showed the highest deacclimation rates at both low and high temperatures.

Linear models showed a good fit of the estimated parameters for k_{deacc} and Ψ_{deacc} for all genotypes ($R^2 \geq 0.80$). *V. vinifera* cultivars, which were analysed separately, had higher R^2 values. The better fit for V. *vinifera* cultivars is also seen in their β coefficients, which are very close to 1, although *V. aestivalis* and *V. riparia* had βs of 0.99 and 0.96 respectively. *V. amurensis* had the lowest β, at 0.83.

The model resulting from the forward selection using BIC for budbreak stage was a multiple linear regression using an intercept and GDD × species interaction [*Budbreak stage (species)*$= a + b \times$ GDD], with $P<0.001$ and adjusted-$R^2 = 0.66$. The effect of k_{deacc}, i.e. the effect of temperature, on budbreak can be seen in Fig. 5. When LTE and budbreak are regarded in respect to time, a clear separation was observed between temperatures (Figs. 2-5A, C, E, G). When GDDs are used, accounting for differences in k_{deacc}, LTE and budbreak stages for all temperatures are "stacked" (Figs. 2-5B, D, F, H). Within the same temperature, budbreak occurs at different times for different genotypes (Fig. 2-6A), but is grouped within species when using GDDs (Fig. 2-6B).

Discussion

Chilling accumulation, dormancy state, cold hardiness and budbreak are complex traits driven by the interaction of physiological and climactic attributes. The consistency of winter temperatures is expected to be a major aspect impacting the sustainability and survival of perennial species in a future climate. This study was conducted to gain a better method for predicting dormancy transition and chilling requirement in grapevine, as well as to understand how deacclimation processes (loss of cold hardiness) and resulting budbreak are impacted by temperature.

This study provides a quantitative assessment of the transition from endo- to ecodormancy, as evaluated by the Ψ_{deacc}. Unlike the typical dormancy assessment that uses time

to budbreak as a measurement of the transition (Londo and Johnson, 2014), using the deacclimation rates does not require subjective assumptions currently used to determine chilling fulfilment; such as having 50% budbreak occur within 28 days. Budbreak becomes apparent only after the freeze mechanisms associated with cold hardiness are lost (Figs. 2-5, 2-6; Ferguson *et al.*, 2014; Salazar-Gutiérrez *et al.*, 2014), although earlier stages of growth within the dormant bud (e.g., increase in turgor) are likely associated with the loss of hardiness. Thus, the amount of time needed to reach 50% budbreak in forcing assays is a combination of 1) the time needed to fully deacclimate, and 2) time required for deacclimated buds to reach a visible change in phenological stage. This two-part chronology of budbreak likely occurs in all perennial species but this study is unique in that it leverages the ability to assess loss of hardiness through decreasing supercooling ability as a way to quantitatively assess rates of deacclimation and its relation to changes in chilling exposure.

Mid-winter warming events are of major concern both for temperate crop species as well as native and naturalized forests. In native trees within natural ranges, little to no damage occurs during the autumn because the freeze resistance readily withstands the minimum temperatures they usually encounter (Vitasse *et al.*, 2014). However, damage can be substantial in late freeze events during the spring or unusual warm events in early spring as the potential for deacclimation increases exponentially (Vitasse *et al.*, 2014). For example, a late spring freeze in 2007 in North America caused widespread damage in midwestern forests, delaying and reducing canopy establishment by 16-34 days (Gu *et al.*, 2008). Bokhorst *et al.* (2009) reported that dwarf shrub vegetation in a sub-Artic region where midwinter temperatures rose to ~7 °C for 2 weeks followed by further cold temperatures resulted in an 87% reduction in growth during the summer compared to neighbouring undamaged areas. Cannell and Smith (1983) show results from

different authors for forest species in which the time to budbreak is reduced in an exponential manner. This is similar to our assessment of Ψ_{deacc}, where the upper portion of the logistic is like the exponential decrease in time to budbreak. The logistic behaviour of Ψ_{deacc} in relation to chill accumulation explains the continuous increase risk of damage of mid-winter warm spells followed by the return of low temperatures the later they occur until 100% Ψ_{deacc} is achieved. This is in contrast with the model developed by Ferguson *et al.* (2011, 2014), where a hard limit for the dormancy boundary is used to model grape cold hardiness. It is likely that, similar to the behaviour described in our study, forest species also have increased deacclimation rates with higher chill accumulation, seen as a decrease in the time to budbreak. Additionally, it is important to note that while canopies may be able to recover from midwinter bud kill events, damage to the reproductive buds in the case of fruit and nut crops will reduce yields in the season following damage.

Our assessment of Ψ_{deacc} leading to increases in k_{deacc} agrees with the general observation that warm temperatures in the early winter are negligible for bud growth (Cannell and Willett, 1975) and that increasing chill accumulation reduces the heat requirements for budbreak in fruit species (Couvillon and Erez, 1985; Citadin *et al.*, 2001), and forest species (Hunter and Lechowicz, 1992; Dantec *et al.*, 2014), considering that loss of hardiness is required for budbreak to occur (Figs. 2-5, 2-6; Ferguson *et al.*, 2014). Analysing bud phenology at approximately full chilling (1440 Chill accumulation $\geq$ 95% Ψ_{deacc} for all genotypes), we have seen that k_{deacc} is responsible for differences in early phenological development in the spring between genotypes within *V. vinifera*, but species still had different phenology with regard to GDD. Planted in the same environment, Taulavuori *et al.* (2004) observed that deacclimation occurs faster in mountain birch [*Betula pubescens* ssp. *czerepanovii* (Orl.) Hämet-Ahti] ecotypes

collected from areas with historical low chill accumulation. If the mechanisms in birch are similar to those described here, what may have been observed in their study may not reflect different rates of deacclimation, but instead plants that were at different stages in their deacclimation potential, or a combination of both. Climate warming appears to speed the loss of cold hardiness and promote earlier leaf-out, although the response is not linear due to interactions with chilling and photoperiod (Vitasse *et al.*, 2014). In our case (e.g. Northeast United States), a predicted increase in chill accumulation (Luedeling *et al.*, 2011) could contribute to higher Ψ_{deacc} and higher risk of cold damage should midwinter warm spells increase in a future climate (Vitasse *et al.*, 2014; Walsh *et al.*, 2014).

Ferguson *et al.* (2011, 2014) used a linear response of the rates of deacclimation in relation to temperature for 21 *V. vinifera* and two *V. labruscana* Bailey cultivars, with a different rate and base temperature for endo- and ecodormant buds. In our experiments, deacclimation occurred in temperatures below those established as the threshold for deacclimation by Ferguson *et al.* (2014). This suggests that although it may produce a good fit for field data in Western Washington, the current prediction model (Ferguson *et al.*, 2014) may be over-simplifying the response to temperature from a physiological standpoint. Takeuchi and Kasuga (2017) have also seen deacclimation through electrolyte leakage of bark and xylem of Japanese white birch [*Betula platyphylla* Sukatchiev var. *japonica* (Miq.)] at low temperatures, including high below-freezing temperatures (−5 to 0 °C). In our study the temperature dependency of k_{deacc} appears to follow simple enzymatic kinetics, affected by both the catalytic rate (Arrhenius' law) in lower temperatures, and the denaturation of enzymes in higher temperatures. This behaviour suggests that an active temperature sensing, as defined by Ruelland and Zachowski (2010), is not necessary for deacclimation.

Cultivar or accession differences are seen within species in cold hardiness (Arora *et al.*, 2004; Ferguson *et al.*, 2011, 2014; Salazar-Gutiérrez *et al.*, 2014, 2016; Szalay *et al.*, 2017), although deacclimation rates may or may not differ (Arora *et al.*, 2004; Ferguson *et al.*, 2011, 2014; Szalay *et al.*, 2017). The effect of genotypes within species in k_{deacc} is suggested by the better fit of our curves to *V. vinifera* cultivars as compared to the other species, where parameters were estimated by combining different accessions in the wild material. However, our dataset did not allow us to properly analyse each genotype of the wild accessions separately. It has been suggested that there is no correlation among species between the maximum cold hardiness or climate of origin and the rate of deacclimation (Arora *et al.*, 2004; Kalberer *et al.*, 2006). Vitasse *et al.* (2014), however, suggests that the rate of deacclimation is more related to temperature fluctuations in the area where species evolved, diminishing the potential for deacclimation in locations where frequent temperature fluctuations occur in the winter. In our case, *V. riparia* and *V. amurensis*, two species from colder climates as compared to *V. vinifera*, had higher k_{deacc} at all (*V. amurensis*) or at moderate to high temperatures (*V. riparia*) than *V. vinifera*. *V. aestivalis*, however, did not appear to differ from the *V. vinifera* cultivars, in agreement with the assessment by Kalberer *et al.* (2006). Kalberer *et al.* (2006) also suggested that field and controlled studies can result in different responses to temperature. In our study, however, we observed higher rates of deacclimation in *V. amurensis* and *V. riparia* compared to *V. aestivalis*, which is comparable and follows the same behaviour as the "responsiveness" described by Londo and Kovaleski (2017) using field observations.

Bud phenology timing appears to follow the same temperature response as deacclimation within species. Therefore, it is possible that loss of cold hardiness may represent early stages of growth within the bud, such as increase in turgor of cells, and that the differences in bud

development in regard to GDDs (Fig. 2-6B) between species are due to different bud morphology. However, there have been no studies comparing early morphological development in buds of different *Vitis* species. In *V. vinifera*, however, Andreini *et al.* (2009) showed a difference in thermal time requirements between different genotypes grouped in late, intermediate and early budbreak. They used a single temperature exposure to evaluate all cultivars, however. This is similar to the assessment of budbreak by Londo and Johnson (2014), in which 'Riesling' and 'Cab. Sauvignon' had different times to budbreak within the same chill accumulation. In our case, 'Riesling' also had earlier budbreak compared to 'Cab. Sauvignon' (Fig. 2-6A), and it is clear that GDDs calculated with the same base temperature would result in different thermal time requirements to reach budbreak. However, when we account for the difference in thermal efficiency for deacclimation (e.g., $k_{\mathrm{deacc}_{Riesling}} > k_{\mathrm{deacc}_{Cab.Sauvignon}}$ at any given temperature), both *V. vinifera* genotypes have the same GDD requirements for budbreak (Fig. 6B). Therefore, forcing assays using budbreak phenology as the method of determining chilling fulfilment would determine that inherently slow deacclimators, such as 'Cabernet Sauvignon', require higher chill accumulation. Our results demonstrate that high-chill requirement phenotypes may actually be a combination of higher chill requirement and low temperature efficiency (low k_{deacc}).

Conclusions

Specific studies linking environmental factors to understand plant phenology in order to evaluate impacts of climate change are needed (Cleland *et al.*, 2007; Chmielewski *et al.*, 2018), especially during spring phenology (Vitasse *et al.*, 2014). In this study, we have demonstrated that early bud phenology and deacclimation to cold are linked and therefore results based on budbreak alone are confounded by dynamics of the loss of hardiness. It is clear that assessments

of deacclimation rates simply using “endo-” and “ecodormant” material is not appropriate, as there is a continuum of response in deacclimation rates as chill is accumulated. In this study, we demonstrate an objective, quantitative method for determining the chilling requirement and dormancy transition of perennial species that utilize supercooling for cold hardiness [e.g. peach, cherry (*Prunus* spp. L.), azalea (*Rhododendron* spp. L.), larch (*Larix kaempferi* Sarg.)]. In addition, this method provides a measure of thermal efficiency that appears to be species and genotype specific. These metrics may prove useful for modelling how perennial species will be impacted by future shifts of winter and spring temperatures.

Table 2-1 Parameter estimates and model fits for deacclimation potential, low and high temperature deacclimation rates, and linear relationship between LTE and the deacclimation rate × deacclimation potential for 7 *Vitis* genotypes.

		Deacclimation potential[a]			
Species	Cultivar	b	e	Convergence	Pseudo-R^2
V. vinifera	'Cab. Franc'	−9.47	6.79	Relative	0.93
	'Cab. Sauvignon'	−8.27	6.80	Relative	0.65
	'Riesling'	−7.23	6.88	Relative	0.87
	'Sauvignon blanc'	−43.66	6.77	Relative	0.93
V. aestivalis		−22.31	6.86	Relative and x	0.97
V. amurensis		−12.94	6.85	Relative	0.79
V. riparia		−9.79	6.82	Relative	0.96
		Low temperature[b]			
		m	n	Convergence	Pseudo-R^2
V. vinifera	'Cab. Franc'	0.0600	0.253	Relative	0.89
	'Cab. Sauvignon'	0.0620	0.218	Relative	0.87
	'Riesling'	0.0675	0.236	Relative	0.92
	'Sauvignon blanc'	0.0542	0.235	Relative and x	0.84
V. aestivalis		0.0965	0.187	Relative and x	0.80
V. amurensis		0.1988	0.211	Relative	0.75
V. riparia		0.0754	0.259	Relative	0.81
		High temperature[c]			
		q	r	Convergence	Pseudo-R^2
V. vinifera	'Cab. Franc'	0.762	7.52	Relative	0.92
	'Cab. Sauvignon'	0.593	7.73	Relative	0.84
	'Riesling'	0.732	7.39	Relative	0.88
	'Sauvignon blanc'	0.513	6.66	Relative	0.83
V. aestivalis		0.830	7.91	Relative and x	0.80
V. amurensis		0.913	3.34	Relative	0.80
V. riparia		0.977	7.32	Relative	0.84
		Linear model[d]			
		β	R^2	N	n (%)
V. vinifera	'Cab. Franc'	0.962	0.88	853	0.96
	'Cab. Sauvignon'	0.997	0.84	1160	0.93
	'Riesling'	1.018	0.90	1260	0.93
	'Sauvignon blanc'	1.002	0.86	745	0.90
V. aestivalis		0.963	0.80	700	0.92
V. amurensis		0.828	0.83	730	0.81
V. riparia		0.987	0.82	1499	0.93

[a] $\Psi_{deacc}\ (\%) = {}^{1}/_{1+\,e^{[b\,\times\,(\ln Chill\,-\,c)]}}$, where *Chill* = chill accumulation

[b] $k_{deacc} = m \times e^{(n \times T)}$, where T = temperature

[c] $k_{deacc} = q \times \ln(T - r)$, where T = temperature

[d] $\Delta_{LTE}(T, Chill) = \beta \times k_{deacc} \times \Psi_{deacc} \times t$, where t = time

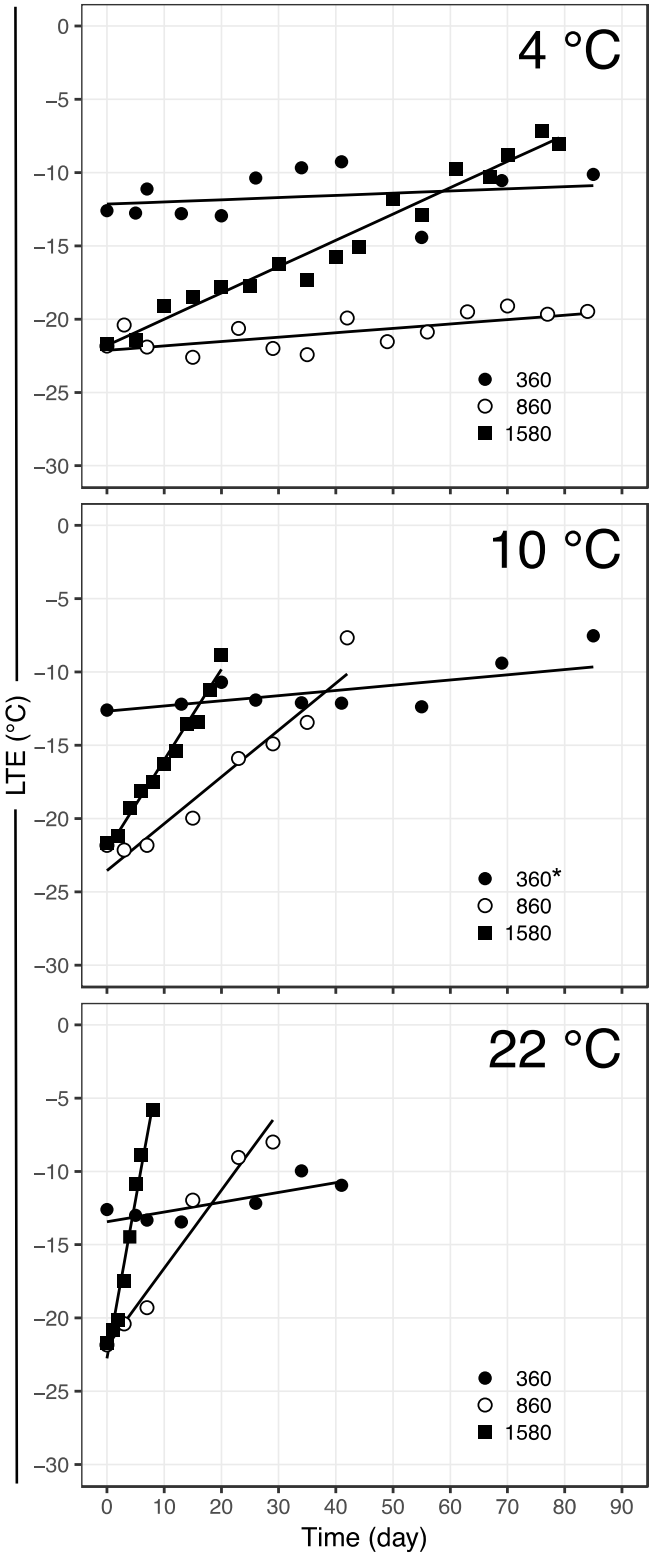

Figure 2-1. Deacclimation of *V. vinifera* 'Riesling' buds at three temperatures (4, 10, and 22 °C) collected from the field at three different chill accumulations (360, 860, 1580). *Buds at 360 chill accumulation were deacclimated at 11 °C.

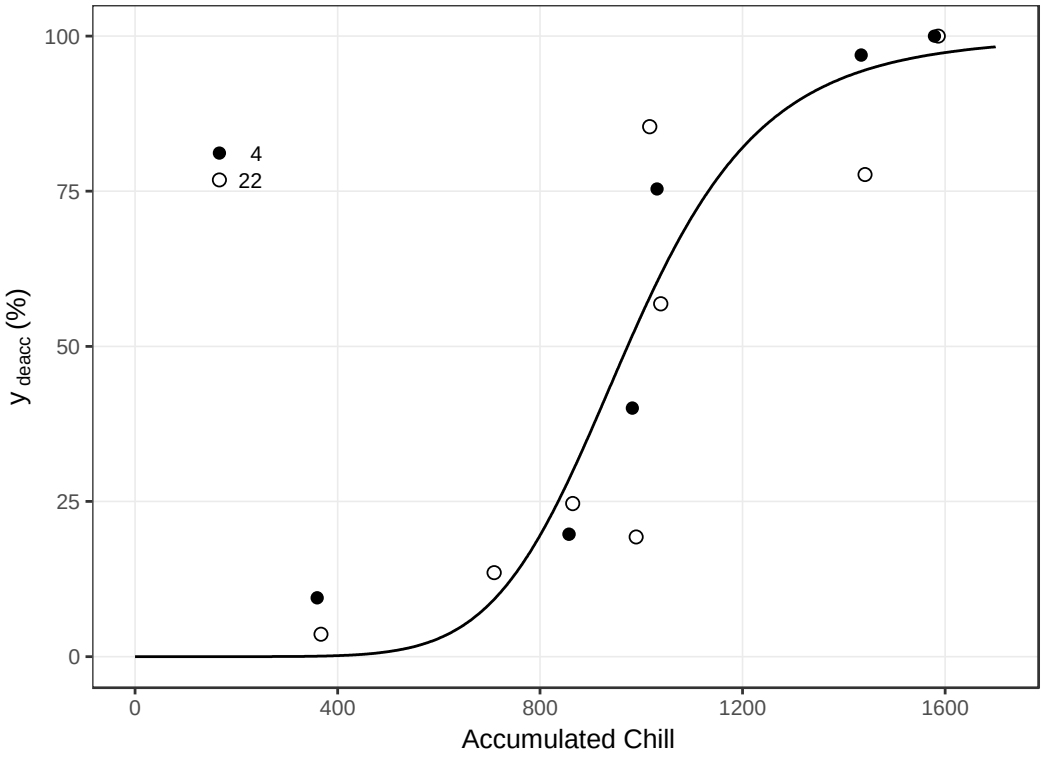

Figure 2-2. Deacclimation potential of *V. vinifera* 'Riesling' buds collected at different chill accumulations in two temperatures. Deacclimation rate at 1580 chill units was used as reference (100 %). The relationship between deacclimation potential and accumulated chill was described by the equation: $\Psi_{deacc}\ (\%) = {}^{1}/_{1+\,e^{[-7.23 \times (\ln Chill\ -6.88)]}}$, with a pseudo-$R^2$ = 0.87.

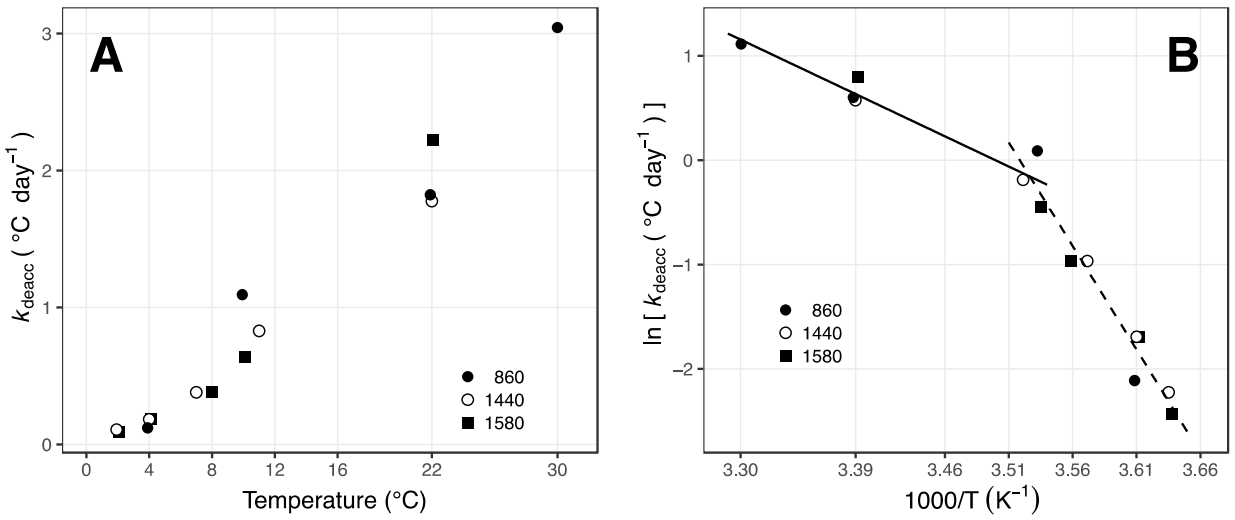

Figure 2-3. Effect of temperature on deacclimation rates of *V. vinifera* 'Riesling'. A) Scaled deacclimation rates (based on deacclimation potential) at three different chill accumulations in response to temperature; B) Arrhenius plot of scaled deacclimation rates. Tick marks in both panels are equivalent and mirrored (e.g. 0 °C = 3.66 × 1000 K^{-1}).

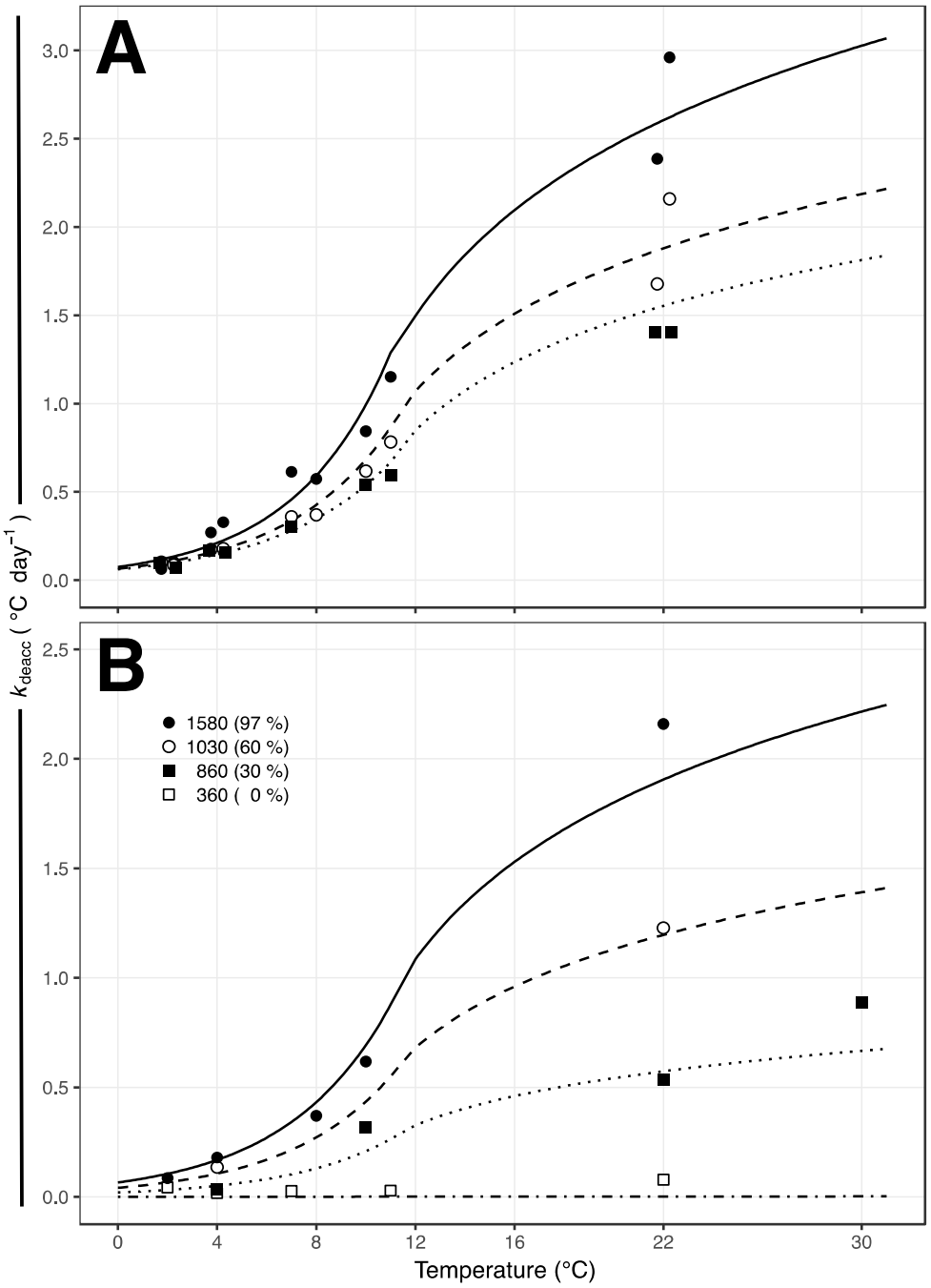

Figure 2-4. Deacclimation rates of *Vitis* buds as a function of temperature. A) Deacclimation rates at >90 % deacclimation potential for three different *Vitis* genotypes: *V. riparia* (closed circle – full line; mean of 4 genotypes), *V. vinifera* 'Riesling' (open circles – dashed line), and *V. vinifera* 'Cabernet Sauvignon' (closed squares – dotted line); B) Deacclimation rates of *V. vinifera* 'Riesling' at different chill accumulations as a function of temperature: 1580 (closed circle – full line), 1030 (open circle – dashed line), 860 (closed square – dotted line), 360 (open square – dashdotted line).

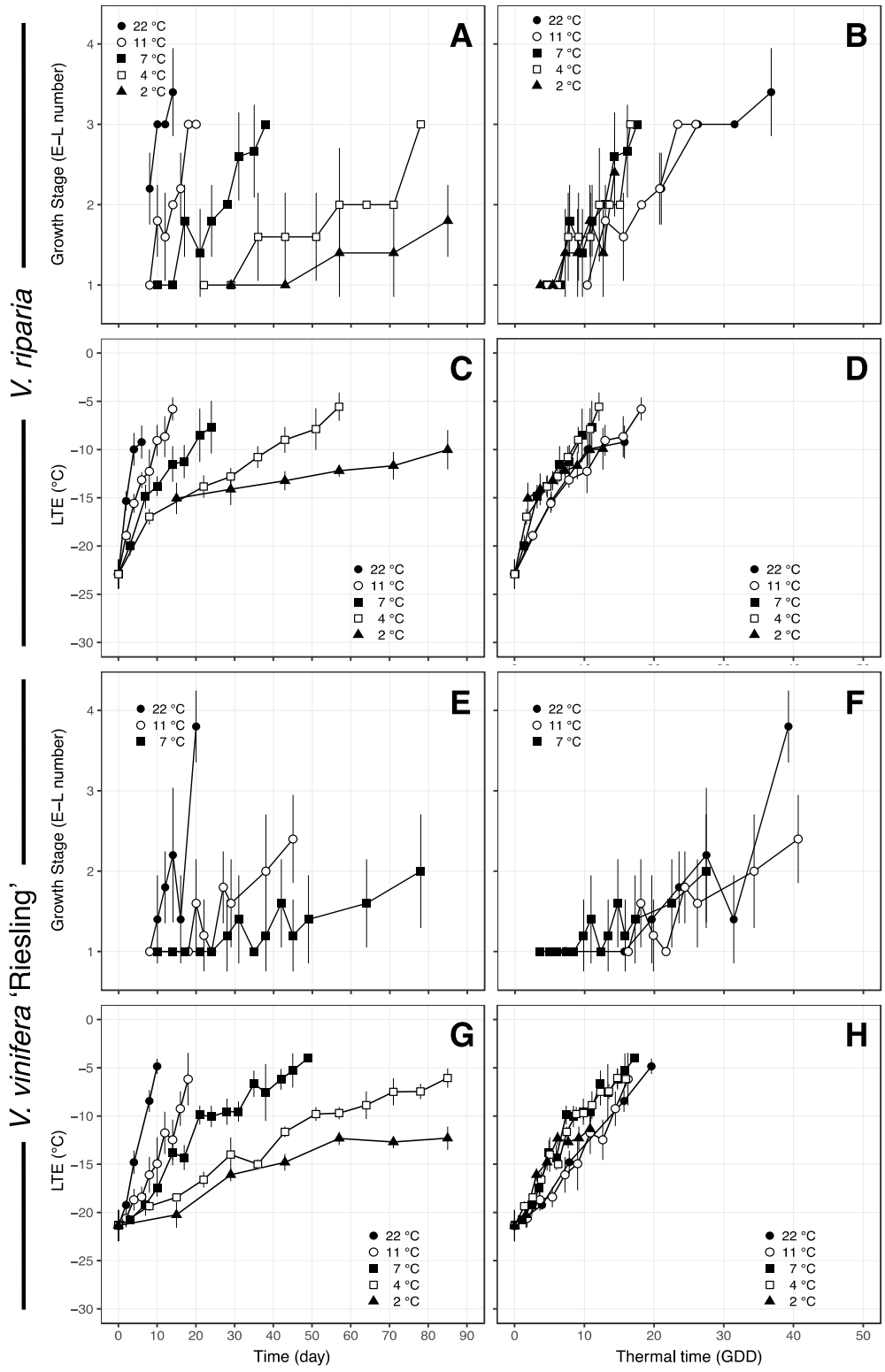

Figure 2-5. Deacclimation and bud phenology of *V. riparia* and *V. vinifera* 'Riesling' in relation to time (A, C, E, G) and thermal time in GDD (B, D, F, H). Bud phenology as the

Figure 2-5. (*Cont.*) “E-L number” (Coombe & Iland, 2005) is shown for 5 temperatures in *V. riparia* and 3 temperatures in ‘Riesling’, as no bud development was recorded within 90 days at 2 and 4 °C for ‘Riesling’. GDDs were calculated based on k_{deacc} for each genotype (see Table 1) at any given temperature multiplied by time in days. Bars indicate standard deviation.

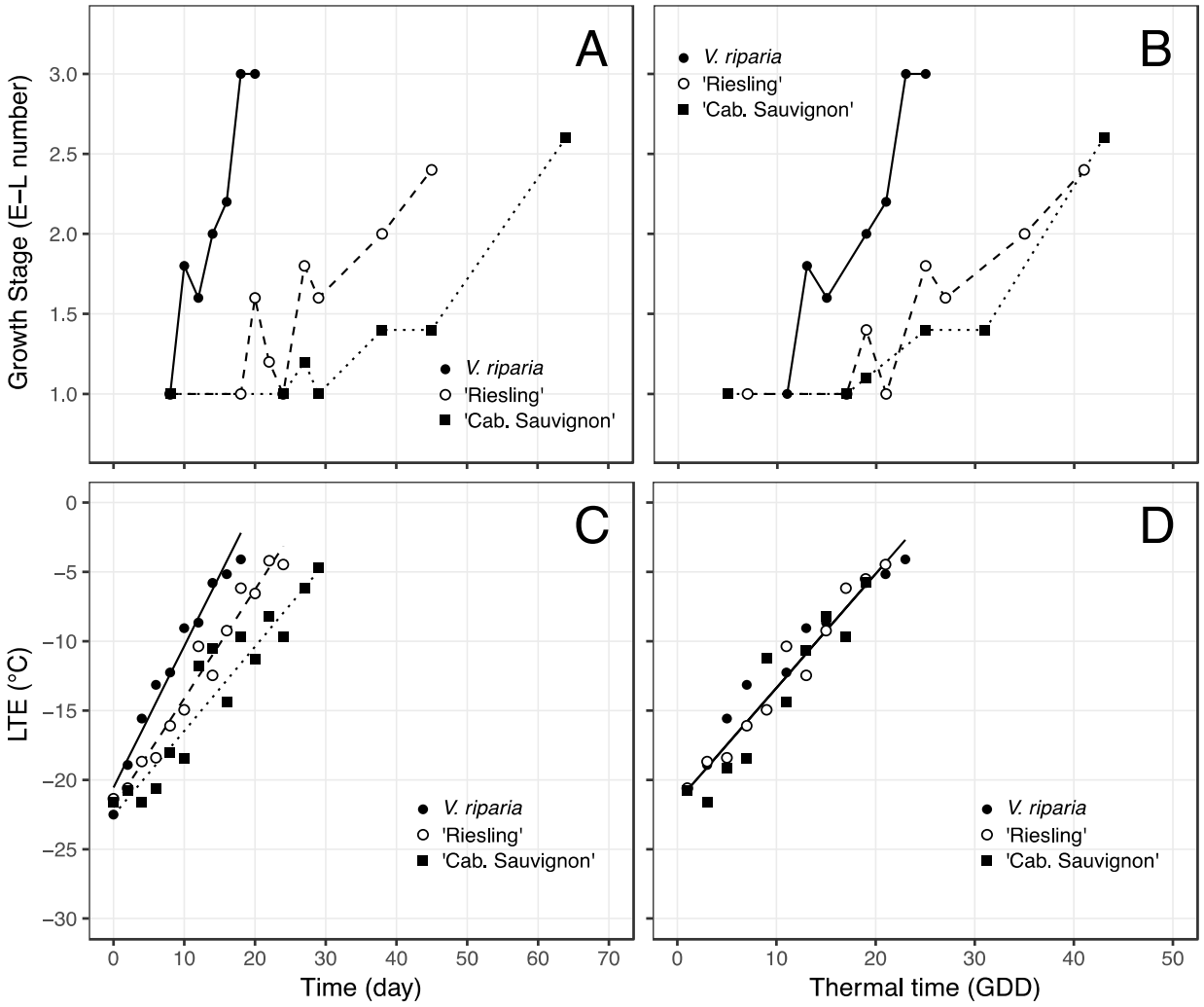

Figure 2-6. Deacclimation and bud phenology of *V. riparia* (closed circle – full line), *V. vinifera* 'Riesling' (open circle – dashed line), and *V. vinifera* 'Cabernet Sauvignon' (closed square – dotted line) at 11 °C in relation to time (A, C) and thermal time in GDD (B, D).

References

Andreini L, Viti R, Scalabrelli G. 2009. Study on the morphological evolution of budbreak in *Vitis vinifera* L. *Vitis* **4** : 153-158.

Andrews PK, Sandidge III CR, Toyama TK. 1984. Deep supercooling of dormant and deacclimating *Vitis* buds. *American Journal of Enology and Viticulture* **35** : 175-177.

Antivilo FG, Paz RC, Keller M, Borgo R, Tognetti J, Juñent FR. 2017. Macro- and microclimate conditions may alter grapevine deacclimation: variation in thermal amplitude in two contrasting wine regions from North and South America. *International Journal of Biometeorology* **61** : 2033-2045.

Arora R, Rowland LJ, Ogden EL, *et al*. 2004. Dehardening kinetics, bud development, and dehydrin metabolism in blueberry cultivars during deacclimation at constant, warm temperatures. *Journal of the American Society for Horticultural Sciences* **129** : 667-674.

Bigg EK. 1953. The supercooling of water. *Proceedings of the Physical Society Section B* **66** : 688-694.

Bokhorst SF, Bjerke JW, Tømmervik H, Callaghan TV, Phoenix GK. 2009. Winter warming events damage sub-Arctic vegetation: consistent evidence from an experimental manipulation and a natural event. *Journal of Ecology* **97** : 1408-1415.

Burke MJ, Gusta LV, Quamme HA, Weiser CJ, Li PH. 1976. Freezing and injury in plants. *Annual Review of Plant Physiology* **27** : 507-528.

Campoy JA, Ruiz D, Egea J. 2011. Dormancy in temperate fruit trees in a global warming context: A review. *Scientia Horticulturae* **130** : 357-372.

Cannell MGR, Smith RI. 1983. Thermal time, chill days and prediction of budburst in *Picea sitchensis*. *Journal of Applied Ecology* **20** : 951-963.

Cannell MGR, Willett SC. 1975. Rates and times at which needles are initiated in buds of different provenances of *Pinus contorta* and *Picea sitchensis* in Scotland. *Canadian Journal of Forest Research* **5** : 367-380.

Chmielewski F, Götz K, Weber KC, Moryson S. 2018. Climate change and spring frost damages for sweet cherries in Germany. *International Journal of Biometeorology* **62** : 217-228.

Citadin I, Raseira MCB, Herter FG, Silva JB. 2001. Heat requirement for blooming and leafing in peach. *HortScience* **36** : 305-307.

Cleland EE, Chuine I, Menzel A, Mooney HA, Schwartz MD. 2007. Shifting plant phenology in response to global change. *Trends in Ecology & Evolution* **22** : 357-365.

Cook C, Jacobs G. 2000. Progression of apple (*Malus* × *domestica* Borkh.) bud dormancy in two mild winter climates. *The Journal of Horticultural Science and Biotechnology* **75** : 233-236.

Couvillon GA, Erez A. 1985. Influence of prolonged exposure to chilling temperatures on bud break and heat requirement for bloom of several fruit species. *Journal of the American Society for Horticultural Sciences* **110** : 47-50.

Dantec CF, Vitasse Y, Bonhomme M, Louvet J, Kremer A, Delzon S. 2014. Chilling and heat requirements for leaf unfolding in European beech and sessile oak populations at the southern limit of their distribution range. *International Journal of Biometeorology* **58** : 1853-1864.

Coombe BG, Iland P. 2005. Grapevine phenology. In Dry PR, Coombe BG, eds. *Viticulture, vol 1: Resources*. Winetitles, Ashford, Australia, 210-248.

Fan S, Bielenberg DG, Zhebentyayeva TN, Reighard GL, Okie WR, Holland D, Abbott AG. 2010. Mapping quantitative trait loci associated with chilling requirement, heat requirement and bloom date in peach (*Prunus persica*). *New Phytologist* **185** : 917-930.

Ferguson JC, Tarara JM, Mills LJ, Grove GG, Keller M. 2011. Dynamic thermal time model of cold hardiness for dormant grapevine buds. *Annals of Botany* **107** : 389-396.

Ferguson JC, Moyer MM, Mills LJ, Hoogenboom G, Keller M. 2014. Modeling dormant bud cold hardiness and budbreak in twenty-three *Vitis* genotypes reveals variation by region of origin. *American Journal of Enology and Viticulture* **65** : 59-71.

Gray LK, Hamann A. 2013. Tracking suitable habitat for tree populations under climate change in western North America. *Climatic Change* **117** : 289-303.

Gu L, Hanson PJ, Post WM, Kaiser DP, *et al*. 2008. The 2007 Eastern US spring freeze: increased cold damage in a warming world? *BioScience* **58** : 253-262.

Horvath DP, Anderson JV, Chao WS, Foley ME. 2003. Knowing when to grow: signals regulating bud dormancy. *Trends in Plant Science* **8** : 534-540.

Hunter AF, Lechowicz MJ. 1992. Predicting the timing of budburst in temperate trees. *Journal of Applied Ecology* **29** : 597-604.

Kalberer SR, Wisniewski M, Arora R. 2006. Deacclimation and reacclimation of cold-hardy plants: Current understanding and emerging concepts. *Plant Science* **171** : 3-16.

Kolstad EW, Breiteig T, Scaife AA. 2010. The association between stratospheric weak polar vortex events and cold air outbreaks in the Northern Hemisphere. *Quarterly Journal of the Royal Meteorological Society* **136** : 886-893.

Lang GA, Early JD, Martin GC, Darnell RL. 1987. Endo-, para-, and ecodormancy: physiological terminology and classification for dormancy research. *HortScience* **22** : 371-377.

Lloyd J, Firth D. 1990. Effect of defoliation time on depth of dormancy and bloom time for low-chill peaches. *HortScience* **25** : 1575-1578.

Londo JP, Johnson LM. 2014. Variation in the chilling requirement and budburst rate of wild *Vitis* species. *Environmental and Experimental Botany* **106** : 138-147.

Londo JP, Kovaleski AP. 2017. Characterization of wild North American grapevine cold hardiness using differential thermal analysis. *American Journal of Enology and Viticulture* **68** : 203-212.

Luedeling E, Girvetz EH, Semenov MA, Brown PH. 2011. Climate change affects winter chill for temperate fruit and nut trees. *PLoS ONE* https://doi.org/10.1371/journal.pone.0020155

Mills LJ, Ferguson JC, Keller M. 2006. Cold-hardiness evaluation of grapevine buds and cane tissues. *American Journal of Enology and Viticulture* **57** : 194-200.

Penfield S. 2008. Temperature perception and signal transduction in plants. *New Phytologist* **179** : 615-628.

Ruelland E, Zachowski A. 2010. How plants sense temperature. *Environmental and Experimental Botany* **69** : 225-232.

Salazar-Gutiérrez MR, Chaves B, Anothai J, Whiting M, Hoogenboom G. 2014. Variation in cold hardiness of sweet cherry flower buds through different phenological stages. *Scientia Horticulturae* **172** : 161-167.

Salazar-Gutiérrez MR, Chaves B, Hoogenboom G. 2016. Freezing tolerance of apple flower buds. *Scientia Horticulturae* **198** : 344-351.

Shaltout AD, Unrath CR. 1983. Rest completion prediction model for 'Starkrimson Delicious' apples. *Journal of the American Society for Horticultural Sciences* **108** : 957-961.

Szalay L, Molnár A, Kovács S. 2017. Frost hardiness of flower buds of three plum (*Prunus domestica* L.) cultivars. *Scientia Horticulturae* **214** : 228-232.

Takeuchi M, Kasuga J. 2017. Bark cells and xylem cells in Japanese white birch twigs initiate deacclimation at different temperatures. *Cryobiology* https://doi.org/10.1016/j.cryobiol.2017.11.007

Taulavuori KMJ, Taulavuori EB, Skre O, Nilsen J, Igeland B, Laine KM. 2004. Dehardening of mountain birch (*Betula pubescens* ssp. *czerepanovii*) ecotypes at elevated winter temperatures. *New Phytologist* **162** : 427-436.

Vitasse Y, Lenz A, Körner C. 2014. The interaction between freezing tolerance and phenology in temperate deciduous trees. *Frontiers in Plant Science* doi: 10.3389/fpls.2014.00541

Walsh J, Wuebbles D, Hayhoe K, *et al*. 2014. Chapter 2: Our Changing Climate. In Melillo JM, Richmond T, Yohe GW, eds. *Climate Change Impacts in the United States: The Third National Climate Assessment.* U.S. Global Change Research Program, 19-67. doi: 10.7930/J0KW5CXT

Weinbaum SA, Polito VS, Muraoka TT. 1989. Assessment of rest completion and its relationship to appearance of tetrads in anthers of 'Nonpareil' almond. *Scientia Horticulturae* **38** : 69-76.

Wolf TK, Cook MK. 1994. Cold hardiness of dormant buds of grape cultivars: comparison of thermal analysis and field survival. *HortScience* **29** : 1453-1455.

Zhang J, Taylor C. 2011. The dynamic model provides the best description of the chill process on 'Sirora' pistachio trees in Australia. *HortScience* **46** : 420-425.

CHAPTER 3
TIMING OF GENE REGULATION REVEALS DIFFERENCES BETWEEN LOSS OF COLD HARDINESS AND BUDBREAK IN FOUR GRAPEVINE GENOTYPES

Introduction

Buds of woody perennials are subjected to dormancy during periods of environmental conditions that are non-conducive for growth. On a typical cycle for deciduous plants, the onset of dormancy is usually programmed based on day length, or day length and low temperatures (Cooke *et al.*, 2012). Once dormancy is established, buds gradually transition from a state where growth is suppressed through endogenous factors (endodormancy) to a state where growth is only suppressed by unsuitable environmental conditions (ecodormancy; Lang *et al.*, 1987). The transition occurs through time spent in low, above freezing temperatures, termed as chill accumulation. During ecodormancy, if buds are placed under conducive conditions, they will resume growth and break bud (Lang *et al.*, 1987; Cooke *et al.*, 2012). Timing of budbreak is an extensively studied temperature-controlled trait in plants that depends on both winter (i.e., chill accumulation) and spring temperatures [growing degree-days (GDD) accumulation; Prentice *et al.*, 1992]. Time to budbreak can be described by the dynamics of the loss of cold hardiness (deacclimation; Ferguson *et al.*, 2011, 2014; Kovaleski *et al.*, 2018). The timing to budbreak is dependent on the initial cold hardiness and the rate of deacclimation, which is itself species specific and dependent on both accumulated chill and temperature of deacclimation (Kovaleski *et al.*, 2018). It has been a decade since Penfield (2008), while reviewing temperature perception and signal transduction in plants, stated that the timing of budbreak in woody perennials is poorly understood from a molecular level. Since then, buds have been the subject of many studies regarding dormancy control (Olukolu *et al.*, 2009; van Dyk *et al.*, 2010; Hedley *et al.*, 2010; Díaz-Riquelme *et al.*, 2012; Busov *et al.*, 2016; Sudawan *et al.*, 2016; Wu *et al.*, 2017;

Meitha *et al.*, 2018). However, these studies have not considered deacclimation aspects of budbreak, and how this may affect the recalcitrant phenotype of some genotypes.

Cold hardiness kinetics and budbreak phenology are tightly linked (Kovaleski *et al.*, 2018). *V. amurensis* and *V. riparia* are frequently used in breeding programs to increase cold hardiness of *V. vinifera* cultivars. However, *V. amurensis* and *V. riparia* have higher rates of deacclimation during the spring when compared to *V. vinifera* (Londo & Kovaleski, 2017; Kovaleski *et al.*, 2018). Comparisons between *Vitis* species could help identify the molecular drivers of cold hardiness and deacclimation. In addition, the quantitative nature of deacclimation also responds to chill accumulation (Kovaleski *et al.*, 2018). Therefore, understanding the genetic regulation of cold hardiness loss could elucidate some of the mechanisms that control dormancy in buds.

Low temperatures during the winter are the most important factor for plant distribution (Burke *et al.*, 1976). Perennial plants have to withstand these low temperatures in wood and other overwintering structures (i.e., buds), but a great number of studies have focused on chill or freeze stress in annual plants or actively growing tissues of perennial plants (Ruelland *et al.*, 2002; Li *et al.*, 2004; Nguyen *et al.*, 2017; Liu *et al.*, 2017b,a; Ban *et al.*, 2017; Londo *et al.*, 2018). Dehydration-responsive element-binding 1 (DREB1)/C-repeat-binding factors (CBF) genes are known to be elicitors of cold responsive genes, following low temperature perception (Liu *et al.*, 1998). Other stress related transcription factors [other DREBs, heat shock factors (HSFs), NAC and WRKY families] are also involved in the signaling, much of these shared between heat shock, drought, and biotic stresses (Liu *et al.*, 1998, 2017a; Birkenbihl *et al.*, 2012). However, responses may not be shared between actively growing and dormant tissues. The circadian clock is likely involved in the regulation of bud dormancy (Penfield, 2008; Cooke

et al., 2012), where low temperatures disrupt the circadian clock of woody perennials but not *Arabidopsis* (Ramos *et al.*, 2005). The regulation of budbreak has many parallel processes shared with germination (Penfield, 2008), such as signaling through hypoxia via ERFs regulation (Meitha *et al.*, 2018). Therefore, buds present the opportunity to study the unique condition of shared characteristics between growing and dormant tissues.

Although known to be central in senescence and dormancy, the role of abscisic acid (ABA) in bud dormancy is not fully understood (Cooke *et al.*, 2012). ABA promotes the induction of dormancy by blocking cell-cell communication (Tylewicz *et al.*, 2018). Exogenous ABA applications during the growing season have been shown to enhance hardiness earlier in the fall (Li & Dami, 2016), and budbreak can be delayed by ABA when applied in dormant buds (Zheng *et al.*, 2015). Considering recent evidence that budbreak phenology follows similar kinetics as deacclimation (Kovaleski *et al.*, 2018), it is possible that ABA acts on maintenance of the cold hardiness, rather than preventing growth itself.

The objective of this study was to understand the relationship between loss of cold hardiness and growth through regulation of the transcriptomic landscape in grapevine buds. The hypothesis regarding loss of cold hardiness and budbreak is that genotypes which have been observed to break bud early in the spring may have faster transcriptomic responses tied to growth and development when placed under forcing conditions. Differences between genotypes with rapid or slow phenology may be due to acceleration of gene regulation cascades, or acceleration of "bottleneck" genes which trigger specific regulatory cascades. This study leverages differences between species (*V. amurensis*, *V. riparia*, *V. vinifera*) and between cultivars (*V. vinifera* 'Cabernet Sauvignon' and 'Riesling') within species to uncover gene regulation during deacclimation. We expect that genes related to maintaining the cold hardy and dormant

phenotype will be quickly down-regulated in all genotypes; genes related to deacclimation will either be transiently expressed or have a slow increase, but mostly synchronized between genotypes; and genes related to growth and budbreak will be staggered. Further, we explore the use of ABA as a deacclimation inhibitor in grapevine buds.

Materials and Methods

Plant material

Canes of four different genotypes of grapevine were collected: two wild species, *V. amurensis* and *V. riparia*; and two cultivars of cultivated grapevines (*V. vinifera*), 'Cabernet Sauvignon' and 'Riesling'. Dormant canes were collected in late winter [February 2015; 1030 chill units (NC model; Shaltout & Unrath, 1983] and prepared into single node cuttings. The cuttings were placed in cups of water and into a growth room with forcing conditions: 22 °C and 16h/8h:light/dark.

Loss of cold hardiness and budbreak

Starting at day 0 (field samples), 8 buds were collected daily to estimate cold hardiness through differential thermal analysis (DTA; Mills *et al.*, 2006). Buds were cut from the cane and placed in sample trays equipped with thermoelectric modules and arranged into sample plates. These plates were placed in programmable freezers and subjected to decreasing temperatures at a rate of −4 °C/hour. The release of heat resulting from freezing of water inside the bud was measured as changes in voltage by the thermoeletric modules, and recorded using a Keithley data logger (Tektronix, Beaverton, OR) attached to a computer. In this analysis, a high temperature exotherm occurs in the vicinity of −5 °C and is non-lethal, while a low temperature exotherm happens below that temperature, and its occurrence is lethal to the bud. Phenology was visually assessed, and budbreak was noted to start when buds had reached stage 3 of the modified E-L scale (Coombe & Iland, 2005).

RNAseq Libraries and data analysis

Samples were collected daily for each genotype, with three replicates containing three buds each, until buds reached E-L stage 3 on day 10, 12, 15, and 17 for *V. amurensis*, *V. riparia*, 'Riesling', and 'Cabernet Sauvignon', respectively. Material was collected and frozen immediately with liquid nitrogen. Total RNA was extracted using Sigma Spectrum kits (Sigma-Aldrich, St. Louis, MO, USA), and strand-specific libraries were prepared. The libraries were multiplexed (25-plex) using unique barcode adapters (6 bp), and sequenced at 100 bp single-end reads on HiSeq 2500 (Illumina, Inc., San Diego, CA, USA).

Raw reads were de-multiplexed, and residual adapter and low quality sequences were removed. Quality reads were aligned to the *V. vinifera* 12xV2 genome and the V3 annotation (Canaguier *et al.*, 2017) using STAR (Dobin *et al.*, 2013). Uniquely aligned reads were quantified for all annotated genes using HTSeq (Anders *et al.*, 2015). A second set of libraries where prepared from extra tissue for those with initially low number of quality reads, when tissue was available.

Within each genotype, counts were normalized and grouped by days using the *edgeR* library in R (ver. 3.3.0, R Foundation for Statistical Computing). Multidimensional scaling and correlation plots were produced to visually verify outliers in the libraries. After outliers were removed, remaining data were analyzed using the *DESeq2* library (Love *et al.*, 2014) in R. In *DESeq2*, a full model containing a fourth order polynomial for time (t, in days) as a continuous variable and intercept, was compared to a null model of intercept only, using likelihood ratio test. Genes with an adjusted p-value < 0.10 were used for subsequent filtering. Using the parameter estimates extracted from *DESeq2*, predicted counts were calculated for the time span of each genotype's experiment (e.g., 0-10 days for *V. amurensis*, 0-17 days for *V. vinifera* 'Cabernet

Sauvignon'). Considering that counts for any given gene are a function of time, $CPM(t) = \beta_0 + \beta_1 t + \beta_2 t^2 + \beta_3 t^3 + \beta_4 t^4$, the filters used were: $max\{CPM(t) \mid 0 \le t \le t_f\} \ge 10$ (i.e., maximum predicted CPM >10), where t_f is the last time point for any given genotype (e.g., for 'Cabernet Sauvignon', t_f = 10); and $log_2\left(max\{CPM(t) \mid 0 \le t \le t_f\} / min\{CPM(t) \mid 0 \le t \le t_f\}\right) \ge 2$ (i.e., logFC ≥2). The remaining genes were considered to be relevant differentially expressed genes (DEGs).

Predicted logFC for each day calculated using *DESeq2* model estimates were used for cluster analysis of DEGs using Cluster 3.0 (ver. 3.0, Human Genome Center, University of Tokyo). Data were centered based on gene means, then on array means, followed by normalization by genes and arrays. Twenty *k*-Means clusters were used for genes, using Euclidian distances as the similarity metric, and 100 permutations. The average behavior of the genes placed in each cluster was visually inspected, and placed into 4 general categories: up-regulated, with relative expression increasing over time; down-regulated, with relative expression decreasing over time; transient expression, where peak expression occurred within the duration of the experiment; and random, where most of the clusters in this category had genes with a transient low expression within the duration of the experiment.

The produced list of DEGs for each genotype was used in VitisPathways for pathway enrichment analysis (Osier, 2016). VitisPathways uses the biological pathways and molecular functions from the Vitisnet database (Grimplet *et al.*, 2009). Enriched pathways were determined using 1000 permutations, and a permuted p-value of <0.10. Pathway enrichment analysis was conducted for each genotype using all DEGs, as well as DEGs in the up-regulated, down-regulated, and transient expression groups. Enriched pathways that were shared between genotypes were identified as pathways of interest. To observe trends in gene expression, genes encoding the same protein were aggregated, and mean expression was used for each day.

Qualitative comparisons of gene behavior were done on a relative basis, using the maximum mean counts within the duration of the experiment as 100%.

ABA treatment of single node cuttings

Single node cuttings of ecodormant *V. vinifera* 'Riesling' were collected from the field. The cuttings were placed in a growth chamber with average temperature of 7 ºC and a 0/24h light/dark photoperiod. ABA treatments were applied as the solution inside cups where cuttings were placed. Two concentrations were used, 1mM and 5mM. After 42 days, the cuttings were washed in running water, the bottom ~1 cm of the stems was cut, and the cuttings were placed in cups with water and moved to forcing conditions (22 °C, 16h/8h light/dark). Cold hardiness was measured using DTA, as previously described, twice a week for 8 weeks, or until LTEs were no longer detectable. Phenology was evaluated using the modified E-L scale (Coombe & Iland, 2005) until buds reached stage 8 (2 separated leaves).

Results

Deacclimation and budbreak

Both wild species had a higher initial cold hardiness upon collection from the field (−29.8 and −28.0 °C for *V. amurensis* and *V. riparia*, respectively) compared to *V. vinifera* genotypes (−23.4 and −23.9 °C for 'Cabernet Sauvignon' and 'Riesling', respectively; Fig. 3-1). The wild species also had higher deacclimation rates than the two *V. vinifera* genotypes (2.87, 2.81, 1.76, and 1.58 °C day^{-1} for *V. amurensis*, *V. riparia*, and *V. vinifera* 'Cab. Sauvignon' and 'Riesling', respectively). Budbreak occurred latest on *V. vinifera* genotypes, starting at 13 days and spanning through day 17 for 'Riesling' and 'Cabernet Sauvignon'. Budbreak under forcing conditions occurred after 8 days in *V. amurensis* and 10 days for *V. riparia*.

Analysis of Differential Gene Expression

The number of DEGs for all genotypes ranged from 8326 (*V. riparia*) to 9123 (*V. vinifera* 'Cabernet Sauvignon'; Fig. 3-2). DEGs uniquely expressed in each species were 1348 for *V. amurensis*, 1006 for *V. riparia*, and 2232 for *V. vinifera* ('Cabernet Sauvignon' + 'Riesling'). The majority of DEGs, 4551, were shared among all four genotypes. When grouping by specific behaviors, 1065 DEGs of the up-regulated and 1192 DEGs of the down-regulated genes were shared by all 4 genotypes.

As a limitation to available analysis tools in grapevine and in order to perform pathway enrichment analysis using VitisPathways, annotations were back converted to the V1 annotation designations. In this process, some genes in the V2 annotation were unable to be assigned to specific pathways, but datasets kept between 92.3% and 93.7% of the DEGs. There were 21 enriched pathways when all genes were queried, 22 for genes with down-regulated patterns, 15 for up-regulated patterns, and 5 for transient patterns that were shared among all genotypes (Table 3-1). Overall, there were 43 enriched pathways that were shared among the 4 genotypes: 16 were defined as associated with Metabolism, 4 with Environmental Information Processing, 2 with Cellular Processes, 4 with Transport, and 17 with Transcription Factors.

Abscisic acid (ABA), ethylene, cytokinin, and auxin related pathways were the plant hormone related pathways that were enriched. ABA biosynthesis and signaling pathways were enriched with genes showing a general down-regulation trend. Ethylene signaling was enriched with down-regulated and transiently expressed genes, while auxin-related pathways appeared in up-regulated and transient expression. Zeatin biosynthesis, involved in cytokinin-related pathways, appeared enriched when all DEGs were used in VitisPathways. Carotenoid biosynthesis, which leads to ABA biosynthesis, was also enriched for down-regulated genes. Photosynthesis related pathways (e.g., photosynthesis antenna proteins and transport electron

carriers) were enriched when genes with a general up-regulation were used for pathway enrichment analysis. This was also the case for fatty acid biosynthesis, cell cycle, and regulation of actin cytoskeleton pathways.

Within ABA biosynthesis, zeaxanthin epoxidase (ZEP) and 9-cis-epoxycarotenoid dioxygenase (NCED), which lead to the synthesis of ABA, were quickly down-regulated once buds were moved into warm conditions for all genotypes (Fig. 3-3). ABA 8'-hydroxylase (ABA8'OH), which breaks down ABA, was also down-regulated. ABA glucosidase (ABA BG), which re-activates ABA bound to glucose esters in the vacuole, had an initial decrease in transcripts, followed by strong up-regulation. For ABA signaling, AREB2 and KEG genes were down-regulated. AREB2 appears to be very synchronized between genotypes, while the expression of KEG is reduced at a faster rate in the wild species than in *V. vinifera*. Both ABI1 and ABR1 appear to have transient expressions. ABR1 is quickly up-regulated in day 1 for all genotypes, and then expression is reduced over time. ABI1 is initially down-regulated, followed by another peak of expression, and then expression is lowered again. MARD1 and Phospholipase D (PLD) are both generally up-regulated.

ACC oxidase and ACC synthase, which participate in the synthesis of ethylene, had peak expression after placement in warm conditions, or a temporary up-regulation (Fig. 3-4). E8, however, was up-regulated in all genotypes. Although not enriched, key components of jasmonate and gibberellin (GA) synthesis pathways were observed (Fig. 3-5). For jasmonate, it appears that the synthesis is down-regulated, as seen by 12-oxophytodienoate reductase (OPR), with precursors being led to medium chain fatty acids via up-regulation of lipoxygenase. MEJAE, which converts methyl-jasmonate to jasmonic acid (JA), is down-regulated, whereas Jasmonate-O-methyltransferase, which catalyzes the reaction in the opposite direction, is up-

regulated. For GAs, the expression of GA-44 dioxygenase appears to not change much over time, GA-3 β-dioxygenase is up-regulated in all genotypes, while GA-2 β-dioxygenase is down-regulated.

Indole-3-acetic acid-amino acid hydrolases (IAA-AA-hydrolases), which reactivates IAA, was up-regulated in all genotypes, reaching maximum expression earlier in *V. amurensis* than other genotypes (Fig. 3-6). IAA6, IAA19, ARF5 and AUX1 were up-regulated, with relative expression increasing faster in *V. amurensis* than other genotypes. PIN1 was down-regulated over time for all genotypes, while PIN3 was up-regulated. Cytokinin dehydrogenase (CKX) was up-regulated for all genotypes, while PUP1, a cytokinin transporter, was down-regulated (Fig. 3-7). ARR11 was down-regulated, and ARR17 was up-regulated.

CIR1, ELF3, CCA1, APR5, and Catalase CAT3, from the circadian rhythm pathway were down-regulated in all genotypes (Fig. 3-8). CIR1, ELF3, and APR5 had a strong down-regulation in the first few days, whereas CCA1 and CAT3 reduced in a slower rate. The nitrogen metabolism shows that NH_3 conversion to nitrile or nitrite is down-regulated, while the production of amino acids (Gly and Glu) is up-regulated (Fig. 3-9). In the phenylpropanoid biosynthesis pathway, phenylalanine ammonia lyase was initially down-regulated, followed by up-regulation that happens earlier in *V. amurensis*, followed by *V. riparia*, and the *V. vinifera* genotypes (Fig. 3-10). Trihydroxystilbene synthase (stilbene synthase) was quickly down-regulated in all genotypes, but faster in the wild species than *V. vinifera*. Of the 44 predicted genes for stilbene synthase, between 29 and 35 were differentially expressed towards down-regulation for all genotypes. The genes encoding catechol oxidase, the enzyme which leads L-tyrosine to a different path, is up-regulated. DODA is down-regulated, indicating that betalamic acid or betanin production is not the fate of L-tyrosine.

Starch and Glycogen [starch] synthases, and beta amylase are down-regulated (Fig. 3-11). However, Glycogen [starch] synthase and beta amylase are synchronized in all genotypes, whereas starch synthase reduces its expression earlier in the wild genotypes. Sucrose synthase is initially down-regulated in all genotypes, while a return to high levels of expression is seen in *V. riparia* and *V. vinifera*, but not in *V. amurensis*. Fructokinase and hexokinase are generally up-regulated in all genotypes.

Genes related to cell expansion and cell division (cyclins and cytoskeleton proteins) were up-regulated and staggered in accordance to species: *V. amurensis*, followed by *V. riparia*, and *V. vinifera* (Fig. 3-7). Within the cell cycle pathway, cyclin D was up-regulated earlier compared to cyclins A and B for all genotypes. Similarly, genes in the fatty acid biosynthesis pathway were generally up-regulated over time (Fig. 3-12). FAD5, however, was strongly down-regulated for all genotypes.

In photosynthesis related pathways, light harvesting complex I (LHCI) and II (LHCII) and photosystem I (PSI) subunits also follow the trend of growth related genes, with earlier up-regulation in wild species (Fig. 3-13). RBOHB (all genotypes) and RBOHE (all but *V. riparia*) had a transient up regulation in the earlier days. RBOHF was also up-regulated in the first few days, returning to ~50% relative expression. RBOHD appeared to have an increasing expression trend.

Ethylene signaling, which includes Ethylene Responsive Factors (ERFs), WRKY, and HSF pathways were enriched when down-regulated genes were used for pathway enrichment analysis. ERFs were generally down-regulated (DDF2, DREB2C, DREB2E, DREB2F, ETR2, RAP2-11), but some were up-regulated (CRF4 and EREBP4; Fig. 3-4). WRKY6-1, WRKY6-3, WRKY33-1, WRKY33-3, and WRKY75-1 were down-regulated (Fig. 3-14). HSFB4-1 and

HSFB4-2 were up-regulated, while HSFA4A-3, HSFA8, and HSFC1 were down-regulated in all genotypes (Fig. 3-15). HSFA6B-2 is generally down-regulated, but shows a transient up-regulation in the two *V. vinifera* genotypes. Vacuole localize aquaporins TIP3;1 and TIP3;2 were down-regulated, while TIP1;3 and TIP4;1 were up-regulated (Fig. 3-16). CNGC15 was down-regulated in all genotypes.

ABA effects on cold hardiness

ABA had no effect on cold hardiness until 16 days post application (Fig. 3-17). Starting on day 20, both ABA treatments prevented further loss of cold hardiness, whereas deacclimation continued in the water control treatment. A light gain in hardiness appears to occur in ABA treated buds, although this was not tested statistically. Upon washing of the canes, pruning of the bottom part, and move to 22 ºC at 42 days, previously ABA treated buds started losing hardiness. When looking at the phenology, non-treated buds reached budbreak (E-L stage 3) at ~50 days after the beginning of the experiment. For 1mM ABA, budbreak occurred at ~75 days, while buds in 5mM did not resume growth before the end of the experiment at 84 days.

Discussion

Deacclimation and growth are processes that occur in tandem, although most or all of the cold hardiness is lost before growth is visible. The processes are different in nature: deacclimation is to some extent reversible, whereas growth is by definition irreversible. However, it is important to acknowledge that some of the aspects of both processes, such as the influx of water leading to cell turgor and reorganization of the cytoskeleton, are shared. This is the first study exploring long-term RNA-Seq data for the exploration of genes and pathways important for each of these processes. A novel approach for time-series data analysis is used, and the use of species of contrasting phenotypes allows for hypotheses that explore the genes that are

likely related to the cold hardy, dormant phenotype, those related to growth and budbreak, and those that may be shared between both.

The approach used for data analysis in this study was important to detect many trends in the long term RNA-Seq data for differential expression. Here we treated time as a continuous variable, modeling counts with a fourth degree polynomial to allow transient expression of genes to be properly predicted, and using the predicted counts for filtering. Meitha *et al.* (2018) also reported data collected from grapevine (*V. vinifera* 'Crimson Seedless') buds in a budbreak experiment. In their study, budbreak occurred within 7-10 days, and RNA-Seq samples were collected at 0h, 3h, 24h (1 day), 72h (3 days), and 144h (6 days). The authors analyzed the data using pairwise comparisons between adjacent time points. While discrete comparisons may yield genes that have extreme changes in expression between time points, our approach acknowledges that some genes may slowly change in expression over time. This might explain the orders of magnitude difference in the number of DEGs found by Meitha *et al.* (2018) in comparison to the present study. It is clear that many of the DEGs in our study would not be considered significantly DE if we analyzed our data such as in Meitha *et al.* (2018). Additionally, the differences in time between sampling points (3h difference vs. 21h and so on) also advocate towards the use of time as a continuous variable. Fu *et al.* (2018) used a similar approach to that of Meitha *et al.* (2018), evaluating seeds of two genotypes of *Elymus nutans* under forcing conditions after cold stress. Fu *et al.* (2018) collected samples at 0h, 3h, 24h, and 120h (5d) under forcing conditions. Differently from Meitha *et al.* (2018), their pairwise comparisons were between each time point and 0h (control) within each genotype, which may be more appropriate for genes that have a slow increase, and may result in a larger number of DEGs (Díaz-Riquelme *et al.*, 2012). While the approach in Meitha *et al.* (2018) would more likely detect genes with

transient expression or genes with extreme changes in expression, and the approach of Fu *et al.* (2018) might miss genes that have a peak following the first time point, and then an abrupt decrease in expression (or vice-versa), our approach makes no assumption as to when maximum and minimum expression levels for any given gene occur.

Sampling within a 24h period following treatment can also result in the detection of "false" DEGs due to circadian oscillations in genes (Grundy *et al.*, 2015). In our case, samples were always taken within a 3h window in the day. Samplings that do not follow regular intervals could benefit from using time as a continuous variable and sine/cosine functions that may elucidate some of the variation in gene expression due to their natural daily oscillation. Therefore, using continuous variables for RNA-Seq studies with more than 3 data points might be more appropriate.

The change in environment that buds are exposed to in our experiment likely resulted in temperature sensing transcriptional changes, followed by those related to loss of cold hardiness, ultimately leading to growth. Membrane rigidity has long been suggested as the most upstream temperature sensor for thermal signaling (Horváth *et al.*, 1998, 2012; Saidi *et al.*, 2010; Bahuguna & Jagadish, 2015). The fast down-regulation of FAD5 observed demonstrates this quick response to excessive fluidity of membranes caused by the move from low temperatures (field, average temperature of −7 °C) to high above freezing temperatures (22 °C), likely leading to an increase in the content of saturated fatty acids in the membrane (Wallis & Browse, 2002; Falcone *et al.*, 2004). In general, the biosynthesis of fatty acids is up-regulated, with a trend towards synthesis of saturated fatty acids, as indicated by the up-regulation of 3-hydroxyacyl dehydrase, likely further decreasing the fluidity of membranes (Filek *et al.*, 2017). At higher

temperatures, a membrane with more saturated fatty acids would have the appropriate fluidity to maintain integrity and avoid electrolyte leakage (Holmstrup & Slotsbo, 2018).

Ca^{2+} signaling has been implicated in bud dormancy release (Pang *et al.*, 2007). Bahuguna & Jagadish (2015) review the importance of cyclic nucleotide-gated ion channels (CNGCs) in thermosensing as channel proteins for Ca^{2+} signaling. Although plasma membrane localized CNGCs have more clear roles in cold sensing (Bahuguna & Jagadish, 2015), down-regulation of CNGC15 was detected in all genotypes in the present study, which is a CNGC localized to the nucleus (DeFalco *et al.*, 2016). This indicates that in grapevine buds, Ca^{2+} stored in the nuclear envelope lumen or endoplasmic reticulum may be transported into the nucleus (DeFalco *et al.*, 2016), and not only Ca^{2+} influx from the apoplast (Bahuguna & Jagadish, 2015), may play a role in calcium signaling during the dormant period. The down-regulation of this gene also indicates that the Ca^{2+} signaling is relieved during the loss of hardiness and resumption of growth.

Regulation of circadian clock genes is important for abiotic stress tolerance (Grundy *et al.*, 2015), and alternative splicing has been indicated as a mechanism of signaling in response to low temperature (Calixto *et al.*, 2016). Most of the genes in the circadian rhythm pathway were down-regulated. Both CCA1 and its promoter CIR1 are down-regulated in all genotypes. CCA1 is a TF that regulates low temperature responses through the control of CBF gene expression (Grundy *et al.*, 2015), and also represses TOC1 expression. The higher expression of CCA1 in the field may be causing a disruption of the circadian clock, as observed by Ramos *et al.* (2005) in *Castanea sativa*. CIR1 also triggers the expression of CAT3, which is itself down-regulated. Catalases are important antioxidant enzymes, and the decrease in their activity during dormancy release may result in the temporary increase of ROS (i.e., H_2O_2) that precedes budbreak (Pérez &

Lira, 2005; Khalil-Ur-Rehman *et al.*, 2017). H_2O_2 is also involved in the regulation of cold-responsive genes expression during acclimation (Fedurayev *et al.*, 2018), demonstrating contrasting roles. ELF3, an inhibitor of PHYA and PHYB, is down-regulated, although neither PHYA or PHYB are differentially expressed. The release of the repression on PHYA and PHYB expression, however, may be important for further action during regulation of flowering (Andrés & Coupland, 2012). APRR5, also involved in flowering time and development controlled by light signaling (Sato *et al.*, 2002; Yamamoto *et al.*, 2003), was down-regulated. Altogether, it appears that some circadian clock genes may be required at a higher level of expression during the dormant period in order to properly maintain the circadian rhythm without strong effects of day length or light.

PLD has been observed to be up-regulated during cold and freezing stress (Ruelland *et al.*, 2002) as well as many other stress conditions (Meijer & Munnik, 2003), and is indicated as a signaling protein in thermal sensing (Bahuguna & Jagadish, 2015). PLD activity is Ca^{2+} dependent (Meijer & Munnik, 2003), and Ca^{2+} influx during cold stress lead to activation of PLD (Wang & Nick, 2017). Overexpression of PLD results in higher freezing tolerance (Li *et al.*, 2004), and more rapid and sensitive response to ABA and stress (Sang *et al.*, 2001; Meijer & Munnik, 2003). Considering our treatment can be seen as a release from cold stress, but PLD expression increased, we speculate that the effects of PLD in cold stress relief signaling are likely related to the changes in plasma membrane composition. PLD activity also has an effect on cytoskeleton reorganization – a temperature sensing process (Nick, 2008; Shimono *et al.*, 2016). Similarly, β-tubulin has been described as a QTL associated with budbreak (Hedley *et al.*, 2010). Therefore, early changes in cytoskeleton related proteins might be due to changes in cold hardiness. In this experiment, PLD regulation appears to follow a two-step up-regulation. An

initial up-regulation is synchronous among all 4 genotypes, which may be related to the signaling effects of PLD. However, the earlier up-regulation that follows in *V. amurensis* compared to the other genotypes likely indicates its effect on membrane remodeling through selective hydrolysis of membrane phospholipids (Wang, 1999).

ROS participate in temperature sensing and signaling. The down-regulation of TIP3 genes can result in accumulation of ROS, considering they participate in H_2O_2 diffusion (Mao & Sun, 2015). Some NADPH oxidases (RBOHB, RBOHE, and RBOHF) had transient up-regulations in the first few days of exposure to warm temperatures, which may indicate their role in inducing budbreak. However, ROS scavengers, such as betalains and trihydroxystilbene (resveratrol) are also involved in stress signaling. An interesting aspect in this study is the observation of strong down-regulation of stilbene synthase, as well as DODA, in the phenylpropanoid biosynthesis pathway. This indicates a different fate for L-tyrosine other than that of the production of trihydroxystilbene (resveratrol) or betalains during warming. Stilbene synthase has previously been described by Londo *et al.* (2018) as up-regulated in grapevine leaves during cold or freeze stress, but is also involved in other types of stress during the growing season (Carvalho *et al.*, 2015). Chalcone synthase, an enzyme similar to stilbene synthase (Melchior & Kindl, 1990), was up-regulated in white spruce due to wounding and jasmonate application (Richard *et al.*, 2000). The phenylpropanoid biosynthesis KEGG pathway, which may lead to synthesis of resveratrol, was enriched in cold tolerant *Passiflora edulis* (Liu *et al.*, 2017a) and ecodormant *Pyrus pyrifolia* (Bai *et al.*, 2013). The very strong and quick down-regulation of the majority of genes encoding for stilbene synthase in all 4 genotypes indicates that resveratrol may be an important molecule for maintaining cold hardiness. For DODA, there is an interesting up-regulation from day 0 to day 1 in all 4 genotypes. This phenotype may be

related to the control of ROS that form when buds are exposed to warm temperatures and lead to the budbreak process (Pérez & Lira, 2005). The presence of ROS scavengers may be an important control in the loss of cold hardiness cascades that lead to budbreak in case of mid-winter warming events. Regulation of these genes could therefore also be related to chill accumulation and dormancy state.

In our experiment, following the sensing of warm temperatures, it was expected that a decrease in cold-related transcription factors would occur. Interestingly, none of the DREB1 homologs (CBFs) were differentially expressed, regardless of CCA1 down-regulation. Alternatively, DREB2 homologs were differentially expressed and down-regulated. This is in disagreement with Liu *et al.* (1998) and Nguyen *et al.* (2017), who suggested DREB1 and DREB2 are two independent DREB families that lead to signal transduction pathways for low temperature and dehydration conditions, respectively. It is possible that CBFs are involved in the gain of cold hardiness and in response to cold stress (Liu *et al.*, 2017a; Ban *et al.*, 2017), but are not maintained in a high level of transcription throughout the winter. This way, when buds were moved into forcing conditions, down-regulation of these transcripts was not detected.

HSFs are transcription factors involved in heat shock and drought responses (Czarnecka-Verner *et al.*, 2000; Dossa *et al.*, 2016). In this study, HSFA transcripts were down-regulated over time, whereas HSFBs were up-regulated. Class A HSFs are responsible for activation of stress induced heat shock genes, while class B HSFs are likely repressors of the heat shock response (Czarnecka-Verner *et al.*, 2000). The expression pattern seen in HSFs here gives further evidence that plants responding to cold stress may perceive cold as drought stress, perhaps due to the decreased water potential caused by extracellular ice during supercooling (George & Burke, 1977).

WRKY6, WRKY33, and WRKY75 are involved in several types of stress response, such as high temperature, salt, Pi deficiency, wounding (Devaiah *et al.*, 2007; Skibbe *et al.*, 2008; Chen *et al.*, 2009; Li *et al.*, 2011). Perhaps most importantly in this case, all three WRKY family TFs have been described to be up-regulated in oxidative stress when exposed to ROS (Davletova *et al.*, 2005; Jiang *et al.*, 2017). These TFs also interact with hormone signaling: WRKY6 is a positive regulator of ABA signaling (Huang *et al.*, 2016), while WRKY33 regulates components of SA and JA pathways during *Botrytis cinerea* infection (Birkenbihl *et al.*, 2012).

ABA biosynthesis is a requirement for cold acclimation and thermotolerance (Gilmour & Thomashow, 1991; Larkindale *et al.*, 2005; Penfield, 2008), and ABA is a clear antagonist of the loss of cold hardiness and growth. Both the biosynthesis and the signaling pathways appear enriched with down-regulated genes in this study. The pivotal role of the reduction in ABA synthesis for the loss of hardiness appears very clear when looking at gene expression data. Both ZEP and especially NCED, the rate-limiting enzyme in ABA biosynthesis (Grundy et al., 2015), are quickly down-regulated in all genotypes, indicating that carotenoids are likely no longer moving toward the synthesis of new ABA during deacclimation. The down-regulation of NCED is also supported by the observation that DREB2C was down-regulated, as DREB2C positively regulates the expression of NCED (Je *et al.*, 2014). A decrease in NCED transcripts was also observed in *Pyrus pyrifolia* flower buds when transitioning from endo- to ecodormant floral buds (Bai *et al.*, 2013) further supporting the role of ABA in dormancy processes. ABR1, an AP2 TF repressor of ABA response (Pandey *et al.*, 2005), is quickly up-regulated from day 0 to the highest relative level of expression in all genotypes at day 1, indicating the move to warm temperatures quickly signals for reduction of ABA synthesis as well as repression of ABA responses from the present pool. ABA BH, which re-activates the inactive pool of ABA-glu-ester

is up-regulated, while the degradation of ABA is down-regulated. This could indicate that initially, ABA levels may not be reduced despite reduction in signaling for synthesis. Supporting the role of ABA concentration as a limiting aspect of deacclimation, high ABA concentrations were seen to halt the loss of cold hardiness in this study. This provides some evidence that a lag in the loss of cold hardiness would have been expected if concentration of ABA was maintained by ABA BH acting on the inactive ABA pool during warming, which did not occur. It is possible that the reactivated ABA is going into signaling such as that of MARD1, which promotes genes related to seed germination. Future studies should examine the fates and concentrations of newly synthesized ABA and reactivated ABA during deacclimation.

Control of water status during the winter is critical for cell survival (George & Burke, 1977), and aquaporins may be important during exposure to low temperatures (Bilska-Kos *et al.*, 2016). The expression of TIP3;1 and TIP3;2 aquaporins is regulated by ABA through ABI3 (Mao & Sun, 2015). Although ABI3 was not differentially expressed in our study, the down-regulation of TIP3s (TIP3;1, *V. vinifera*; TIP3;2, all genotypes) opposed the general up-regulation of aquaporins (e.g., TIP1;3 and TIP4;1). This demonstrates that ABA may be affecting water movement in the bud during the dormant season, positively influencing cold hardiness. This regulation during the dormant season, when low temperatures are common, is likely important to maintain the equilibrium in water potential while there is extracellular ice under negative temperatures. Although located in the vacuole, TIP aquaporins may contribute to water flow from cell to cell, considering the difference in area available for flow in the vacuole as compared to the cytoplasm (Pou *et al.*, 2013).

The pathways leading to ethylene biosynthesis appears to be transiently up-regulated in the first few days of warm period in this study. This may be due to the antagonistic effect of

ABA on the synthesis of ethylene, and the quick reduction of ABA synthesis following move to forcing conditions. Ethylene, along with H_2O_2, lead to the activation of antioxidative stress genes in grapevine (Vergara *et al.*, 2012). The synthesis of jasmonates is likely decreased over time as seen by the down-regulation of OPR. This is in agreement with Li *et al.* (2016), where cold acclimation lead to up-regulation of jasmonic acid biosynthesis in *Camellia japonica*. Additionally, the decrease in expression of MEJAE over time and increase in expression of Jasmonate-O-methyltransferase indicate that methyl-jasmonate may be the preferred jasmonate during budbreak. This is similar to what was described by Bai *et al.* (2013), where jasmonate O-methyltransferase was up-regulated in eco- compared to endodormant buds. Bai *et al.* (2013) also reported down-regulation of GA2 beta dioxygenase. We also observed a down-regulation of GA2 beta dioxygenase, and an up-regulation of GA3 beta dioxygenase, while the upstream GA44-dioxygenase maintained similar levels through the whole experiment. This suggests the control of bioactive GA levels may actually be by GA 2 beta dioxygenase during dormancy transition (Bai *et al.*, 2013), and by both GA-3 beta dioxygenase and GA-2 beta dioxygenase during budbreak.

Since the growth phenotype (budbreak) was staggered in the different species, we expected that genes related to growth would also appear staggered. Cytokinin signaling appears to indicate that cell division is being promoted. CKX, which degrades cytokinins, is being up-regulated, as well as TFs that lead to the repression of the cytokinin responses. The transport of cytokinins also appears to be down-regulated over time (i.e., PUP1). Each of these patters suggest a potential decrease in the expression of TFs that elicit cytokinin responses, such as ARR11. In result, we see a clear up-regulation of cyclins, which are involved in the signaling of the different phases of cell division. There is a clear staggering in the down-regulation of PUP1

and ARR11, where expression levels are lowered earlier in the wild species as compared to *V. vinifera*. This is likely influencing the staggered expression of cyclins in the three species, and further, cytoskeleton proteins related to growth. For all of these proteins we see *V. amurensis* clearly has an earlier up-regulation, followed by *V. riparia*, and the two *V. vinifera* genotypes. This is in line with the observed difference in timing of budbreak of the three species. In addition, the expression of the three cyclins, D, A, and B, which are expressed at different times during the cell division cycle following a specific order (Mironov *et al.*, 1999), can be used as a gauge of the data collection: in all of the genotypes, cyclin D is up-regulated first, then followed by cyclin A, and further by cyclin B. The initially very low expression of both cyclin A and B indicates that these are only expressed after cold hardiness is lost.

Sugar metabolism plays an important role both for signaling and for energy. Genes in carbohydrate metabolism likely have significant roles during the dormancy period in grapevine buds (Khalil-Ur-Rehman *et al.*, 2017). In the synthesis and metabolism of sugars, the synthesis of starch is down-regulated. Enzymes in the degradation of starch are also generally down-regulated, although expression levels of alpha amylase are kept higher for a longer period of time, using starch as a source of simple carbohydrates. Sucrose synthase is also initially down-regulated in all genotypes, but returns to higher levels of expression in *V. riparia* and in the two *V. vinifera* genotypes. Sucrose can aid in maintaining the structure of proteins during freeze events (Fediuk *et al.*, 2017). In contrast, fructokinase and hexokinase are both up-regulated, indicating that the pools of sugar are being used in glycolysis to generate energy. The up-regulation of Enoyl CoA hydratase and Acetyl CoA c-Acyltransferase in the fatty acid metabolism indicates that energy is also being produced from free fatty acids such as those resulting from the degradation of phospholipids by PLD (Wang, 1999).

Our results demonstrate that exogenous ABA prevents loss of cold hardiness during deacclimation, with no return to the initial cold hardiness, and delays budbreak. Zheng *et al.* (2015) also demonstrated that ABA treatments delay budbreak of grapevine buds, although those authors did not evaluate cold hardiness. In their study, budbreak promoters such as hydrogen cyanamide and hypoxia resulted in faster budbreak compared to non-treated buds. This would suggest that these promoters may also increase the rate of deacclimation (Kovaleski *et al.*, 2018) through an increase in ROS or decrease in antioxidants and antioxidant enzymes activity, and therefore comparative studies using ABA and budbreak promoters using RNA-Seq could be helpful for understanding the machinery that leads to the loss of cold hardiness. ABA may also be an alternative for field application to prevent loss of cold hardiness during midwinter warming events, or delay budbreak in areas prone to late frosts, although further studies are warranted.

Conclusion

As RNA-Seq and other genetics-based technologies become increasingly cheaper, datasets will continue increasing in size, and we must find new ways to deal with these data. In this study, we describe a new way to deal with time-series data such that a single list of DEGs is produced from all time-points, although further development in this area is required. Most of the DEGs and mechanisms explored in this study have been previously described elsewhere. While RNA Seq data is only correlational, here we have shown indications of a great number of processes that have been tested in an array of different plants to likely be occurring in the *Vitis* species examined. We attempted to separate the genes that are related to cold hardiness and the loss of it (deacclimation), the release of dormancy, and budbreak, by exploring phenotypic or temporal differences in the genotypes used. Our results also indicate that loss of cold hardiness is not only the opposite of gain of hardiness, and molecular processes involved (e.g., PLD regulation) are not only in reverse mode. Moreover, we tested the effect of exogenous ABA in

deacclimating buds, which halted the loss of cold hardiness and prevented budbreak, further demonstrating that loss of hardiness is required for budbreak (Kovaleski *et al.*, 2018). This also confirms that ABA and its signaling are upstream from what defines cold hardiness, or the loss of it, in buds that go through supercooling.

Table 3-1. Enriched Vitisnet pathways shared among *V. amurensis*, *V. riparia*, and *V. vinifera* 'Cabernet Sauvignon' and 'Riesling' during deacclimation and budbreak. Pathway enrichment analysis was conducted in VitisPathways using all differentially expressed genes (DEGs), as well as DEGs in the up-regulated, down-regulated, and transient expression groups.

All DEGs	Down-regulated	Up-regulated	Transient
Fatty acid biosynthesis	Galactose metabolism	Fatty acid biosynthesis	Fatty acid metabolism
Photosynthesis antenna proteins	Tyrosine metabolism	Photosynthesis	Anthocyanin biosynthesis
Tyrosine metabolism	Glutathione metabolism	Photosynthesis antenna proteins	Auxin signaling
Zeatin biosynthesis	Starch and sucrose metabolism	Flavonoid biosynthesis	Ethylene signaling
ABA signaling	Inositol phosphate metabolism	Cell cycle	Auxin transport
Auxin Transport	Carotenoid biosynthesis	Regulation of actin cytoskeleton	
Transport electrol carriers	Nitrogen metabolism	Auxin transport	
Thylakoid targeting pathway	Phenylpropanoid biosynthesis	Transport electron carriers	
AP2-EREBP	ABA biosynthesis	Thylakoid targeting pathway	
AUXIAA	ABA signaling	Porters cat7 to 17	
BZIP	Ethylene signaling	BHLH	
C2C2-DOF	Circadian rhythm	C2C2-GATA	
C2C2-GATA	AP2-EREBP	C2C2-YABBY	
C2C2-YABBY	C2C2-DOF	MYB	
GRAS	DBP	OFP	
HSF	GRAS		
NAC	HSF		
TCP	MYB		
Orphans zf-b box	NAC		
OFP	WRKY		
	Orphans zf-b box		
	Other zf-C3HC4		

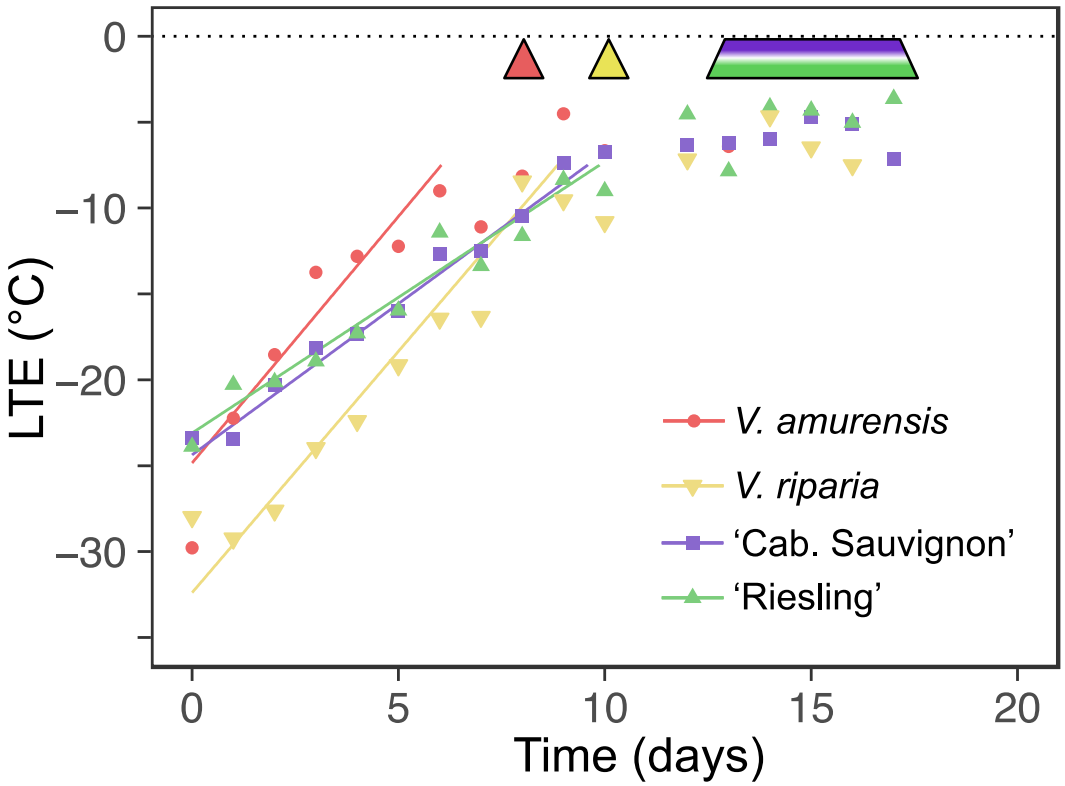

Figure 3-1. Cold hardiness and budbreak of *V. amurensis*, *V. riparia*, and *V. vinifera* 'Cabernet Sauvignon' and 'Riesling'. Cold hardiness, indicated by symbols and predicted linear deacclimation for each genotype. Arrow heads (*V. amurensis* and *V. riparia*) or trapezoid (*V. vinifera*) at 0 °C line indicate timing of budbreak (E-L stage 3; Coombe & Iland, 2005).

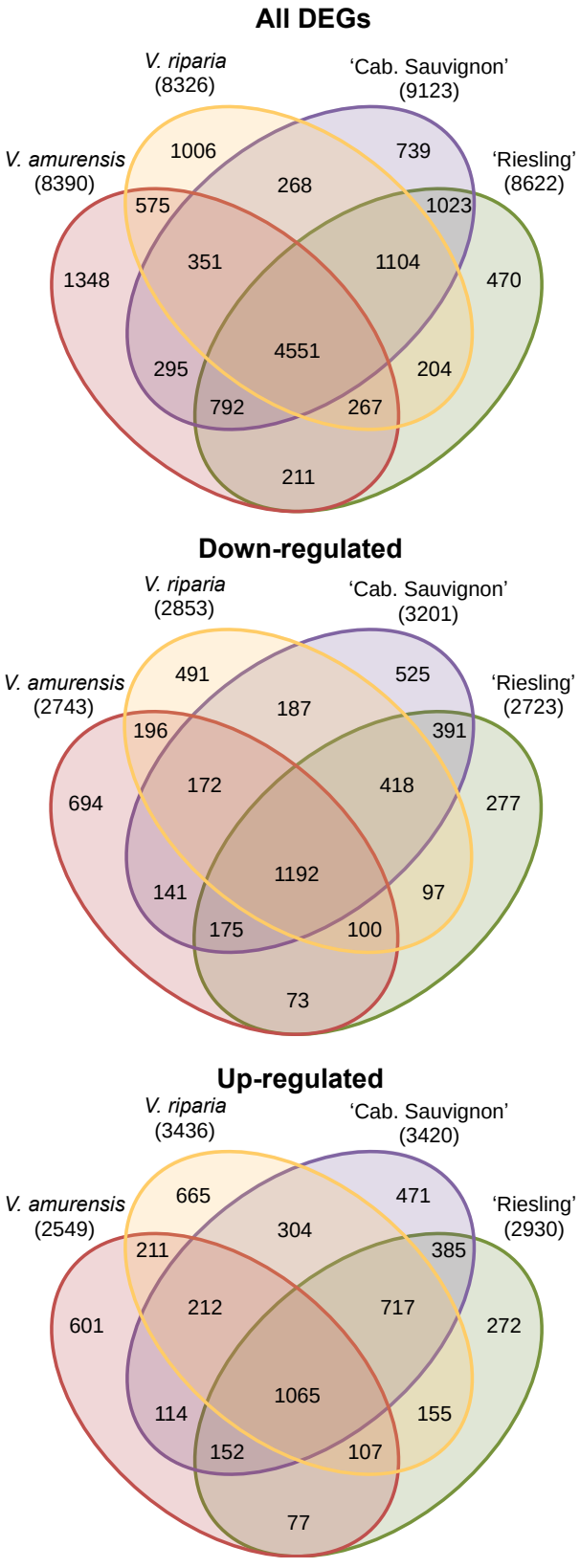

Figure 3-2. Venn diagrams of shared differentially expressed genes (DEGs) between *V. amurensis* (red), *V. riparia* (yellow), and *V. vinifera* 'Cabernet Sauvignon' (purple) and 'Riesling' (green) during deacclimation and budbreak. Venn diagrams were produced using all DEGs, down-regulated, and up-regulated genes.

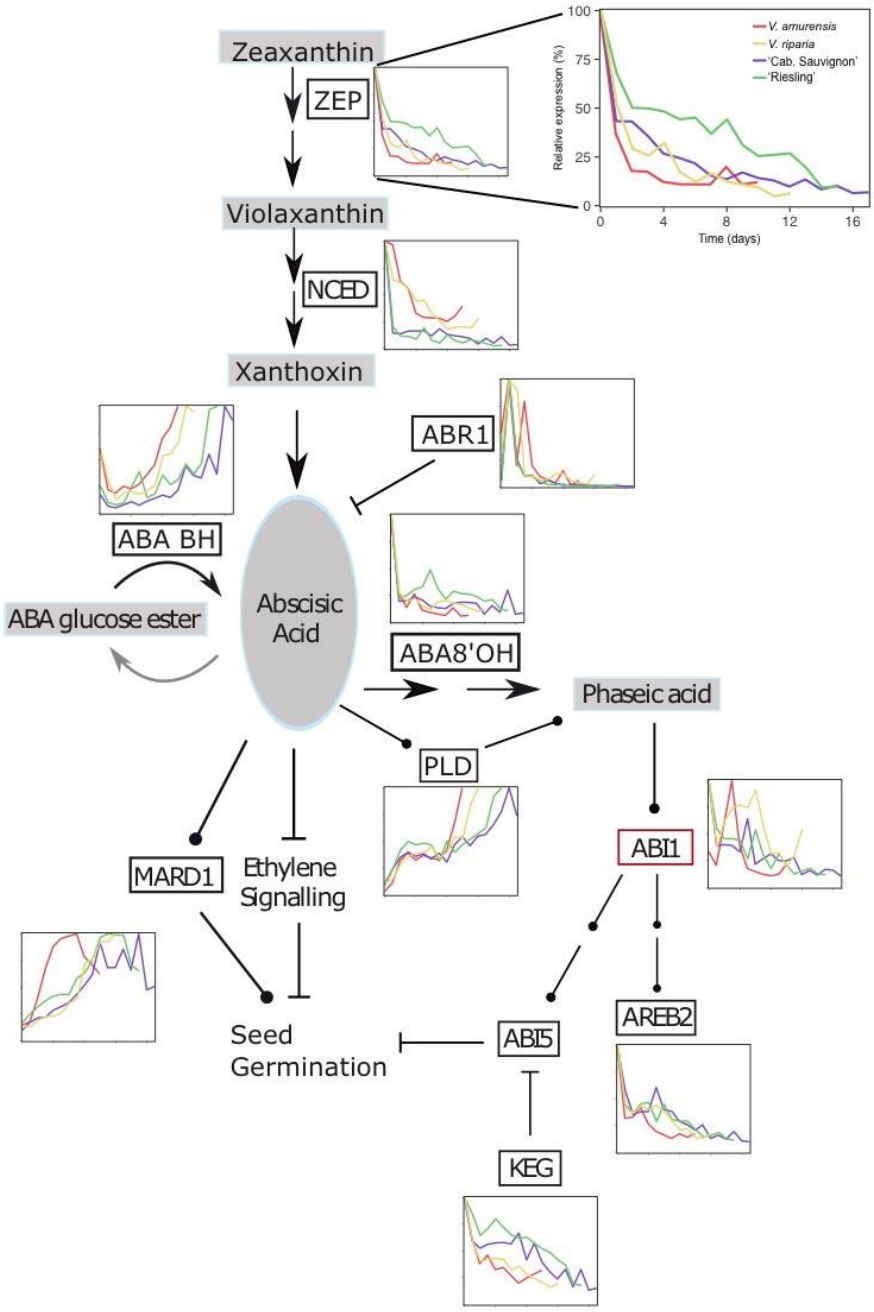

Figure 3-3. Reduced Vitisnet ABA biosynthesis and signaling pathway. Mini-graphs indicate relative level of expression of any given protein for *V. amurensis* (red), *V. riparia* (yellow), and *V. vinifera* 'Cabernet Sauvignon' (purple) and 'Riesling' (green) during deacclimation and budbreak. Multiple DEGs encoding for the same protein had their expression pooled. Arrows indicate transition; circular arrows indicate positive regulation; and "T" indicates negative regulation. Multiple arrows indicate transition or signaling steps omitted. Detail shows expanded graph for axis information.

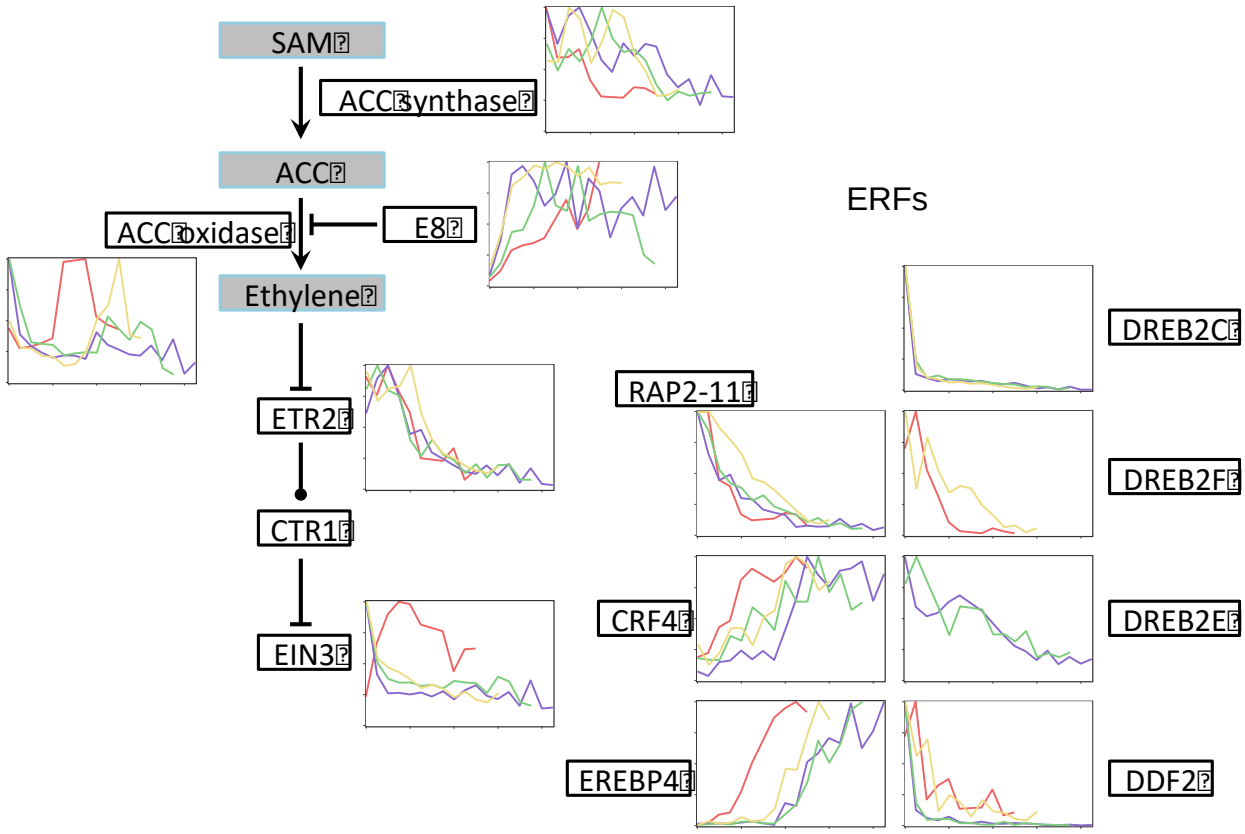

Figure 3-4. Reduced Vitisnet ethylene biosynthesis and signaling pathway, and ethylene response factors (ERFs). Mini-graphs indicate relative level of expression of any given protein for *V. amurensis* (red), *V. riparia* (yellow), and *V. vinifera* 'Cabernet Sauvignon' (purple) and 'Riesling' (green) during deacclimation and budbreak. Multiple DEGs encoding for the same protein had their expression pooled. Arrows indicate transition; circular arrows indicate positive regulation; and "T" indicates negative regulation. Multiple arrows indicate transition or signaling steps omitted.

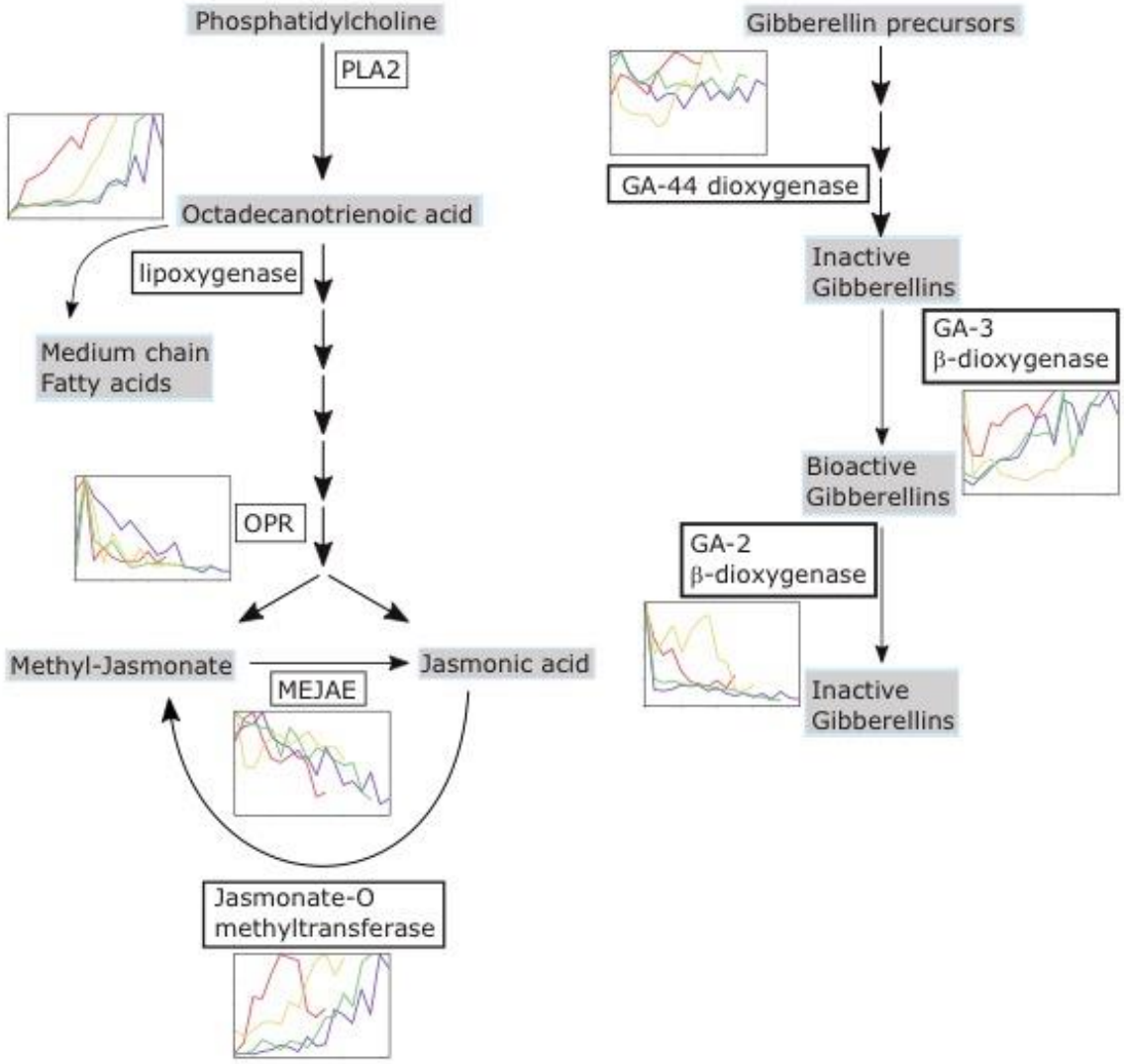

Figure 3-5. Reduced Vitisnet Jasmonic Acid and Giberellin biosynthesis pathways. Mini-graphs indicate relative level of expression of any given protein for *V. amurensis* (red), *V. riparia* (yellow), and *V. vinifera* 'Cabernet Sauvignon' (purple) and 'Riesling' (green) during deacclimation and budbreak. Multiple DEGs encoding for the same protein had their expression pooled. Arrows indicate transition; circular arrows indicate positive regulation; and "T" indicates negative regulation. Multiple arrows indicate transition or signaling steps omitted.

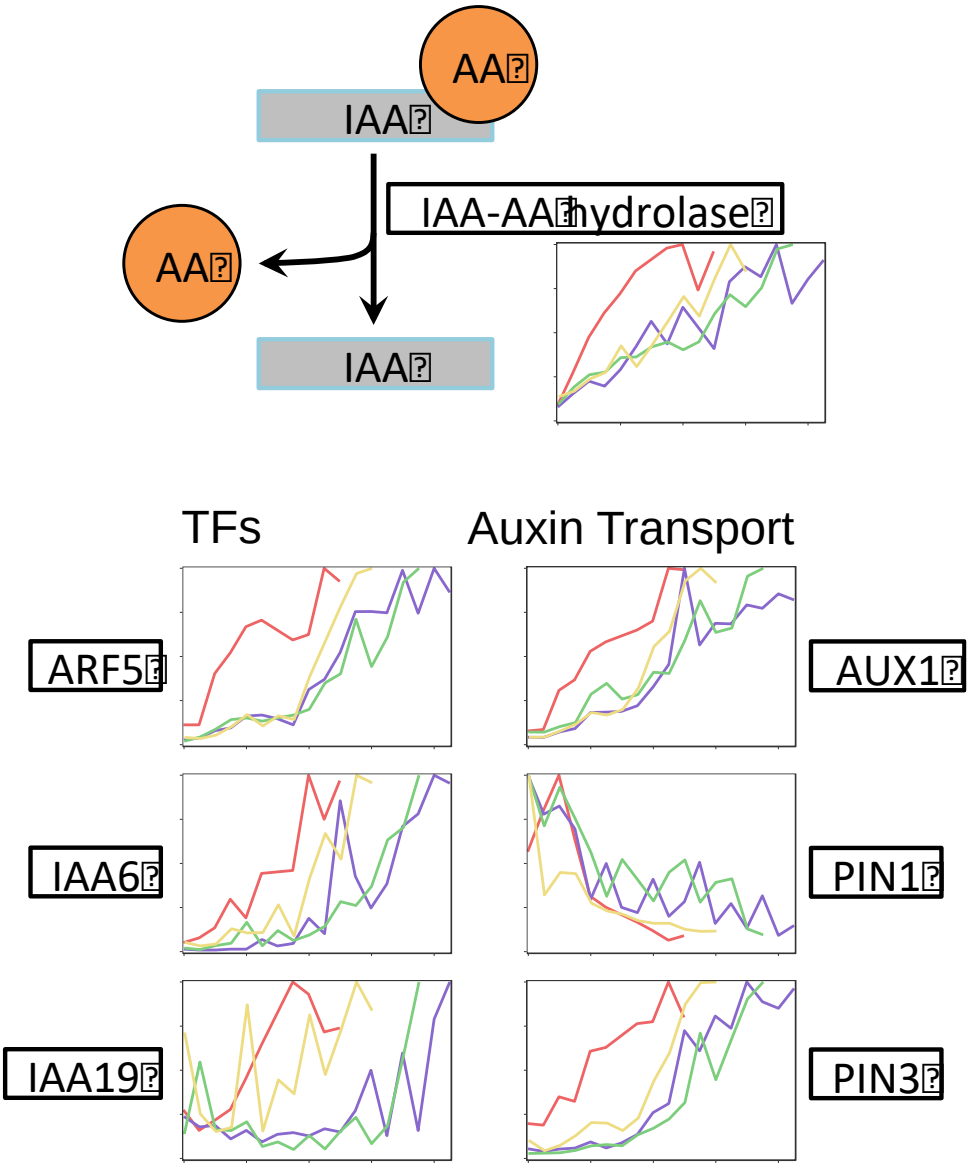

Figure 3-6. Reduced Vitisnet auxin biosynthesis pathway and auxin-regulated transcription factors (TFs) and transport-related genes. Mini-graphs indicate relative level of expression of any given protein for *V. amurensis* (red), *V. riparia* (yellow), and *V. vinifera* 'Cabernet Sauvignon' (purple) and 'Riesling' (green) during deacclimation and budbreak. Multiple DEGs encoding for the same protein had their expression pooled. Arrows indicate transition; circular arrows indicate positive regulation; and "T" indicates negative regulation. Multiple arrows indicate transition or signaling steps omitted.

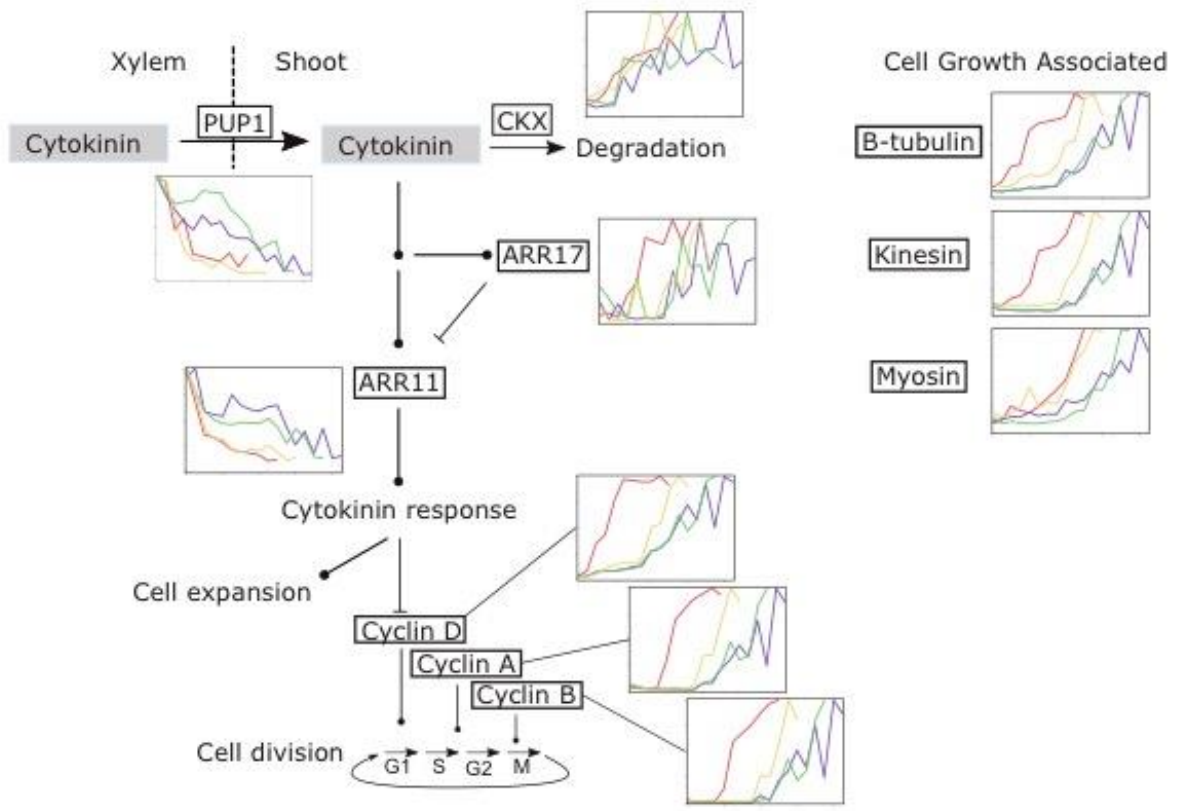

Figure 3-7. Reduced Vitisnet cytokinin biosynthesis and signaling pathway, and growth associated genes. Mini-graphs indicate relative level of expression of any given protein for *V. amurensis* (red), *V. riparia* (yellow), and *V. vinifera* 'Cabernet Sauvignon' (purple) and 'Riesling' (green) during deacclimation and budbreak. Multiple DEGs encoding for the same protein had their expression pooled. Arrows indicate transition; circular arrows indicate positive regulation; and "T" indicates negative regulation. Multiple arrows indicate transition or signaling steps omitted.

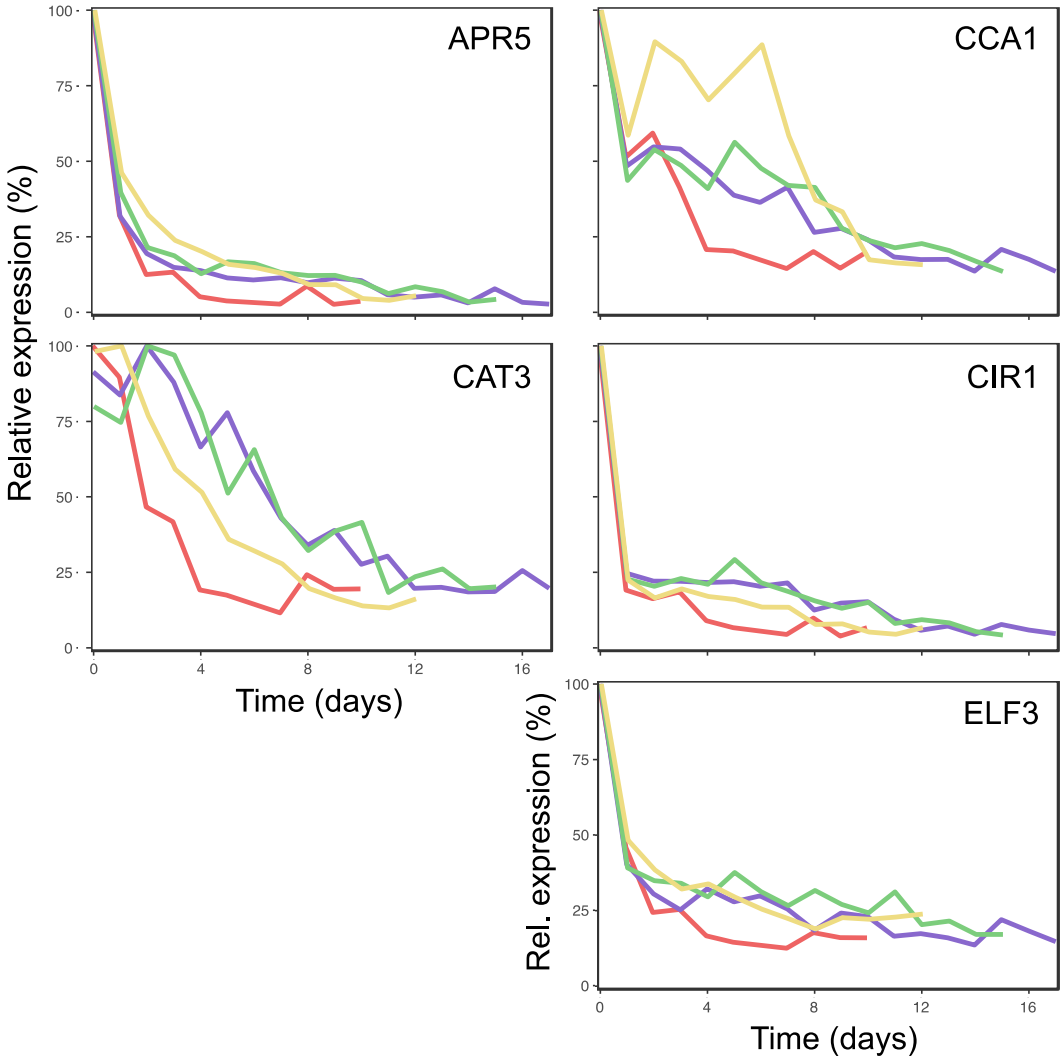

Figure 3-8. Relative expression of genes in the Vitisnet circadian rhythm pathway during deacclimation and budbreak in *V. amurensis* (red), *V. riparia* (yellow), and *V. vinifera* 'Cabernet Sauvignon' (purple) and 'Riesling' (green).

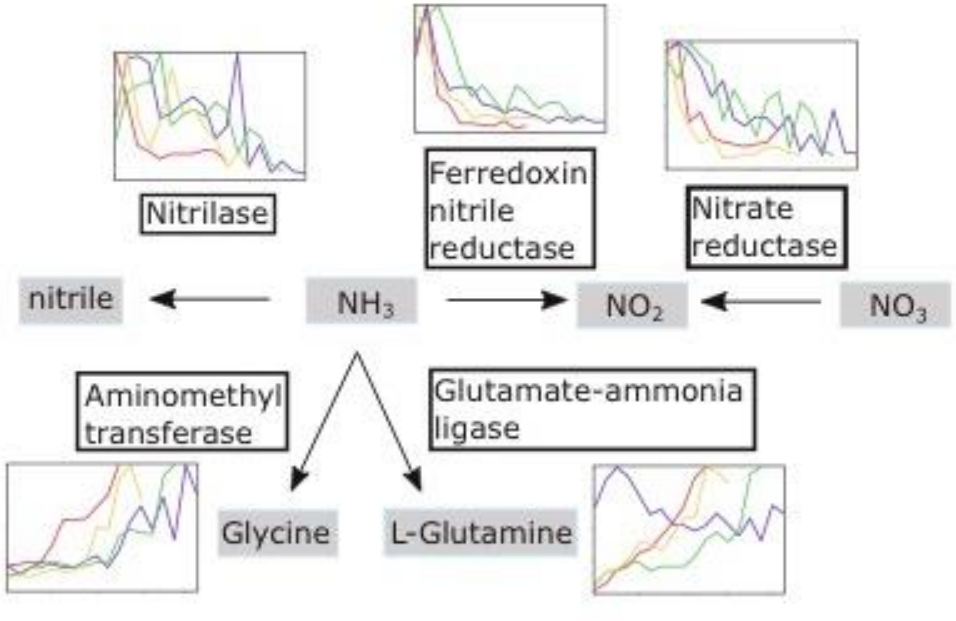

Figure 3-9. Reduced Vitisnet nitrogen metabolism pathway. Mini-graphs indicate relative level of expression of any given protein for *V. amurensis* (red), *V. riparia* (yellow), and *V. vinifera* 'Cabernet Sauvignon' (purple) and 'Riesling' (green) during deacclimation and budbreak. Multiple DEGs encoding for the same protein had their expression pooled. Arrows indicate transition.

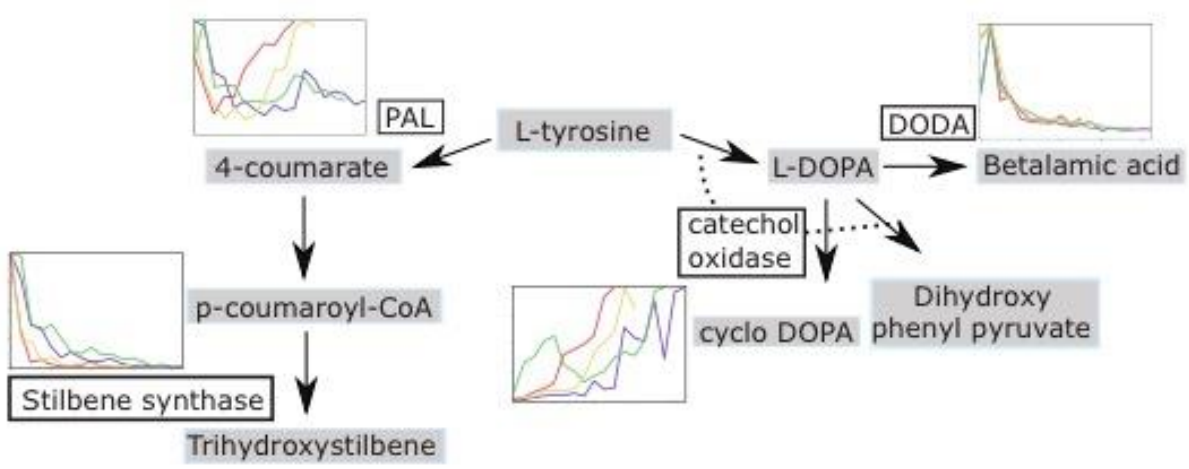

Figure 3-10. Reduced Vitisnet phenylpropanoid biosynthesis pathway. Mini-graphs indicate relative level of expression of any given protein for *V. amurensis* (red), *V. riparia* (yellow), and *V. vinifera* 'Cabernet Sauvignon' (purple) and 'Riesling' (green) during deacclimation and budbreak. Multiple DEGs encoding for the same protein had their expression pooled. Arrows indicate transition; circular arrows indicate positive regulation; and "T" indicates negative regulation. Multiple arrows indicate transition or signaling steps omitted.

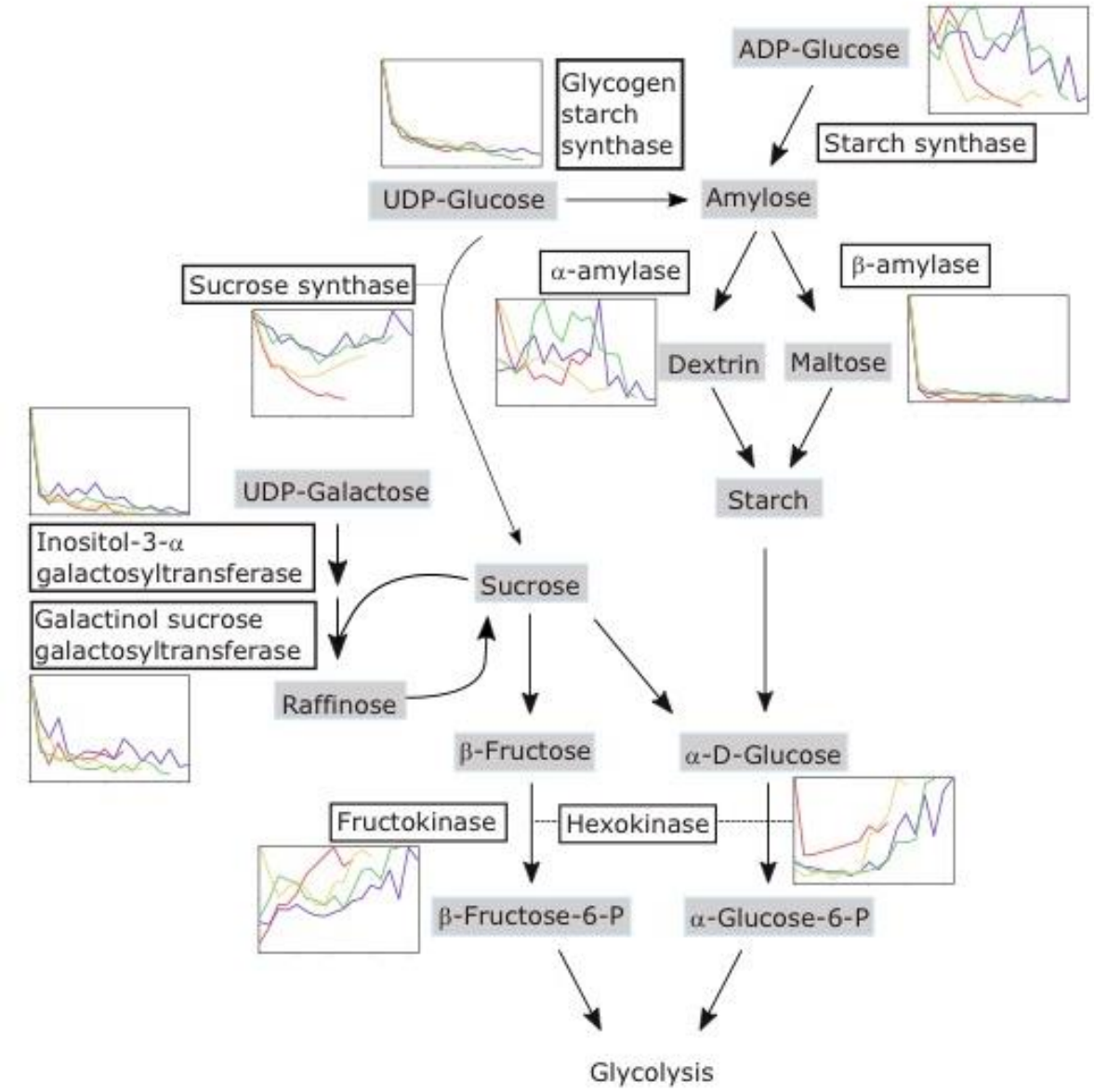

Figure 3-11. Reduced Vitisnet starch, sucrose, and galactose metabolism pathways. Mini-graphs indicate relative level of expression of any given protein for *V. amurensis* (red), *V. riparia* (yellow), and *V. vinifera* 'Cabernet Sauvignon' (purple) and 'Riesling' (green) during deacclimation and budbreak. Multiple DEGs encoding for the same protein had their expression pooled. Arrows indicate transition; circular arrows indicate positive regulation; and "T" indicates negative regulation. Multiple arrows indicate transition or signaling steps omitted.

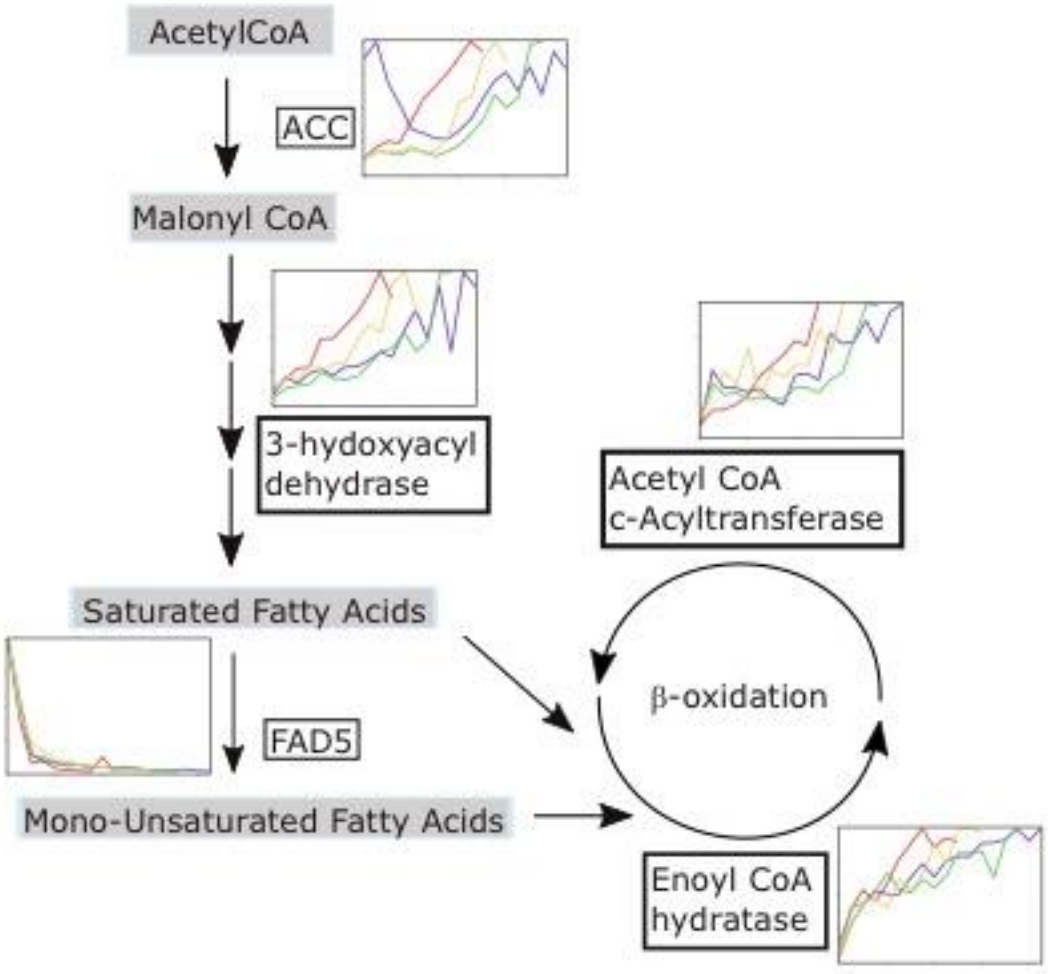

Figure 3-12. Reduced Vitisnet fatty acids synthesis and metabolism pathway. Mini-graphs indicate relative level of expression of any given protein for *V. amurensis* (red), *V. riparia* (yellow), and *V. vinifera* 'Cabernet Sauvignon' (purple) and 'Riesling' (green) during deacclimation and budbreak. Multiple DEGs encoding for the same protein had their expression pooled. Arrows indicate transition; circular arrows indicate positive regulation; and "T" indicates negative regulation. Multiple arrows indicate transition or signaling steps omitted.

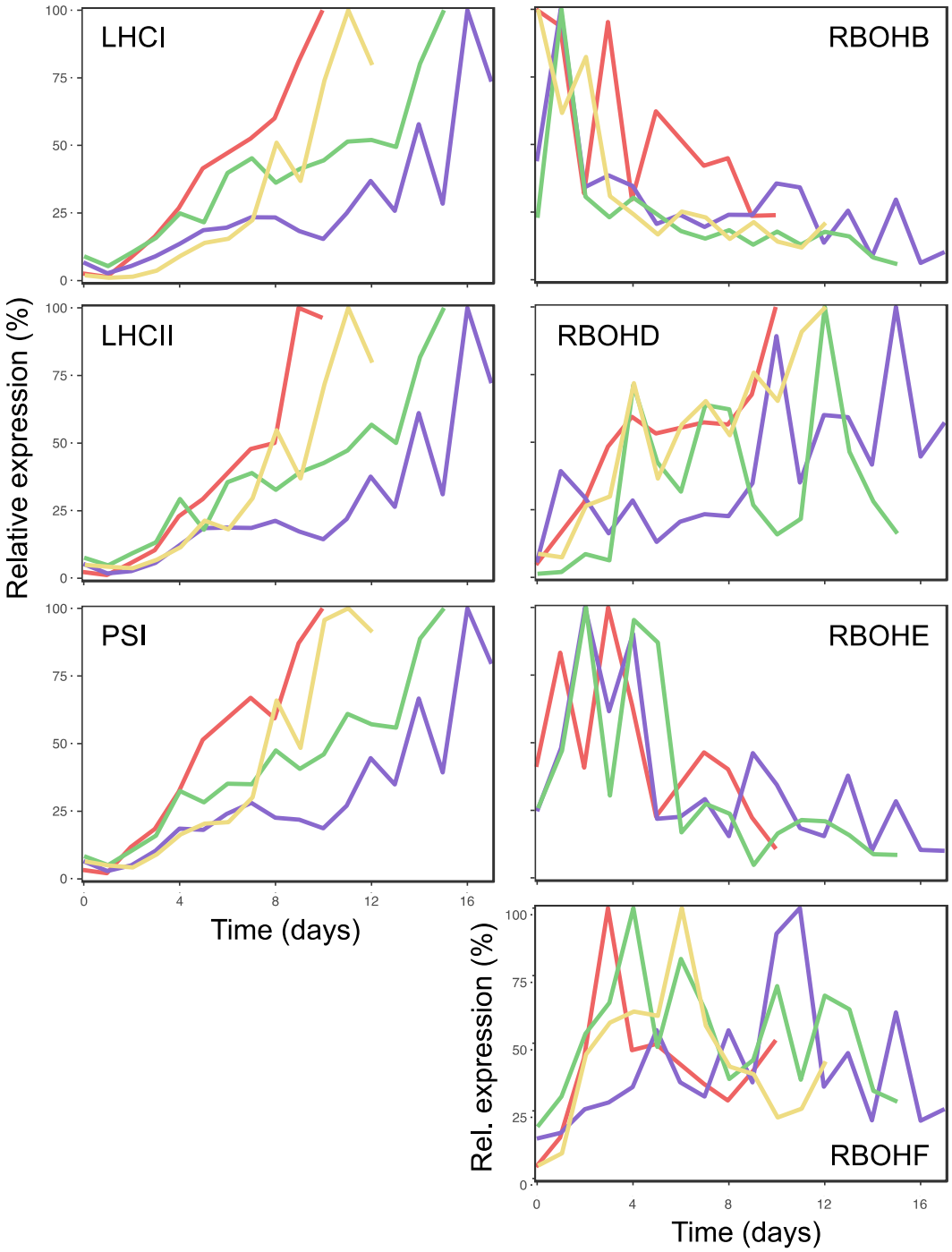

Figure 3-13. Relative expression of genes in the Vitisnet photosynthesis antenna proteins and transport electron carriers pathways during deacclimation and budbreak in *V. amurensis* (red), *V. riparia* (yellow), and *V. vinifera* 'Cabernet Sauvignon' (purple) and 'Riesling' (green).

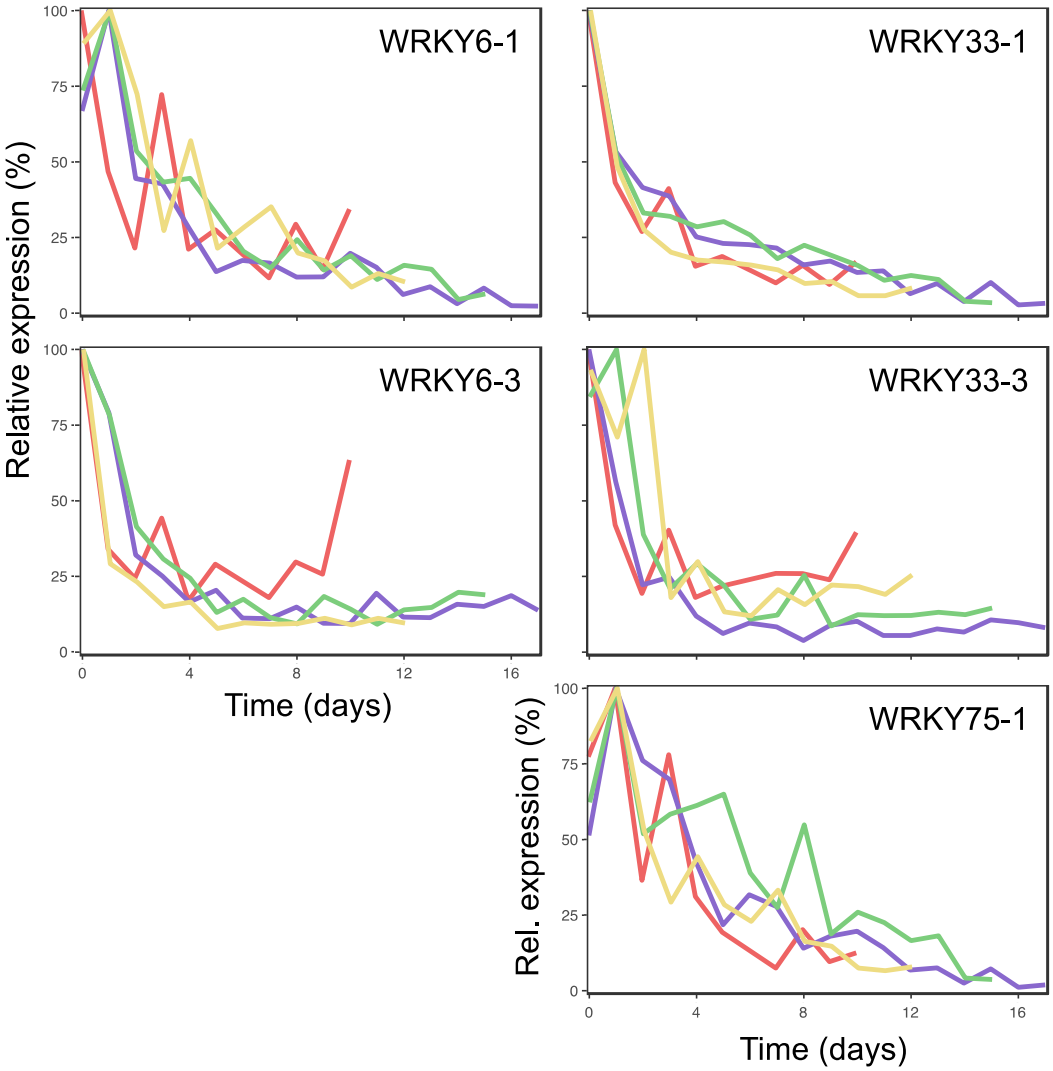

Figure 3-14. Relative expression of genes in the WRKY family of transcription factors during deacclimation and budbreak in *V. amurensis* (red), *V. riparia* (yellow), and *V. vinifera* 'Cabernet Sauvignon' (purple) and 'Riesling' (green).

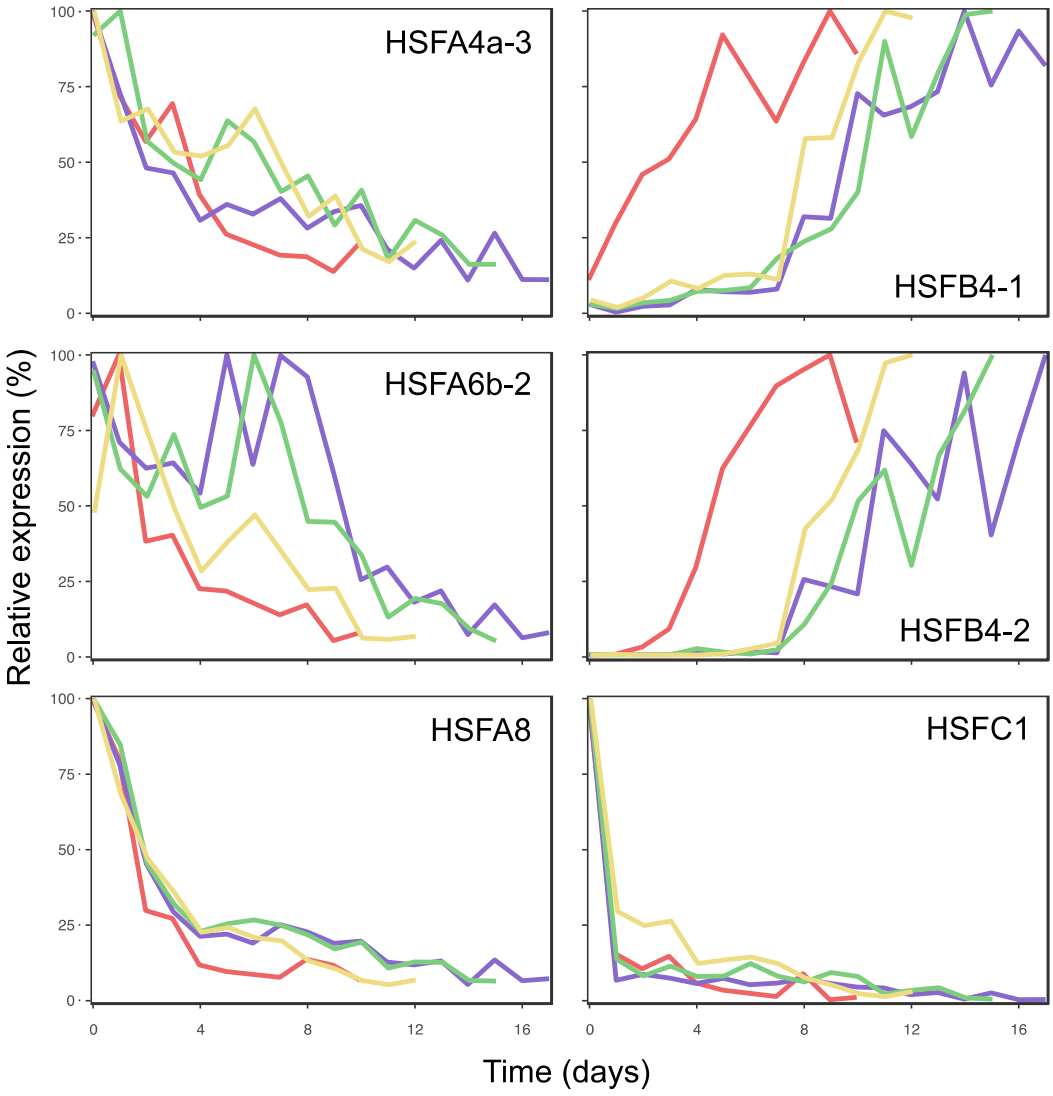

Figure 3-15. Relative expression of genes in the HSF family of transcription factors during deacclimation and budbreak in *V. amurensis* (red), *V. riparia* (yellow), and *V. vinifera* 'Cabernet Sauvignon' (purple) and 'Riesling' (green).

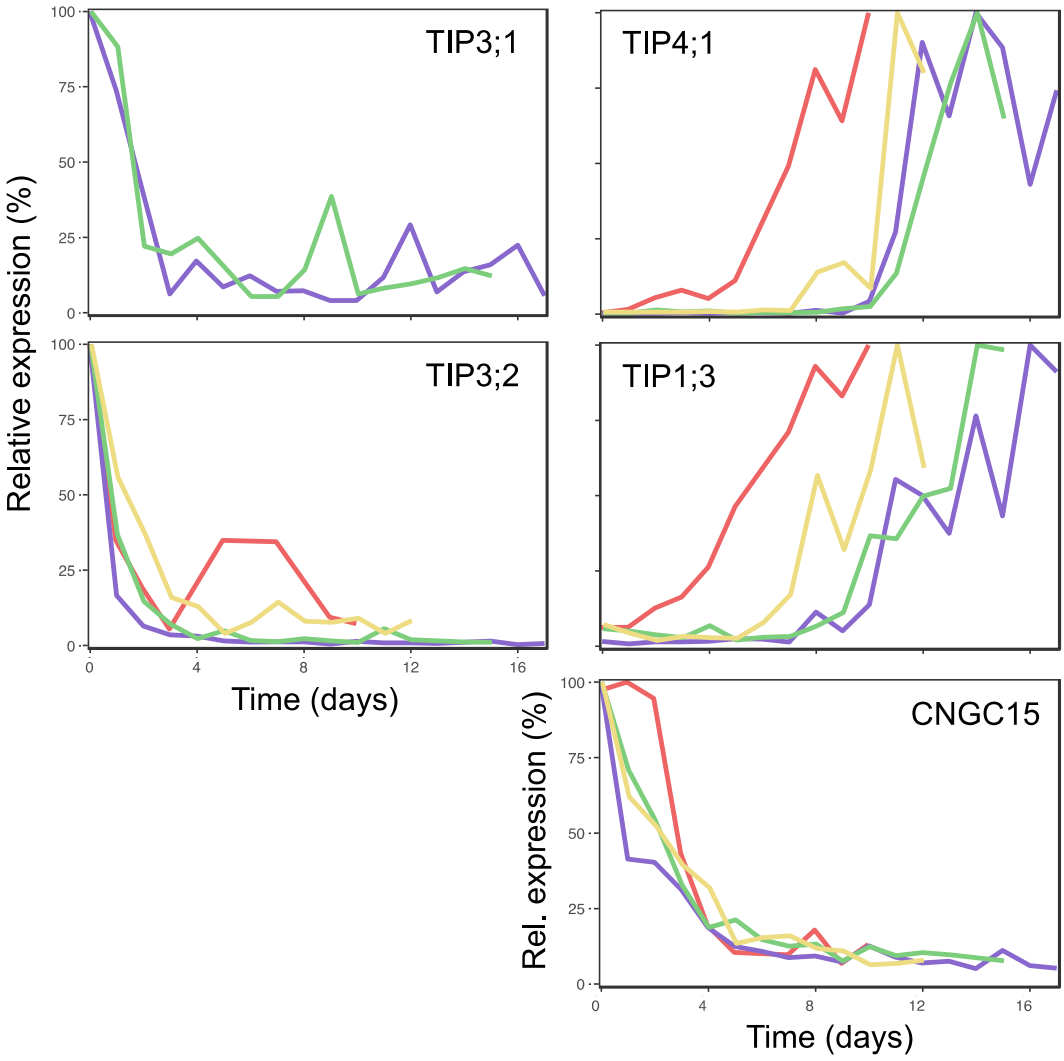

Figure 3-16. Relative expression of channel protein genes during deacclimation and budbreak in *V. amurensis* (red), *V. riparia* (yellow), and *V. vinifera* 'Cabernet Sauvignon' (purple) and 'Riesling' (green).

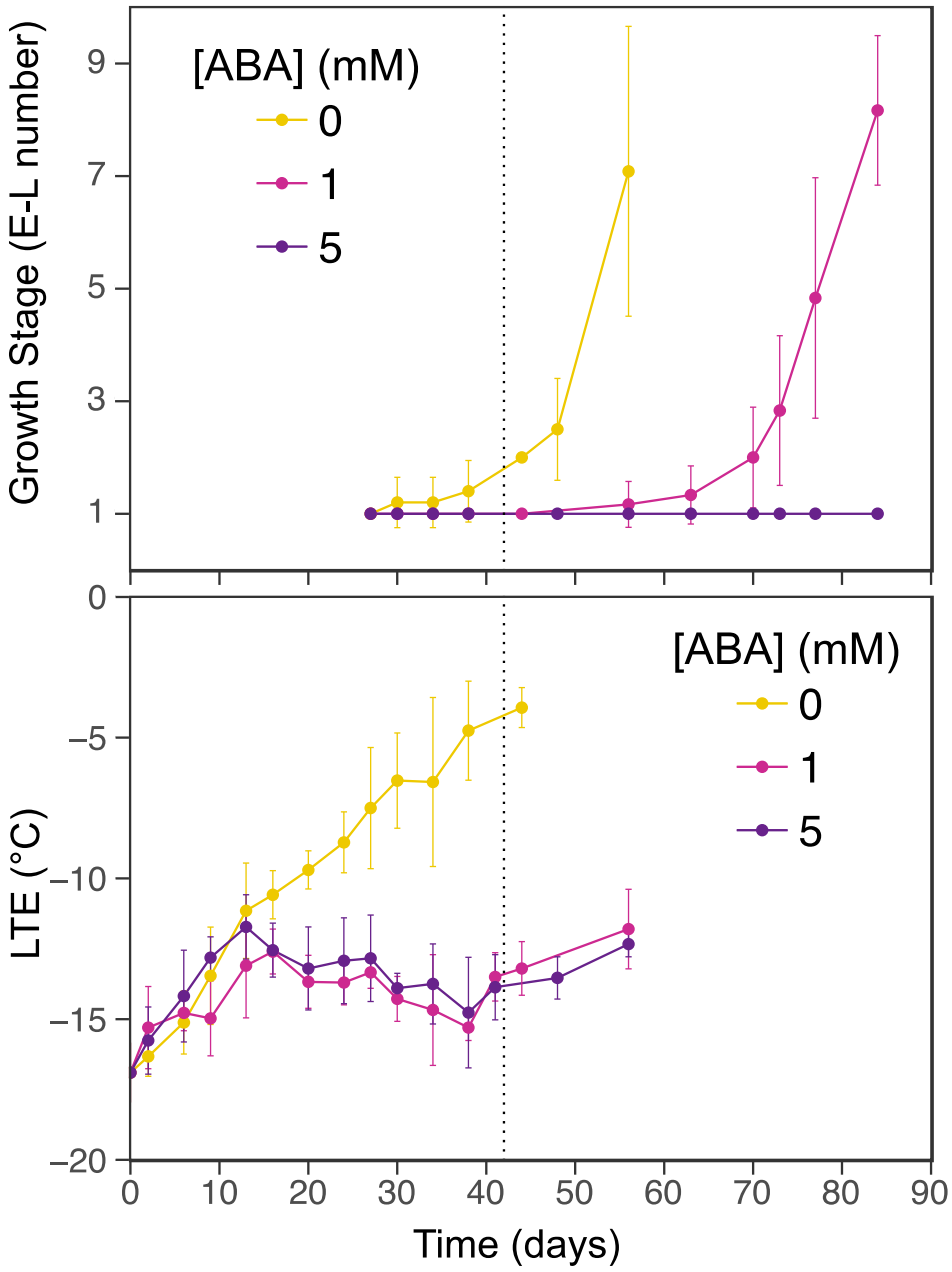

Figure 3-17. Stage of development (E-L number; Coombe & Iland, 2005) and cold hardiness of V. vinifera 'Riesling' buds in 0, 1, and 5 mM abscisic acid solution at an average temperature of 7 °C 0/24h light/dark photoperiod. After 42 days (vertical dotted line) samples were moved to 22 °C 16/8h light/dark photoperiod. Error bars represent standard deviations of the mean.

References

Anders S, Pyl PT, Huber W. **2015**. HTSeq--a Python framework to work with high-throughput sequencing data. *Bioinformatics* **31**: 166–169.

Andrés F, Coupland G. **2012**. The genetic basis of flowering responses to seasonal cues. *Nature reviews. Genetics* **13**: 627–639.

Bahuguna RN, Jagadish KSV. **2015**. Temperature regulation of plant phenological development. *Environmental and Experimental Botany* **111**: 83–90.

Bai S, Saito T, Sakamoto D, Ito A, Fujii H, Moriguchi T. **2013**. Transcriptome analysis of Japanese pear (*Pyrus pyrifolia* Nakai) flower buds transitioning through endodormancy. *Plant & Cell Physiology* **54**: 1132–1151.

Ban Q, Wang X, Pan C, Wang Y, Kong L, Jiang H, Xu Y, Wang W, Pan Y, Li Y, *et al.* 2017. Comparative analysis of the response and gene regulation in cold resistant and susceptible tea plants. *PLOS ONE* **12**: e0188514.

Bilska-Kos A, Szczepanik J, Sowiński P. **2016**. Cold induced changes in the water balance affect immunocytolocalization pattern of one of the aquaporins in the vascular system in the leaves of maize (*Zea mays* L.). *Journal of Plant Physiology* **205**: 75–79.

Birkenbihl RP, Diezel C, Somssich IE. **2012**. Arabidopsis WRKY33 is a key transcriptional regulator of hormonal and metabolic responses toward *Botrytis cinerea* infection. *Plant Physiology* **159**: 266–285.

Burke MJ, Gusta LV, Quamme HA, Weiser CJ, Li PH. **1976**. Freezing and Injury in Plants. *Annual Review of Plant Physiology* **27**: 507–528.

Busov V, Carneros E, Yakovlev I. **2016**. EARLY BUD-BREAK1 (EBB1) defines a conserved mechanism for control of bud-break in woody perennials. *Plant Signaling & Behavior* **11**: e1073873.

Calixto CPG, Simpson CG, Waugh R, Brown JWS. **2016**. Alternative splicing of barley clock genes in response to low temperature. *PLOS ONE* **11**: e0168028.

Canaguier A, Grimplet J, Di Gaspero G, Scalabrin S, Duchêne E, Choisne N, Mohellibi N, Guichard C, Rombauts S, Le Clainche I. 2017. A new version of the grapevine reference genome assembly (12X.v2) and of its annotation (VCost.v3). *Genomics Data* **14**: 56–62.

Carvalho LC, Vidigal P, Amâncio S. **2015**. Oxidative stress homeostasis in grapevine (*Vitis vinifera* L.). *Frontiers of Environmental Science & Engineering in China* **3**: 20.

Chen Y-F, Li L-Q, Xu Q, Kong Y-H, Wang H, Wu W-H. **2009**. The WRKY6 transcription factor modulates PHOSPHATE1 expression in response to low Pi stress in Arabidopsis. *The Plant Cell* **21**: 3554–3566.

Cooke JEK, Eriksson ME, Junttila O. **2012**. The dynamic nature of bud dormancy in trees: environmental control and molecular mechanisms: Bud dormancy in trees. *Plant, Cell & Environment* **35**: 1707–1728.

Czarnecka-Verner E, Yuan CX, Scharf KD, Englich G, Gurley WB. **2000**. Plants contain a novel multi-member class of heat shock factors without transcriptional activator potential. *Plant Molecular Biology* **43**: 459–471.

Davletova S, Rizhsky L, Liang H, Shengqiang Z, Oliver DJ, Coutu J, Shulaev V, Schlauch K, Mittler R. **2005**. Cytosolic ascorbate peroxidase 1 is a central component of the reactive oxygen gene network of Arabidopsis. *The Plant Cell* **17**: 268–281.

DeFalco TA, Moeder W, Yoshioka K. **2016**. Opening the gates: Insights into cyclic nucleotide-gated channel-mediated signaling. *Trends in Plant Science* **21**: 903–906.

Devaiah BN, Karthikeyan AS, Raghothama KG. **2007**. WRKY75 transcription factor is a modulator of phosphate acquisition and root development in Arabidopsis. *Plant Physiology* **143**: 1789–1801.

Díaz-Riquelme J, Grimplet J, Martínez-Zapater JM, Carmona MJ. **2012**. Transcriptome variation along bud development in grapevine (*Vitis vinifera* L.). *BMC Plant Biology* **12**: 181.

Dobin A, Davis CA, Schlesinger F, Drenkow J, Zaleski C, Jha S, Batut P, Chaisson M, Gingeras TR. **2013**. STAR: ultrafast universal RNA-seq aligner. *Bioinformatics* **29**: 15–21.

Dossa K, Diouf D, Cissé N. **2016**. Genome-wide investigation of HSF genes in sesame reveals their segmental duplication expansion and their active role in drought stress response. *Frontiers in Plant Science* **7**: 1522.

Coombe BG, Iland P. 2005. Grapevine phenology. In Dry PR, Coombe BG, eds. *Viticulture, vol 1: Resources*. Winetitles, Ashford, Australia, 210-248.

van Dyk MM, Soeker MK, Labuschagne IF, Rees DJG. **2010**. Identification of a major QTL for time of initial vegetative budbreak in apple (*Malus x domestica* Borkh.). *Tree genetics & genomes* **6**: 489–502.

Falcone DL, Ogas JP, Somerville CR. **2004**. Regulation of membrane fatty acid composition by temperature in mutants of Arabidopsis with alterations in membrane lipid composition. *BMC Plant Biology* **4**: 17.

Fediuk OM, Bilyavska NO, Zolotareva OK. **2017**. Effects of sucrose on structure and functioning of photosynthetic apparatus of *Galanthus nivalis* l. leaves exposed to chilling stress. *Annals of R.S.C.B.* **21**: 43–51.

Fedurayev PV, Mironov KS, Gabrielyan DA, Bedbenov VS, Zorina AA, Shumskaya M, Los DA. **2018**. Hydrogen peroxide participates in perception and transduction of cold stress signal in *Synechocystis*. *Plant & Cell Physiology* **59**: 1255–1264.

Ferguson JC, Moyer MM, Mills LJ, Hoogenboom G, Keller M. **2014**. Modeling dormant bud cold hardiness and budbreak in twenty-three *Vitis* genotypes reveals variation by region of origin. *American Journal of Enology and Viticulture* **65**: 59–71.

Ferguson JC, Tarara JM, Mills LJ, Grove GG, Keller M. **2011**. Dynamic thermal time model of cold hardiness for dormant grapevine buds. *Annals of Botany* **107**: 389–396.

Filek M, Rudolphi-Skórska E, Sieprawska A, Kvasnica M, Janeczko A. **2017**. Regulation of the membrane structure by brassinosteroids and progesterone in winter wheat seedlings exposed to low temperature. *Steroids* **128**: 37–45.

Fu JJ, Geng JC, Miao YJ, Xu YM, Hu TM, Yang PZ. **2018**. Transcriptomic analyses reveal genotype- and organ-specific molecular responses to cold stress in *Elymus nutans*. *Biologia plantarum*.

George MF, Burke MJ. **1977**. Cold hardiness and deep supercooling in xylem of shagbark hickory. *Plant Physiology* **59**: 319.

Gilmour SJ, Thomashow MF. **1991**. Cold acclimation and cold-regulated gene expression in ABA mutants of *Arabidopsis thaliana*. *Plant Molecular Biology* **17**: 1233–1240.

Grimplet J, Cramer GR, Dickerson JA, Mathiason K, Van Hemert J, Fennell AY. 2009. VitisNet: "omics" integration through grapevine molecular networks. *PLOS ONE* **4**: e8365.

Grundy J, Stoker C, Carré IA. **2015**. Circadian regulation of abiotic stress tolerance in plants. *Frontiers in Plant Science* **6**: 648.

Hedley PE, Russell JR, Jorgensen L, Gordon S, Morris JA, Hackett CA, Cardle L, Brennan R. **2010**. Candidate genes associated with bud dormancy release in blackcurrant (Ribes nigrum L.). *BMC Plant Biology* **10**: 202.

Holmstrup M, Slotsbo S. **2018**. Combined effects of drought and cold acclimation on phospholipid fatty acid composition and cold-shock tolerance in the springtail Protaphorura fimata. *Journal of comparative physiology B* **188**: 225–236.

Horváth I, Glatz A, Nakamoto H, Mishkind ML, Munnik T, Saidi Y, Goloubinoff P, Harwood JL, Vigh L. **2012**. Heat shock response in photosynthetic organisms: membrane and lipid connections. *Progress in Lipid Research* **51**: 208–220.

Horváth I, Glatz A, Varvasovszki V, Török Z, Páli T, Balogh G, Kovács E, Nádasdi L, Benkö S, Joó F, *et al.* 1998. Membrane physical state controls the signaling mechanism of the heat shock response in *Synechocystis* PCC 6803: Identification of hsp17 as a "fluidity gene". *Proceedings of the National Academy of Sciences* **95**: 3513–3518.

Huang Y, Feng C-Z, Ye Q, Wu W-H, Chen Y-F. **2016**. Arabidopsis WRKY6 Transcription Factor Acts as a Positive Regulator of Abscisic Acid Signaling during Seed Germination and Early Seedling Development. *PLoS genetics* **12**: e1005833.

Je J, Chen H, Song C, Lim CO. **2014**. Arabidopsis DREB2C modulates ABA biosynthesis during germination. *Biochemical and Biophysical Research Communications* **452**: 91–98.

Jiang J, Ma S, Ye N, Jiang M, Cao J, Zhang J. **2017**. WRKY transcription factors in plant responses to stresses. *Journal of Integrative Plant Biology* **59**: 86–101.

Khalil-Ur-Rehman M, Wang W, Xu Y-S, Haider MS, Li C-X, Tao J-M. **2017**. Comparative Study on Reagents Involved in Grape Bud Break and Their Effects on Different Metabolites and Related Gene Expression during Winter. *Frontiers in Plant Science* **8**: 1340.

Kovaleski AP, Reisch BI, Londo JP. **2018**. Kinetics of winter deacclimation in response to temperature determines dormancy status and quantifies chilling requirement in grapevines (Vitis spp.). *bioRxiv*.

Lang GA, Early JD, Martin GC, Darnell RL. **1987**. Endo-, Para-, and Ecodormancy: physiological terminology and classification for dormancy research. *HortScience* **22**: 371–377.

Larkindale J, Hall JD, Knight MR, Vierling E. **2005**. Heat stress phenotypes of Arabidopsis mutants implicate multiple signaling pathways in the acquisition of thermotolerance. *Plant Physiology* **138**: 882–897.

Li S, Dami IE. **2016**. Responses of *Vitis vinifera* 'Pinot gris' Grapevines to Exogenous Abscisic Acid (ABA): I. Yield, Fruit Quality, Dormancy, and Freezing Tolerance. *Journal of Plant Growth Regulation* **35**: 245–255.

Li S, Fu Q, Chen L, Huang W, Yu D. **2011**. Arabidopsis thaliana WRKY25, WRKY26, and WRKY33 coordinate induction of plant thermotolerance. *Planta* **233**: 1237–1252.

Li Q, Lei S, Du K, Li L, Pang X, Wang Z, Wei M, Fu S, Hu L, Xu L. **2016**. RNA-seq based transcriptomic analysis uncovers α-linolenic acid and jasmonic acid biosynthesis pathways respond to cold acclimation in *Camellia japonica*. *Scientific Reports* **6**: 36463.

Li W, Li M, Zhang W, Welti R, Wang X. **2004**. The plasma membrane-bound phospholipase Ddelta enhances freezing tolerance in *Arabidopsis thaliana*. *Nature biotechnology* **22**: 427–433.

Liu Q, Kasuga M, Sakuma Y, Abe H, Miura S, Yamaguchi-Shinozaki K, Shinozaki K. **1998**. Two transcription factors, DREB1 and DREB2, with an EREBP/AP2 DNA binding domain separate two cellular signal transduction pathways in drought- and low-temperature-responsive gene expression, respectively, in Arabidopsis. *The Plant Cell* **10**: 1391–1406.

Liu S, Li A, Chen C, Cai G, Zhang L, Guo C, Xu M. **2017a**. De novo transcriptome sequencing in *Passiflora edulis* Sims to identify genes and signaling pathways involved in cold tolerance. *Forests, Trees and Livelihoods* **8**: 435.

Liu J, Xu Y, Zhang L, Li W, Cai Z, Li F, Peng M, Li F, Hu B. **2017b**. De novo assembly and analysis of the transcriptome of *Rumex patientia* L. during cold stress. *PloS one* **12**: e0186470.

Londo JP, Kovaleski AP. **2017**. Characterization of wild North American grapevine cold hardiness using differential thermal analysis. *American Journal of Enology and Viticulture* **68**: 203–212.

Londo JP, Kovaleski AP, Lillis JA. **2018**. Divergence in the transcriptional landscape between low temperature and freeze shock in cultivated grapevine (*Vitis vinifera*). *Horticulture research* **5**: 10.

Love MI, Huber W, Anders S. **2014**. Moderated estimation of fold change and dispersion for RNA-seq data with DESeq2. *Genome biology* **15**: 550.

Mao Z, Sun W. **2015**. Arabidopsis seed-specific vacuolar aquaporins are involved in maintaining seed longevity under the control of ABSCISIC ACID INSENSITIVE 3. *Journal of Experimental Botany* **66**: 4781–4794.

Meijer HJG, Munnik T. **2003**. Phospholipid-based signaling in plants. *Annual Review of Plant Biology* **54**: 265–306.

Meitha K, Agudelo-Romero P, Signorelli S, Gibbs DJ, Considine JA, Foyer CH, Considine MJ. **2018**. Developmental control of hypoxia during bud burst in grapevine. *Plant, Cell & Environment* **41**: 1154–1170.

Melchior F, Kindl H. **1990**. Grapevine stilbene synthase cDNA only slightly differing from chalcone synthase cDNA is expressed in Escherichia coli into a catalytically active enzyme. *FEBS letters* **268**: 17–20.

Mironov V, De Veylder L, Van Montagu M, Inzé D. **1999**. Cyclin-dependent kinases and cell division in plants— the nexus. *The Plant Cell* **11**: 509–521.

Nguyen HC, Cao PB, San Clemente H, Ployet R, Mounet F, Ladouce N, Harvengt L, Marque C, Teulieres C. **2017**. Special trends in CBF and DREB2 groups in Eucalyptus gunnii vs Eucalyptus grandis suggest that CBF are master players in the trade-off between growth and stress resistance. *Physiologia Plantarum* **159**: 445–467.

Nick P. **2008**. Microtubules as Sensors for Abiotic Stimuli. In: Nick P, ed. Plant Microtubules: Development and Flexibility. Berlin, Heidelberg: Springer Berlin Heidelberg, 175–203.

Olukolu BA, Trainin T, Fan S, Kole C, Bielenberg DG, Reighard GL, Abbott AG, Holland D. **2009**. Genetic linkage mapping for molecular dissection of chilling requirement and budbreak in apricot (*Prunus armeniaca* L.). *Genome* **52**: 819–828.

Osier MV. **2016**. VitisPathways: gene pathway analysis for V. vinifera.

Pandey GK, Grant JJ, Cheong YH, Kim BG, Li L, Luan S. **2005**. ABR1, an APETALA2-domain transcription factor that functions as a repressor of ABA response in Arabidopsis. *Plant Physiology* **139**: 1185–1193.

Pang X, Halaly T, Crane O, Keilin T, Keren-Keiserman A, Ogrodovitch A, Galbraith D, Or E. **2007**. Involvement of calcium signalling in dormancy release of grape buds. *Journal of Experimental Botany* **58**: 3249–3262.

Penfield S. **2008**. Temperature perception and signal transduction in plants. *The New Phytologist* **179**: 615–628.

Pérez FJ, Lira W. **2005**. Possible role of catalase in post-dormancy bud break in grapevines. *Journal of Plant Physiology* **162**: 301–308.

Pou A, Medrano H, Flexas J, Tyerman SD. **2013**. A putative role for TIP and PIP aquaporins in dynamics of leaf hydraulic and stomatal conductances in grapevine under water stress and re-watering: Grapevine leaf conductances and aquaporins. *Plant, Cell & Environment* **36**: 828–843.

Prentice IC, Cramer W, Harrison SP, Leemans R, Monserud RA, Solomon AM. **1992**. A global biome model based on plant physiology and dominance, soil properties and climate. *Journal of Biogeography* **19**: 117–134.

Ramos A, Pérez-Solís E, Ibáñez C, Casado R, Collada C, Gómez L, Aragoncillo C, Allona I. **2005**. Winter disruption of the circadian clock in chestnut. *Proceedings of the National Academy of Sciences of the United States of America* **102**: 7037–7042.

Richard S, Lapointe G, Rutledge RG, Séguin A. **2000**. Induction of chalcone synthase expression in white spruce by wounding and jasmonate. *Plant & Cell Physiology* **41**: 982–987.

Ruelland E, Cantrel C, Gawer M, Kader J-C, Zachowski A. **2002**. Activation of phospholipases C and D is an early response to a cold exposure in Arabidopsis suspension cells. *Plant Physiology* **130**: 999–1007.

Saidi Y, Peter M, Finka A, Cicekli C, Vigh L, Goloubinoff P. **2010**. Membrane lipid composition affects plant heat sensing and modulates Ca^{2+}-dependent heat shock response. *Plant Signaling & Behavior* **5**: 1530–1533.

Sang Y, Zheng S, Li W, Huang B, Wang X. **2001**. Regulation of plant water loss by manipulating the expression of phospholipase Dα: Phospholipase D in plant water loss. *The Plant Journal* **28**: 135–144.

Sato E, Nakamichi N, Yamashino T, Mizuno T. **2002**. Aberrant expression of the Arabidopsis circadian-regulated APRR5 gene belonging to the APRR1/TOC1 quintet results in early

flowering and hypersensitiveness to light in early photomorphogenesis. *Plant & Cell Physiology* **43**: 1374–1385.

Shaltout AD, Unrath CR. **1983**. Rest completion prediction model for 'Starkrimson Delicious' apples. *Journal of the American Society for Horticultural Science* **108**: 957–961.

Shimono M, Lu Y-J, Porter K, Kvitko BH, Henty-Ridilla J, Creason A, He SY, Chang JH, Staiger CJ, Day B. **2016**. The *Pseudomonas syringae* type III effector HopG1 induces actin remodeling to promote symptom development and susceptibility during infection. *Plant Physiology* **171**: 2239–2255.

Skibbe M, Qu N, Galis I, Baldwin IT. **2008**. Induced plant defenses in the natural environment: Nicotiana attenuata WRKY3 and WRKY6 coordinate responses to herbivory. *The Plant Cell* **20**: 1984–2000.

Sudawan B, Chang C-S, Chao H-F, Ku MSB, Yen Y-F. **2016**. Hydrogen cyanamide breaks grapevine bud dormancy in the summer through transient activation of gene expression and accumulation of reactive oxygen and nitrogen species. *BMC Plant Biology* **16**: 202.

Tylewicz S, Petterle A, Marttila S, Miskolczi P, Azeez A, Singh RK, Immanen J, Mähler N, Hvidsten TR, Eklund DM, *et al.* 2018. Photoperiodic control of seasonal growth is mediated by ABA acting on cell-cell communication. *Science* **360**: 212–215.

Vergara R, Parada F, Rubio S, Pérez FJ. **2012**. Hypoxia induces H_2O_2 production and activates antioxidant defence system in grapevine buds through mediation of H_2O_2 and ethylene. *Journal of Experimental Botany* **63**: 4123–4131.

Wallis JG, Browse J. **2002**. Mutants of Arabidopsis reveal many roles for membrane lipids. *Progress in Lipid Research* **41**: 254–278.

Wang X. **1999**. The role of phospholipase D in signaling cascades. *Plant Physiology* **120**: 645–651.

Wang L, Nick P. **2017**. Cold sensing in grapevine-Which signals are upstream of the microtubular 'thermometer'. *Plant, Cell & Environment* **40**: 2844–2857.

Wu R, Wang T, Warren BAW, Allan AC, Macknight RC, Varkonyi-Gasic E. **2017**. Kiwifruit SVP2 gene prevents premature budbreak during dormancy. *Journal of Experimental Botany* **68**: 1071–1082.

Yamamoto Y, Sato E, Shimizu T, Nakamich N, Sato S, Kato T, Tabata S, Nagatani A, Yamashino T, Mizuno T. **2003**. Comparative genetic studies on the APRR5 and APRR7 genes belonging to the APRR1/TOC1 quintet implicated in circadian rhythm, control of flowering time, and early photomorphogenesis. *Plant & Cell Physiology* **44**: 1119–1130.

Zheng C, Halaly T, Acheampong AK, Takebayashi Y, Jikumaru Y, Kamiya Y, Or E. **2015**. Abscisic acid (ABA) regulates grape bud dormancy, and dormancy release stimuli may

act through modification of ABA metabolism. *Journal of Experimental Botany* **66**: 1527–1542.

CHAPTER 4
MORPHOLOGY AND FREEZING OBSERVATION OF BUDS OF DIFFERENT *Vitis* SPECIES USING MICROTOMOGRAPHY AND TIME-RESOLVED X-RAY PHASE CONTRAST

Introduction

Deciduous plants produce buds that remain dormant while environmental conditions are unsuitable for growth. While dormant, buds of temperate climate plants experience temperatures below the freezing point of water, and therefore have developed different strategies to prevent bud death. Some buds present freezing resistance through supercooling of intracellular water (Burke *et al.*, 1976; Andrews *et al.*, 1984). Through this process, water can remain liquid to temperatures close to −42 °C (Bigg, 1953), and therefore supercooling is used as a strategy to resist cold in plants native to regions where temperatures do not commonly drop below those levels (Quamme, 1995). Bud cold hardiness changes throughout the winter, mainly based on air temperature (Ferguson *et al.*, 2011, 2014; Londo & Kovaleski, 2017; Kovaleski *et al.*, 2018). Maximum cold hardiness limits are different for different species, ranging from high negative temperatures (i.e., −7 °C) to very close to the ~−42 °C supercooling limit (Quamme, 1995). Within grapevines, there is variation among species and cultivars within a species, but maximum cold hardiness has been observed to be mostly between −24 °C and −35 °C (Andrews *et al.*, 1984; Ferguson *et al.*, 2011, 2014; Londo & Kovaleski, 2017). Although low temperatures are the most limiting factor in plant distribution (Parker, 1963), the process through which plants control the supercooling point of buds and other structures remains largely unknown.

Once exposed to growing conditions after fulfilling dormancy requirements (i.e., chill requirement; (Lang *et al.*, 1987), buds will resume growth. Budbreak follows the loss of cold hardiness in grapevines (Ferguson *et al.*, 2014; Kovaleski *et al.*, 2018). Observations of budbreak are commonly used for evaluating endo- to ecodormancy transition (Londo & Johnson, 2014).

While the kinetics of the deacclimation process appears to describe budbreak within species, different species within the same genus seem to have differences in the relationship between deacclimation and budbreak (Kovaleski *et al.*, 2018). This might be due to an artifact of scales being produced based on *V. vinifera* buds (Coombe & Iland, 2005; Andreini *et al.*, 2009). Therefore, exploring differences in morphological aspects of *Vitis* species may elucidate differences in time to budbreak.

Damage in grapevine buds occurs when intracellular ice forms (Andrews *et al.*, 1984; Mills *et al.*, 2006), however location of ice nucleation has not been studied in grapevines. The observation of the freezing process is the best means for understanding how the event causes damage (Molisch, 1897). Multiple techniques have been used to observe ice formation in food and biological samples: indirect observation through freeze-substitution, identifying holes left in tissues by ice (Bevilacqua *et al.*, 1979); light microscopy (Morris *et al.*, 1986; Guenther *et al.*, 2006; Stott & Karlsson, 2009; Endoh *et al.*, 2009, 2014); fluorescence microscopy with the aid of a microslicer for 3D ice structure (Do et al., 2004); NMR microscopy (Ishikawa *et al.*, 1997; Kerr *et al.*, 1998); freeze fracture Cryo-SEM (Endoh *et al.*, 2009, 2014); infrared imaging (Workmaster & Palta, 1999; Bauerecker *et al.*, 2008; Livingston *et al.*, 2018); confocal laser scanning microscopy (Baier-Schenk *et al.*, 2005); and X-ray phase contrast imaging (Sinclair *et al.*, 2009).

Avoiding winter damage in buds is important as these structures contain the flowers, or inflorescence primordia in case of grapevines (Pratt, 1971), that produce crops in the following growing season. The identification of the regions of the bud where supercooling fails can help understanding how plants control supercooling. Endoh *et al.* (2009) used light microcopy to examine extracellular ice crystals in buds of larch (*Larix kaempferi*). Freeze fracture Cryo-SEM

was used to evaluate the presence of intracellular ice, based on the presence of crystalline ice vs. amorphous ice inside cells. These methods, however, do not allow for temporal imaging as they are destructive. Using X-ray phase contrast imaging, Sinclair *et al.* (2009) observed the growth of ice crystals in insect larvae in real time. X-ray phase contrast imaging of freezing appears to be an interesting option for imaging freezing in buds, considering the opaque nature of the structure, as well as the fact that it allows for temporal imaging of ice spreading (Sinclair *et al.*, 2009).

The setup used for X-ray phase contrast also allows for tomography-like imaging, an underused technique in plant sciences (Staedler *et al.*, 2013) that allows the study of morphological differences between buds. In plants, this technique has been used and is a consolidated method for the study of xylem and wood characteristics in plants (Mayo *et al.*, 2010; Sedighi Gilani *et al.*, 2014; Cochard *et al.*, 2015; Torres-Ruiz *et al.*, 2015; Choat *et al.*, 2016; Malek *et al.*, 2016; Nardini *et al.*, 2017; Scoffoni *et al.*, 2017; Koddenberg & Militz, 2018). Other plant structures have also been imaged, such as developing maize seeds (Rousseau *et al.*, 2015), tomato leaves (Verboven *et al.*, 2015), and fixed flowers and floral buds, with the imaging of these last plant organs typically performed with the aid of contrasting agents (Staedler *et al.*, 2013).

Understanding morphological changes within buds during deacclimation, as well as the location within the bud where freezing initiates may provide new insights into the mechanistic plant control of supercooling ability. Therefore, the objective of this study was to evaluate morphological development of buds from different *Vitis* species during loss of hardiness and budbreak, as well as image the freezing of buds to identify regions of the bud where the supercooling mechanism fails.

Materials and Methods

Plant material and cold hardiness

Buds of *V. amurensis* PI588641, *V. riparia* PI588711, and *V. vinifera* 'Riesling' were collected from the field on 31 January 2018, prepared into single node cuttings and placed in a 4 °C cold room in cups of water. In preparation for imaging, sets of buds were removed from the cold room and placed under forcing conditions (22 °C, 16h/8h light/dark) periodically to deacclimate. Buds were removed on 31 Jan, 2 Feb, 5 Feb, 7 Feb, and 11 Feb 2018 for *V. riparia* and *V. vinifera*; and 8 Feb and 11 Feb 2018 for *V. amurensis*. On 13 Feb 2018, cold hardiness of buds was determined and buds were moved back into cold room, where they were maintained throughout the imaging period to minimize changes in cold hardiness and developmental stage (Kovaleski *et al.*, 2018). This sampling scheme provided us with buds at 0, 2, 6, 8, 11, and 13 days of deacclimation (0, 2, 5 for *V. amurensis*).

Cold hardiness was determined through differential thermal analysis (DTA), as represented by individual low temperature exotherm (LTE) of buds (Mills *et al.*, 2006). In summary, buds are excised from cane and placed on thermoelectric modules (TEM) in plates, which are then placed in a programmable freezer. The freezer is cooled at a −4 °C $hour^{-1}$ rate, and changes in voltage due to release of heat by freezing of water is measured by the TEMs and recorded via Keithley data logger (Tektronix, Beaverton, OR) attached to a computer. Deacclimation rates were estimated using linear regression (Kovaleski *et al.*, 2018) using R (ver. 3.3.0, R Foundation for Statistical Computing). R was also used to produce all plots.

X-ray phase contrast imaging

Buds with a piece of cane were held on a custom made cylindrical holder with mounting putty. The holder was attached to a small goniometer mounted on a Huber 4-circle diffractometer. Imaging was performed in the C-line at the Cornell High Energy Synchrotron

Source (CHESS). The monochromatic beam was expanded to 7 mm × 7 mm at X-ray energy 15 KeV. The sample-detector distance used was 0.5 m. Phase-contrast is produced when majority unperturbed beam interferes with angular deviations in the wavefront caused by density variations in the sample (Socha *et al.*, 2007). X-rays were converted into visible light using a rare-earth doped GGG ($Gd_3Ga_5O_{12}$) crystal plate and imaged using an Andor Neo CMOS camera with a 5x objective lens.

For morphological changes in buds, tomographic-like imaging was performed with camera resolution at approximately 5 μm, obtained by adapting the objective lens. Buds were scanned while rotating over 180°, with images collected every ¼ or ½ degree. Reconstruction of bud structure based on these datasets was performed using Octopus Reconstruction software (ver. 8.8.1, Inside Matters, Belgium). After reconstruction, buds were visualized in 3D using OsiriX imaging software (ver. 8.0.1, Pixmeo, Switzerland). For volume measurements, a threshold was visually established for each bud to remove noise. The bud cushion (i.e., undifferentiated tissue connecting bud to shoot) was removed from the image, and only the bud itself was used. Volume was determined by counting the number of voxels in the 3D image using the ROI tool within Osirix. Volume was observed as percent increase in volume (ΔV) from the sample in day 0. If more than one bud was imaged for day 0, the average volume of samples was used as the base value.

Freezing of the buds was also observed, using 2D time-lapse with images at 2 μm pixel size. A 1s exposure was used, but image capturing time effectively resulted in 0.56 Hz frequency. During the imaging, buds were cooled using a N_2 gas cryostream (Oxford Cryosystems, UK), with a cooling rate of −50 °C $hour^{-1}$. A thermocouple in a 33-gage needle probe (Omega Engineering, Inc., USA) was inserted in the bud during imaging and used to

measure the temperature inside the bud, and temperature measurements were recorded using an RDXL4SD data logger (Omega Engineering, Inc., USA). LTEs for these samples were observed as temperature deviations from the linear rate of cooling. Image sets were transformed into videos using ImageJ (ver. 2.0.0), and temperature and image information were matched using time stamps in data-logger and images, inserted using the *Series Labeler* plugin.

Results

A linear behavior described well the deacclimation of buds until the limits of detection of LTEs (Fig. 4-1). *V. amurensis* and *V. riparia* had similar deacclimation rates, at 2.24 °C day^{-1} (R^2= 0.89) and 2.12 °C day^{-1} (R^2= 0.92), respectively. *V. vinifera* had a lower deacclimation rate, at 1.33 °C day^{-1} (R^2= 0.95). LTEs determined using needle probes inserted in the buds during imaging of freezing produced similar results to those using the regular DTA method. In *V. riparia*, the last two time points were not used for rate determination as buds had already started to open.

Vitis species produce mixed buds, with both vegetative and reproductive parts, which are visible in micro-CT imaging (Figs. 4-2, 4-3, 4-4). Due to faster deacclimation rate and development under our testing conditions, *V. riparia* buds were imaged through a wider range of development (Fig. 4-2) than *V. vinifera* (Fig. 4-3). Due to the reduced number of sampling dates, *V. amurensis* had the lowest range of development imaged (Fig. 4-4). *V. riparia* was imaged in E-L stages 1 (Figs. 4-2A, B, C), 2 (Fig. 4-2D), and 3 (Fig. 4-2E). *V. vinifera* appears to be at an early stage 2 in Fig. 4-3D, whereas *V. amurensis* buds were all at stage 1. Primary, secondary, and tertiary buds are visible in the still images shown for all three species. Images provide clear identification of inflorescences in the primary bud, even in the fully dormant state (day 0; Figs. 4-2A, 4-3A, 4-4A).

Clear morphological differences can be seen when comparing buds of the different species. *V. riparia* buds are much smaller than *V. vinifera* and *V. amurensis* (4.15 mm^3 vs. 10.4 mm^3 and 20.2 mm^3, respectively). The inflorescence primordia in *V. riparia*, however, take up much more of the volume of day 0 buds in *V. riparia* than in *V. vinifera*. Both *V. vinifera* and *V. riparia* have inflorescence primordia of ~0.5 mm, whereas in *V. amurensis* they are ~1mm long and appear more developed. Buds of *V. vinifera* have much more space between the leaf primordia, inflorescence primordia, and the outer bud scales compared to the two other species, especially *V. amurensis*. This space is occupied by "wool" or "hair", most visible in Figs. 4-1B and C. *V. amurensis* buds are very compact at the dormant stage, and there is very little space between the scales and leaf primordia, which can be seen folding down on the top, as if constrained by the outer scales (Fig. 4-4A).

In *V. riparia*, very few differences could be noted between the buds until day 8 (Figs. 4-2A through C). However, once all the hardiness was lost (lack of measured LTE peaks), there was a greater increase in the bud size. This increase in size appeared to be due primarily to the expansion and development of the inflorescence primordia, and elongation of the base of the primary bud (shoot). In *V. vinifera*, the inflorescence primordia appeared to remain the same size as the buds lost hardiness. However, there was a noticeable expansion of the base of the primary bud. In *V. amurensis*, there are no clear internal differences seen between day 0 and 5.

The visual assessments of expansion in bud tissues are confirmed by analysis of the volume of tissue in the buds (Fig. 4-5). *V. riparia* buds reached the greatest expansion in volume within the time analyzed, reaching at day 13 almost triple the size of buds in day 0. *V. amurensis* appears to have a similar slope when the first days are considered compared to *V. riparia*, while

V. vinifera has the slowest increase in bud volume. Both *V. riparia* and *V. vinifera* buds had increased ~50% in volume when most of the hardiness was lost (day 8 and day 13, respectively).

Freezing was most easily observed in *V. amurensis* and *V. riparia* (Obj. S1 and S2, respectively), although it can also be seen in *V. vinifera* (Obj. S3). In all movies, a slight shift downward of the bud is seen in the first few minutes, possibly due to contraction of the putty that was used to hold the buds during cooling. In *V. amurensis*, a bud from day 0 was imaged, freezing at −17.3 °C. The freezing resulted in an increase in the inner temperature of the bud of almost 8 °C, reaching −9.4 °C. In buds of *V. riparia* that had spent 8 days under forcing conditions, freezing of the primary bud occurred at −16.3 °C, also increasing the inner temperature by ~8 °C. The *V. vinifera* bud from day 13 pictured in movie S3 froze at −5.4 °C, only raising the temperature ~1 °C. Differently from *V. amurensis* and *V. riparia*, in which after the freezing temperature quickly begins to drop again, this bud of *V. vinifera* increased the temperature to −4.2 °C, maintaining at that level for about 1 min – indicating that freezing of tissues continued during that period of time. Perhaps most clearly in *V. amurensis*, but seen in the other species as well, freezing begins in the center of the bud (timestamp ~32:00 in *V. amurensis*, ~22:30 for *V. riparia*, and ~13:30 for *V. vinifera*). The ice spreads throughout the outer scales, and ends at the top of the bud as seen by the slight unfolding of the bud scales in the top. The entire freezing event occurs over ~4 minutes in *V. amurensis* and *V. vinifera*, and ~2 minutes in *V. riparia*. In *V. amurensis*, the freezing of the secondary bud is apparent at 43:10/−25 °C.

Discussion

To our knowledge, this is the first study using X-ray microtomography exploring morphological changes in buds. Moreover, we used quantitative data to explore concepts related to cold hardiness, and X-ray phase contrast imaging to visualize freezing. The non-destructive

nature of X-ray phase contrast imaging is an interesting aspect for study of supercooling in buds, where damage to structure can result in loss of the phenotype (Quamme *et al.*, 1995). Although long-term survivorship of the buds was not tested, and radiation levels could potentially lead to cell death (Socha *et al.*, 2007; Sinclair *et al.*, 2009), buds still showed LTEs that were comparable to those run using standard DTA evaluation. This demonstrates that at least for a few hours (scan for 3D imaging was ~1h, followed by the freezing scan) the buds remained viable and the mechanisms promoting supercooling were intact, as buds which have been killed by freezing temperatures (buds frozen, thawed, and refrozen) lose correlated LTE values (Data not shown).

There were no significant differences in the temperature of LTEs in the buds frozen under the cryostream with the needle probe than what was expected according to DTA and linear models produced, as well as predicted deacclimation rates for buds at this stage (Kovaleski *et al.*, 2018). This is interesting considering two aspects: the high rate of cooling used and the lack of observed high temperature exotherms (HTEs) in the cryostream setup. The rate of cooling used in the cryostream was ~12x higher than the cooling used in typical DTA analysis. The higher rate was required due to the time constrains for beam access, and faster freezing made possible to image a greater number of buds. While the rates of cooling at the level used in this study reportedly cause a decrease in LTE temperature of *V. vinifera* hybrid grapevines (Quamme, 1986), higher rates of cooling result in freezing at warmer temperatures for *Rhododendrum (Ishikawa & Sakai, 1981)*. We did not see a particular trend when all species were taken into account. However, all the buds of *V. amurensis* froze at higher temperatures than the expected, which may be a result of higher rates of deacclimation of this species under the storage temperature (4 °C) compared to the other two (Kovaleski *et al.*, 2018).

HTEs were not measured in terms of temperature changes in most buds through needle probes, or seen as visible changes in the bud through phase contrast imaging. In regular DTAs, HTEs are enhanced by the use of water sprays (Mills *et al.*, 2006), resulting in much larger peaks than LTEs. It is possible, however, that the HTE signal in non-wetted buds comes from the piece of cane attached to the bud, rather than the extracellular space in the bud itself. HTEs may also be a result of condensation followed by freezing, or sublimation of water vapor on TEMs during the cooling in DTAs. The cryostream used in this setup has a ring of warmer, dry N_2 gas surrounding the N_2 cryostream, which prevented any sublimation or condensation on the sample during the cooling. The few HTE-like signals seen were slight lags in the temperature decrease (data not shown). This behavior might indicate extraorgan freezing happens in grapevines, without extracellular ice forming within primordia such as described in other species (Quamme *et al.*, 1995; Endoh *et al.*, 2009, 2014). If the HTE happens in tissues further from the center of the bud, it is possible that the placing of the needle inserted could prevent or diminish the perception of temperature changes caused by tissues away from the center of the bud. However, LTEs corresponding to secondary buds were seen and measured based on temperature changes. Therefore, further testing using multiple needles in buds should be conducted using different forms and rates of cooling to verify the occurrence, location, and importance of HTEs.

The resolution obtained in the freezing images of 2 μm pixel size was not enough to resolve ice crystals in the buds such as observed by (Sinclair *et al.*, 2009) imaging larvae of *Chymomyza amoena* and *Drosophila melanogaster*. Larvae have free lymph in large volumes, allowing the formation of large crystals within their bodies. In grapevine buds, most of the water is located inside cells with diameter less than 20 μm. While imaging at a higher resolution (~1 μm) is possible, increasing the resolution results in a smaller area of imaging (Verboven *et al.*,

2015) that would likely not fit a whole bud. Therefore, we assessed freezing as the movement resulting from volume expansion due to phase change in water, also observed by Sinclair et al. (2009).

Despite the cryostream hitting the bud from the apex, likely generating a temperature gradient that resulted in lower temperatures on the outside of the bud compared to inside, and from top to bottom, freezing appears to occur from the inside, outward in all species. This is very clearly observed in movie S1, where the central portion of the bud of *V. amurensis* expands first, and bud scales located in the distal portion of the bud appear to be the last to freeze as they slightly unfold. This is a similar behavior to what was described by (Quamme *et al.*, 1995) for buds of peach (*Prunus persica*), in which ice propagates from the subtending tissues into the bud. Considering the apparent higher cold hardiness in bud scales compared to the shoot tip area, future studies exploring gene expression differences may want to compare these structures within the bud to identify genes related to cold hardiness.

Clear morphological differences are seen between the three species studied. *V. vinifera* has much less green tissue per bud volume than the other two species analyzed. Much of the bud volume is actually occupied by wool material. Both wild species also have this woolly tissue in the buds but at much lower percent of the total bud space. Initially, it may seem as though this woolly tissue represents an insulative layer, protecting the dormant bud from some of the stress of cold temperature. However, the least cold hardy species has the much greater proportion. This adaptation thus likely linked in some other way to the region of origin for *V. vinifera*. As *V. vinifera* was domesticated in the Mediterranian region of Europe and Africa, it is possible that an adaptation to reduce water loss during the dormant season in a warmer and drier place would be beneficial. In contrast, *V. amurensis* and *V. riparia* are native to riparian areas of Northern Asia

and North America, respectively. The differences in tissue volume of *V. amurensis* and *V. riparia* buds compared to *V. vinifera* also help explain some differences observed during budbreak phenology. *V. riparia* appears to have a more rapid development in the E-L scale compared to *V. vinifera*, even when responses to temperature are corrected (Kovaleski *et al.*, 2018). However, this may be a result of the larger volume of green tissue present in buds of *V. riparia* compared to *V. vinifera*. Although it was not seen, *V. amurensis* would probably have similar or earlier budbreak than *V. riparia*, considering all of the tissues within the bud are extremely compacted and any expansion might result in appearance of early stages of budbreak (opening of the outer scales). It is not clear however how these morphological differences may implicate in greater maximum cold hardiness in *V. amurensis* and *V. riparia* compared to *V. vinifera* (Londo & Kovaleski, 2017).

The increase of volume is positively correlated with deacclimation, and faster increase of volume and deacclimation rates are seen in *V. amurensis* and *V. riparia* as compared to *V. vinifera* (Fig 1 and 5). This could indicate that increases in volume are reducing the ability of buds to supercool, likely as a result of influx of water leading to turgor (Xie *et al.*, 2018) and potentially with differentiation of cells and tissues (chapter 3). Although it is not known how plants are able to control levels of deep supercooling, from a physical aspect it is known that larger volumes of water are at higher risk of ice nucleation at any given temperature (Bigg, 1953). Cold hardiness is correlated to bud water relations (Ishikawa & Sakai, 1981; Richards & Bliss, 1986), and *V. vinifera* buds have an increase in ~25% water content from dormant to budbreak stage (Xie *et al.*, 2018; Meitha *et al.*, 2018). It is important to acknowledge that metabolic changes within the bud during deacclimation can also play a part in the loss of supercooling ability (Meitha *et al.*, 2018; Chapter 2). The more rapid increase in volume in the

later phenological stages may be a result of re-establishment of vascular connections between the bud and the cane (Xie *et al.*, 2018). Early xylem does not appear clearly such as large vessels in the cane (data not shown), but the use of contrasting agents (Staedler *et al.*, 2013) could be used to evaluate the formation of xylem connections such as is done with dyes and light microscopy (Xie *et al.*, 2018). Contrasting agents may also be of potential use to more easily segment different parts of the bud in a virtual histology approach if differential uptake by tissues leads to clear density differences (Rousseau *et al.*, 2015).

Buds took longer than 1 min to completely freeze despite the steep cooling rate and the cooling method based on a cryostream, which would reduce the difference in air to bud temperature by greatly decreasing the boundary layer (Grace, 2006). This contradicts the description of (Quamme, 1995) that the freezing during LTE happens suddenly. There was a difference in the time it took to completely freeze the buds of different species. The size difference might justify why *V. riparia* buds froze more quickly compared to the other species if a similar rate of intracellular ice growth propagation is considered (Acker *et al.*, 2001). Although *V. amurensis* has buds with more volume than *V. vinifera*, it is possible that the wool in *V. vinifera* buds, as well as the shape of it reduced the rate of heat loss to the exterior. Energy balance studies comparing theoretical buds may allow for explanations for the differences in the duration of freezing. However, it is unlikely that insulation capabilities of bud tissues would be an adaptive response to increase cold hardiness, since air temperature changes in nature occur at a much lower rate and low temperature exposure lasts for longer periods of time.

Conclusions

Some expansion early in the deacclimation appears to be correlated to the loss of cold hardiness. Differential development between species is likely due to different order in the development of different organs (flowers vs. leaves). X-ray microtomography proved to be a

useful approach to identify structures within a bud, as well as for quantitative analysis of changes during loss of cold hardiness and early budbreak. Although our setup required removal of the bud from the cane, adaptation of a sample holder could lead to observation of growth in the same bud during development. Future explorations with contrasting agents (Staedler *et al.*, 2013) may aid in anatomical studies of buds, with special interest to water movement in the bud. We identified the differential response between the center of the bud and bud scales, which can be explored further for understanding ice nucleation and propagation in plants. The use of 2D time-lapse X-ray phase contrast associated with a thermocouple was useful in identifying how ice spreads throughout the bud.

Object S-1. Video file of freezing in bud of *V. amurensis* using X-ray phase contrast imaging. Bud had not experienced forcing conditions (same bud from Figure 4A). Time stamp on the left in mm:ss format. Expected (blue background) and measured (red background) temperatures in the bud. Expected temperature was calculated based on linear regression of inner bud temperature during cooling while freezing did not occur. Freezing begins at ~32:00/−17.3 °C. File name: "Movie_S1_V.amurensis_bud_freezing.avi"

Object S-2. Video file of freezing in bud of *V. riparia* using X-ray phase contrast imaging. Bud had been exposed to forcing conditions for 8 days (same bud from Figure 2C). Time stamp on the left in mm:ss format. Expected (blue background) and measured (red background) temperatures in the bud. Expected temperature was calculated based on linear regression of inner bud temperature during cooling while freezing did not occur. Freezing begins at ~22:40/−16.2 °C. File name: "Movie_S2_V.riparia_bud_freezing.avi"

Object S-3. Video file of freezing in bud of *V. vinifera* using X-ray phase contrast imaging. Bud had been exposed to forcing conditions for 13 days (same bud from Figure 3D). Time stamp on the left in mm:ss format. Expected (blue background) and measured (red background) temperatures in the bud. Expected temperature was calculated based on linear regression of inner bud temperature during cooling while freezing did not occur. Freezing begins at ~13:50/−5.3 °C. File name: "Movie_S3_V.vinifera_Riesling_bud_freezing.avi"

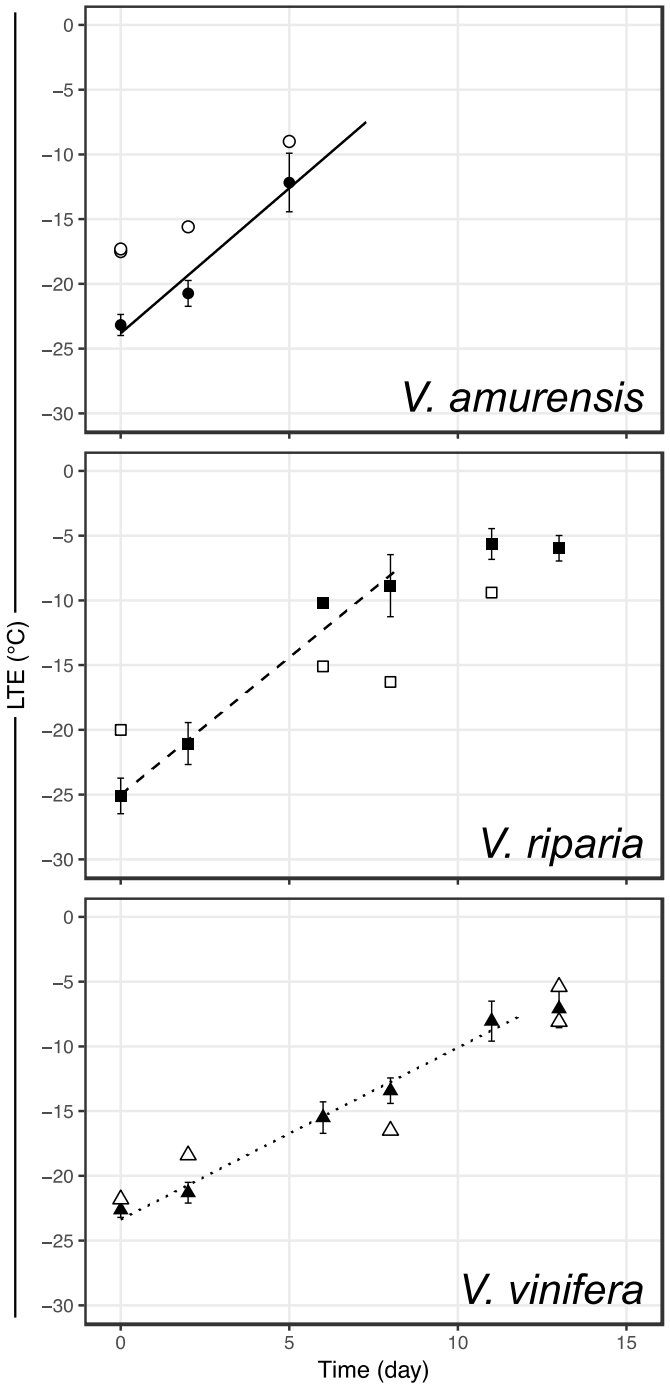

Figure 4-1. Deacclimation of *Vitis amurensis*, *V. riparia*, and *V. vinifera* 'Riesling' under forcing conditions. Full symbols represent average bud cold hardiness estimated through differential thermal analysis, while open symbols represent freezing temperature of single buds under a cryostream. Error bars represent standard deviation of the mean. Deacclimation rates (linear regression) were 2.24 °C day^{-1}(R^2= 0.89), 2.12 °C day^{-1}(R^2= 0.92), and 1.33 °C day^{-1}(R^2= 0.95) for *V. amurensis*,*V. riparia*, and *V. vinifera*, respectively (P<0.001 for all).

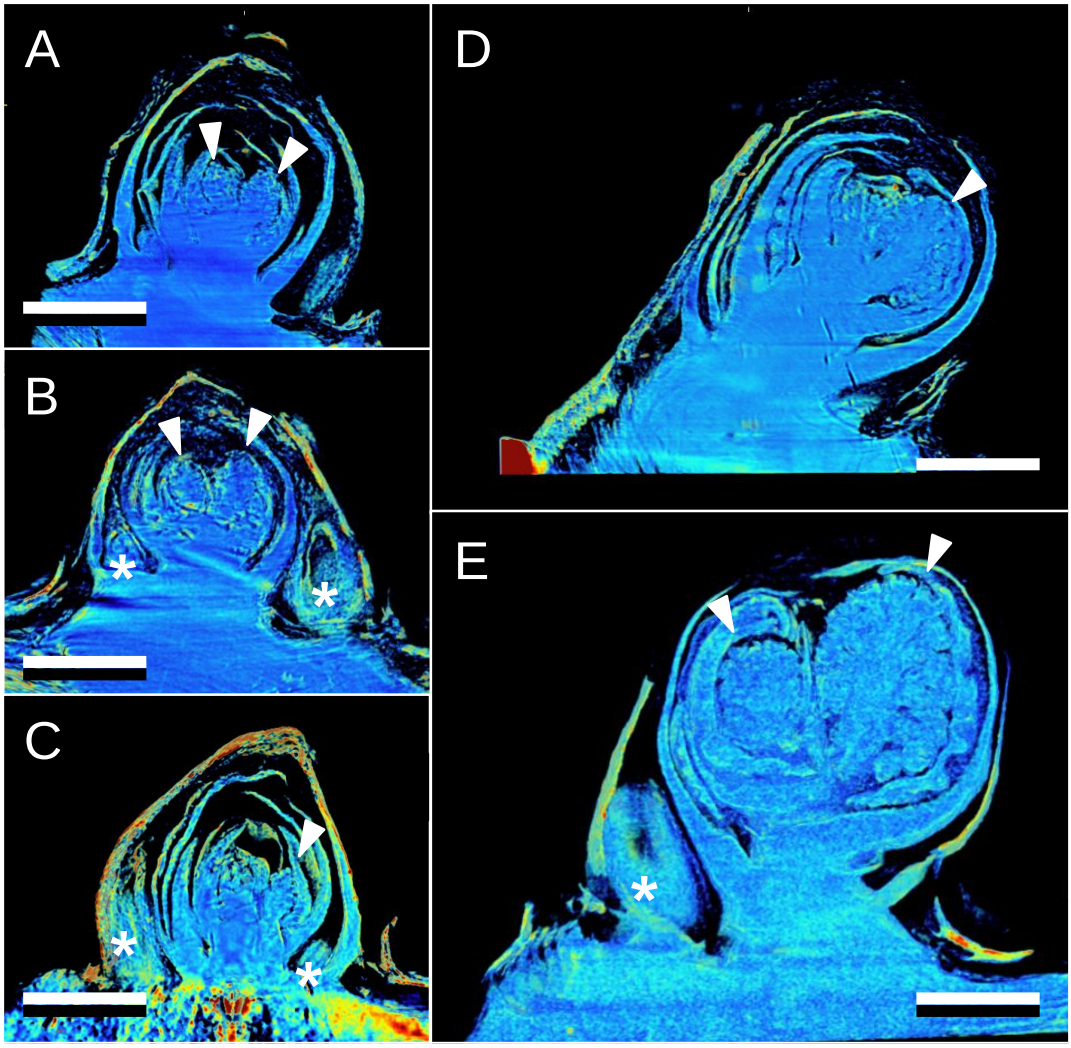

Figure 4-2. Development of *Vitis riparia* buds during budbreak reconstructed using X-ray microtomography. Buds were imaged at 0 (A), 2 (B), 8 (C), 11 (D), and 13 (E) days under forcing conditions. Few differences are observed through day 8, but great expansion of the inflorescence is seen in day 11 and day 13. Full arrow heads indicate inflorescences, asterisks indicate secondary and tertiary bud. Scale bar = 1 mm.

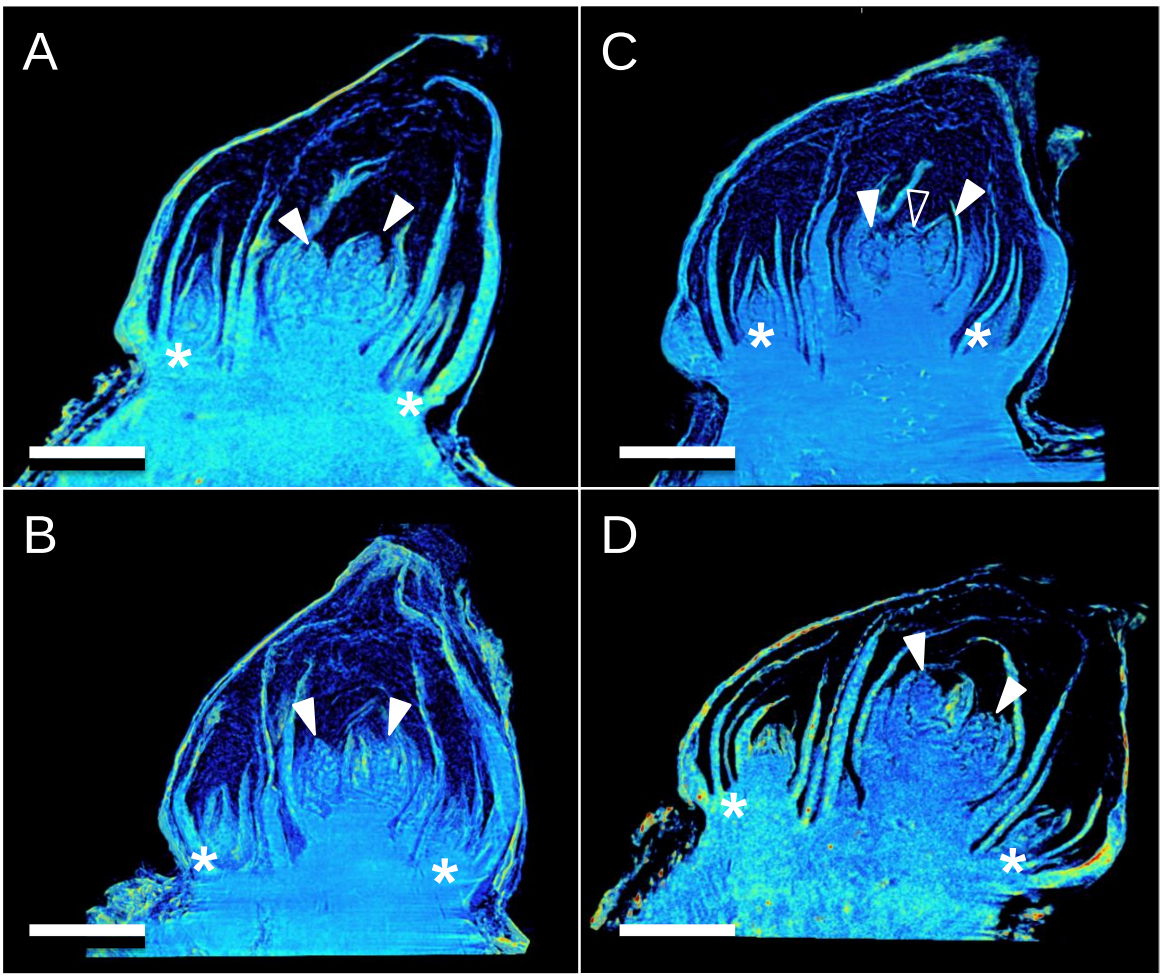

Figure 4-3. Development of *Vitis vinifera* buds during budbreak reconstructed using X-ray microtomography. Buds were imaged at 0 (A), 2 (B), 8 (C), and 13 (D) days under forcing conditions. Expansion of the base of the primary bud is visible throughout the images, and result in opening of the outer bud scales (D). Full arrow heads indicate inflorescences, open arrow head indicates apical meristem, asterisks indicate secondary and tertiary bud. Scale bar = 1 mm.

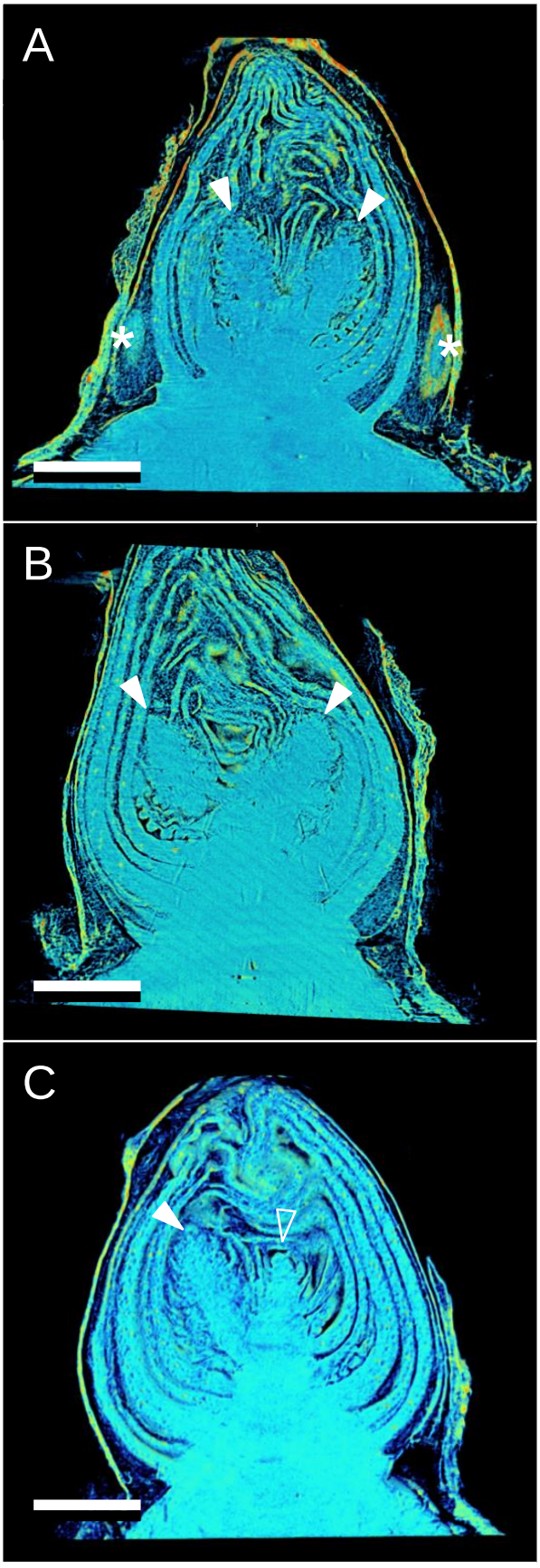

Figure 4-4. Development of *Vitis amurensis* buds during budbreak reconstructed using X-ray microtomography. Buds were imaged at 0 (A), 2 (B), and 5 (C) days under forcing conditions. Few differences are visible in buds of amurensis throughout the development. Full arrow heads indicate inflorescences, open arrow head indicates apical meristem, asterisks indicate secondary and tertiary bud. Scale bar = 1 mm.

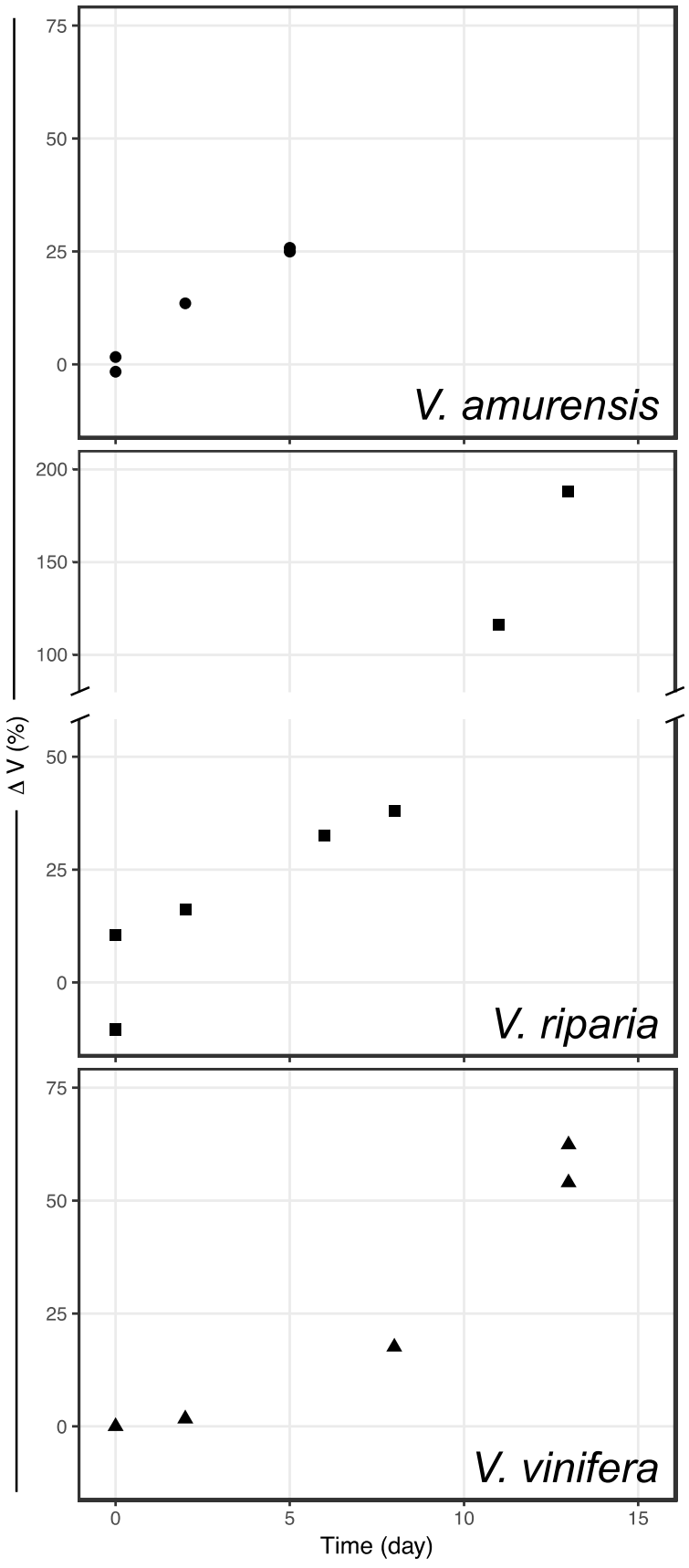

Figure 4-5. Increase in volume (ΔV) of *Vitis amurensis*, *V. riparia*, and *V. vinifera* during deacclimation. Volume was determined by counting the number of voxels in X-ray microtomography-reconstructed buds. ΔV was calculated as the percent increase in volume from sample (or average of samples) at day 0.

References

Acker JP, Elliott JA, McGann LE. **2001**. Intercellular ice propagation: experimental evidence for ice growth through membrane pores. *Biophysical Journal* **81**: 1389–1397.

Andreini L, Viti R, Scalabrelli G. **2009**. Study on the morphological evolution of bud break in *Vitis vinifera* L. *Vitis* **48**: 153–158.

Andrews PK, Sandidge CR III, Toyama TK. **1984**. Deep supercooling of dormant and deacclimating *Vitis* buds. *American Journal of Enology and Viticulture* **35**: 175–177.

Baier-Schenk A, Handschin S, von Schönau M, Bittermann AG, Bächi T, Conde-Petit B. **2005**. In situ observation of the freezing process in wheat dough by confocal laser scanning microscopy (CLSM): Formation of ice and changes in the gluten network. *Journal of Cereal Science* **42**: 255–260.

Bauerecker S, Ulbig P, Buch V, Vrbka L, Jungwirth P. **2008**. Monitoring ice nucleation in pure and salty water via high-speed imaging and computer simulations. *Journal of Physical Chemistry C* **112**: 7631–7636.

Bevilacqua A, Zaritzky NE, Calvelo A. **1979**. Histological measurements of ice in frozen beef. *International Journal of Food Science & Technology*. **14**: 237–251.

Bigg EK. **1953**. The supercooling of water. *Proceedings of the Physical Society. Section B* **66**: 688.

Burke MJ, Gusta LV, Quamme HA, Weiser CJ, Li PH. **1976**. Freezing and injury in plants. *Annual Review of Plant Physiology* **27**: 507–528.

Choat B, Badel E, Burlett R, Delzon S, Cochard H, Jansen S. **2016**. Noninvasive measurement of vulnerability to drought-induced embolism by X-ray microtomography. *Plant Physiology* **170**: 273–282.

Cochard H, Delzon S, Badel E. **2015**. X-ray microtomography (micro-CT): a reference technology for high-resolution quantification of xylem embolism in trees. *Plant, Cell & Environment* **38**: 201–206.

Coombe BG, Iland P. 2005. Grapevine phenology. In Dry PR, Coombe BG, eds. *Viticulture, vol 1: Resources*. Winetitles, Ashford, Australia, 210-248.

Endoh K, Kasuga J, Arakawa K, Ito T, Fujikawa S. **2009**. Cryo-scanning electron microscopic study on freezing behaviors of tissue cells in dormant buds of larch (Larix kaempferi). *Cryobiology* **59**: 214–222.

Endoh K, Kuwabara C, Arakawa K, Fujikawa S. **2014**. Consideration of the reasons why dormant buds of trees have evolved extraorgan freezing as an adaptation for winter survival. *Environmental and Experimental Botany* **106**: 52–59.

Ferguson JC, Moyer MM, Mills LJ, Hoogenboom G, Keller M. **2014**. Modeling dormant bud cold hardiness and budbreak in twenty-three *Vitis* genotypes reveals variation by region of origin. *American Journal of Enology and Viticulture* **65**: 59–71.

Ferguson JC, Tarara JM, Mills LJ, Grove GG, Keller M. **2011**. Dynamic thermal time model of cold hardiness for dormant grapevine buds. *Annals of Botany* **107**: 389–396.

Grace J. **2006**. The temperature of buds may be higher than you thought. *New Phytologist* **170**: 1–3.

Guenther JF, Seki S, Kleinhans FW, Edashige K, Roberts DM, Mazur P. **2006**. Extra- and intra-cellular ice formation in stage I and II *Xenopus laevis* oocytes. *Cryobiology* **52**: 401–416.

Ishikawa M, Price WS, Ide H, Arata Y. **1997**. Visualization of freezing behaviors in leaf and flower buds of full-moon maple by nuclear magnetic resonance microscopy. *Plant Physiology* **115**: 1515–1524.

Ishikawa M, Sakai A. **1981**. Freezing avoidance mechanisms by supercooling in some *Rhododendron* flower buds with reference to water relations. *Plant & Cell Physiology* **22**: 953–967.

Kerr WL, Kauten RJ, McCarthy MJ, Reid DS. **1998**. Monitoring the formation of ice during food freezing by magnetic resonance imaging. *LWT - Food Science and Technology* **31**: 215–220.

Koddenberg T, Militz H. **2018**. Morphological imaging and quantification of axial xylem tissue in *Fraxinus excelsior* L. through X-ray micro-computed tomography. *Micron* **111**: 28–35.

Kovaleski AP, Reisch BI, Londo JP. **2018**. Kinetics of winter deacclimation in response to temperature determines dormancy status and quantifies chilling requirement in grapevines (*Vitis* spp.). *bioRxiv*.

Lang GA, Early JD, Martin GC, Darnell RL. **1987**. Endo-, Para-, and Ecodormancy: physiological terminology and classification for dormancy research. *HortScience* **22**: 371–377.

Livingston DP 3rd, Tuong TD, Murphy JP, Gusta LV, Willick I, Wisniewski ME. **2018**. High-definition infrared thermography of ice nucleation and propagation in wheat under natural frost conditions and controlled freezing. *Planta* **247**: 791–806.

Londo JP, Johnson LM. **2014**. Variation in the chilling requirement and budburst rate of wild Vitis species. *Environmental and Experimental Botany* **106**: 138–147.

Londo JP, Kovaleski AP. 2017. Characterization of wild North American grapevine cold hardiness using differential thermal analysis. *American Journal of Enology and Viticulture* **68** : 203-212.

Malek M, Khelfa H, Picart P, Mounier D, Poilâne C. **2016**. Microtomography imaging of an isolated plant fiber: a digital holographic approach. *Applied Optics* **55**: A111–21.

Mayo SC, Chen F, Evans R. **2010**. Micron-scale 3D imaging of wood and plant microstructure using high-resolution X-ray phase-contrast microtomography. *Journal of Structural Biology* **171**: 182–188.

Meitha K, Agudelo-Romero P, Signorelli S, Gibbs DJ, Considine JA, Foyer CH, Considine MJ. **2018**. Developmental control of hypoxia during bud burst in grapevine. *Plant, Cell & Environment* **41**: 1154–1170.

Mills LJ, Ferguson JC, Keller M. **2006**. Cold-hardiness evaluation of grapevine buds and cane tissues. *American Journal of Enology and Viticulture* **57**: 194–200.

Molisch H. 1897. Untersuchungen über das Erfrieren der Pflanzen. Reprinted in English. 1982 in *Cryo-Letters* **3**:332-390.

Morris GJ, Coulson GE, Engels M. **1986**. A cryomicroscopic study of *Cylindrocystis brebissonii* De Bary and two species of *Micrasterias* Ralfs (Conjugatophyceae, Chlorophyta) during freezing and thawing. *Journal of Experimental Botany* **37**: 842–856.

Nardini A, Savi T, Losso A, Petit G, Pacilè S, Tromba G, Mayr S, Trifilò P, Lo Gullo MA, Salleo S. **2017**. X-ray microtomography observations of xylem embolism in stems of Laurus nobilis are consistent with hydraulic measurements of percentage loss of conductance. *The New Phytologist* **213**: 1068–1075.

Parker J. **1963**. Cold resistance in woody plants. *The Botanical Review* **29**: 123–201.

Pratt C. **1971**. Reproductive anatomy in cultivated grapes - a review. *American Journal of Enology and Viticulture* **22**: 92–109.

Quamme HA. **1986**. Use of thermal analysis to measure freezing resistance of grape buds. *Canadian journal of plant science. Revue Canadienne de Phytotechnie* **66**: 947–952.

Quamme HA. **1995**. Deep supercooling in buds of woody plants. In: Biological ice nucleation and its applications. 183–199.

Quamme HA, Su WA, Veto LJ. **1995**. Anatomical features facilitating supercooling of the flower within the dormant peach flower bud. *Journal of the American Society for Horticultural Science* **120**: 814–822.

Richards JH, Bliss LC. **1986**. Winter water relations of a deciduous timberline conifer, *Larix lyalii* Parl. *Oecologia* **69**: 16–24.

Rousseau D, Widiez T, Di Tommaso S, Rositi H, Adrien J, Maire E, Langer M, Olivier C, Peyrin F, Rogowsky P. **2015**. Fast virtual histology using X-ray in-line phase tomography: application to the 3D anatomy of maize developing seeds. *Plant Methods* **11**: 55.

Scoffoni C, Albuquerque C, Brodersen CR, Townes SV, John GP, Cochard H, Buckley TN, McElrone AJ, Sack L. **2017**. Leaf vein xylem conduit diameter influences susceptibility to embolism and hydraulic decline. *The New Phytologist* **213**: 1076–1092.

Sedighi Gilani M, Boone MN, Mader K, Schwarze FWMR. **2014**. Synchrotron X-ray micro-tomography imaging and analysis of wood degraded by Physisporinus vitreus and Xylaria longipes. *Journal of Structural Biology* **187**: 149–157.

Sinclair BJ, Gibbs AG, Lee W-K, Rajamohan A, Roberts SP, Socha JJ. **2009**. Synchrotron x-ray visualisation of ice formation in insects during lethal and non-lethal freezing. *PLOS ONE* **4**: e8259.

Socha JJ, Westneat MW, Harrison JF, Waters JS, Lee W-K. **2007**. Real-time phase-contrast x-ray imaging: a new technique for the study of animal form and function. *BMC Biology* **5**: 6.

Staedler YM, Masson D, Schönenberger J. **2013**. Plant tissues in 3D via X-ray tomography: simple contrasting methods allow high resolution imaging. *PLOS ONE* **8**: e75295.

Stott SL, Karlsson JOM. **2009**. Visualization of intracellular ice formation using high-speed video cryomicroscopy. *Cryobiology* **58**: 84–95.

Torres-Ruiz JM, Jansen S, Choat B, McElrone AJ, Cochard H, Brodribb TJ, Badel E, Burlett R, Bouche PS, Brodersen CR, *et al.* 2015. Direct x-ray microtomography observation confirms the induction of embolism upon xylem cutting under tension. *Plant Physiology* **167**: 40–43.

Verboven P, Herremans E, Helfen L, Ho QT, Abera M, Baumbach T, Wevers M, Nicolaï BM. **2015**. Synchrotron X-ray computed laminography of the three-dimensional anatomy of tomato leaves. *The Plant Journal* **81**: 169–182.

Workmaster BAA, Palta JP. **1999**. Ice nucleation and propagation in cranberry uprights and fruit using infrared video thermography. *Journal of the American Society for Horticultural Science* **124**: 619–625.

Xie Z, Forney CF, Bondada B. **2018**. Renewal of vascular connections between grapevine buds and canes during bud break. *Scientia Horticulturae* **233**: 331–338.

CHAPTER 5
CONCLUSION

Dormancy is a complex trait that is not well characterized in perennial plants. While our lack of understanding currently leads to problems in agricultural settings, future changes in climate will affect perennial vegetation in ways that are not yet known. Forecasts predict a decrease of chill accumulation in lower latitudes and an increase in chill accumulation in higher latitudes. Insufficient chilling accumulation results in erratic budbreak and growth, and excessive chill accumulation may result in plants that are more prone to mid-winter damage due to unseasonal warm spells. The transition from endodormancy to ecodormancy is understood as the switch between growth-recalcitrant to growth-responsive under conducive conditions. However, a huge knowledge gap still exists in why low temperatures promote chilling, how chilling accumulation is "counted" by plants, and how chilling promotes uniform budbreak. To study some of these aspects, we used grapevines, which have great phenotypic variation between species and cultivars, and are widely cultivated in contrasting environments around the globe. This makes grapevine a good model system for evaluating effects of global climate changes on dormancy aspects – although proper phenotyping for this trait was still lacking. The objectives of this study were to: describe how buds lose cold hardiness and break bud depending on their chill accumulation; characterize the transcriptional landscape of buds during loss of hardiness and budbreak; and identify where ice forms and how it propagates in buds during acute cold events.

Spring phenology is crucial for the growth and flowering of perennial plant species. Through our study, we demonstrated that deacclimation rate is a phenotype that varies quantitatively in response to chill accumulation, and that budbreak phenotype is confounded by dynamics of the cold hardiness loss. We have thus provided a new phenotype that may be used in other perennial species that utilize supercooling for cold hardiness to determine their chilling

requirement. Proper phenotyping may open the way for advanced studies on regulation of dormancy, that have until now relied on budbreak assays. Additionally, we have shown that species, and genotypes within species, have different thermal efficiencies. These appear to be linked to the environment these have originated: genotypes from colder environment have a greater cold hardiness, but also deacclimate faster upon experiencing warm temperatures – likely making use of short growing seasons. Our imaging of developing buds showed that wild species from colder climates also seem to prioritize the development of inflorescences during deacclimation and budbreak, further indicating that early flowering is necessary to complete the cycle in these environments. The use of these species as a source of cold hardiness in breeding programs may result in earlier budbreak that is prone to freeze damage. Most importantly, while plants can recover from damage in leaves during early budbreak, if inflorescences emerge prior to leaves such as in the wild material, spring freeze damage will more easily result in crop losses.

Knowledge of genetic regulation of cold hardiness and budbreak can promote fast advances for agricultural crops facing challenges due to climate change. Our study used genotypes with contrasting phenotypes to uncover gene regulation during deacclimation and early budbreak. Our results demonstrate that loss of cold hardiness is not just the opposite of gain of hardiness, such that molecular processes are not only occurring in the opposite direction and known transcription factors that elicit responses to cold (CBFs) are not differentially expressed. ABA is known to have a pivotal role in preventing growth, but here we demonstrated it also prevents the loss of cold hardiness. Down-regulation of ABA and ethylene allows up-regulation of growth-related hormone pathways (e.g., GA and Auxin). Considering that cold hardiness is related to water volume, the down-regulation of ABA-regulated aquaporins during deacclimation may be a key aspect of the progression to budbreak.

The work presented here also contains information on statistical analysis and imaging methods that are useful for future research. We described a new way to handle time-series RNA-Seq data, with special consideration given to studies that use uneven intervals in sample collection. For imaging, X-ray phase contrast showed great potential as a technology to study ice propagation in plant samples through time-resolved imaging. Microtomography imaging is also possible, and provides an easier and more precise way to both quantitatively and qualitatively assess growth in opaque plant structures such as buds.

The studies presented here have demonstrated that the historical methods of determining chilling requirement and the budbreak phenotype may have delayed our understanding of dormancy. The development of quantitative phenotypes for both the transition out of dormancy and the rate of cold hardiness loss will help enable studies which aim to genetically map the genes and loci that contribute to differences in cold adaptation in grapevine. We provided here groundwork onto which future studies regarding early phenology in plants can build upon from different angles (e.g., modeling responses to current and future climate, genetic regulation of dormancy, etc.), as well as new tools that can be used in the research.

APPENDIX A
SUPPLEMENTAL MATERIAL – CHAPTER 2

Table A-1. Information associated with each deacclimation experiment for each genotype used. Linear models were fit per genotype using chill accumulation and temperature as factors.

Genotype	Chill[1]	T[2]	Length[3]	Interv.[4]	Use[5]			Intercept[6]		Slope	
Vitis vinifera 'Cabernet Franc' (R^2 = 0.921, P<0.001)	360	2	94	8.5				-11.7 ±0.5	***[7]	-0.009 ±0.006	NS
	360	4	94	8.5	a			-11.8 ±0.5	***	-0.038 ±0.006	***
	360	7	94	8.5	a			-12.0 ±0.5	***	-0.009 ±0.006	.
	360	11	94	8.5	a			-11.0 ±0.5	***	-0.023 ±0.007	***
	360	22	55	6.9	a			-12.2 ±0.5	***	0.009 ±0.012	NS
	710	22	7	1.0	a			-19.5 ±0.5	***	0.225 ±0.078	**
	860	4	84	7.0	a	b		-21.1 ±0.5	***	0.032 ±0.006	***
	860	10	29	5.8	a	b	c	-22.3 ±0.6	***	0.469 ±0.028	***
	860	22	15	5.0	a		c	-22.0 ±0.7	***	0.779 ±0.059	***
	860	30	15	5.0			c	-21.4 ±0.6	***	0.645 ±0.095	***
	1020	22	10	1.1	a			-24.8 ±0.4	***	1.591 ±0.064	***
	1440	2	57	14.3		b		-21.7 ±0.6	***	0.172 ±0.013	***
	1440	4	65	7.1	a	b		-21.0 ±0.5	***	0.235 ±0.009	***
	1440	7	35	3.5	a	b		-20.5 ±0.5	***	0.447 ±0.017	***
	1440	11	18	2.0	a	b	c	-22.3 ±0.5	***	0.918 ±0.032	***
	1440	22	8	2.0	a		c	-22.5 ±0.6	***	2.199 ±0.096	***
	1580	2	162	10.8		b		-18.9 ±0.5	***	0.078 ±0.003	***
	1580	4	61	5.1	a	b		-19.4 ±0.5	***	0.206 ±0.010	***
	1580	8	35	2.9		b		-19.8 ±0.5	***	0.441 ±0.019	***
	1580	10	20	2.0	a	b	c	-19.9 ±0.5	***	0.623 ±0.028	***
	1580	22	8	1.1	a		c	-20.9 ±0.6	***	2.163 ±0.103	***
V. vinifera 'Cabernet Sauvignon' (R^2 = 0.879, P<0.001)	360	2	94	8.5				-9.2 ±0.7	***	-0.022 ±0.008	**
	360	4	94	8.5	a			-9.4 ±0.7	***	-0.062 ±0.008	***
	360	7	94	8.5	a			-10.3 ±0.7	***	-0.019 ±0.008	*
	360	11	85	8.5	a			-9.7 ±0.7	***	-0.005 ±0.010	NS
	360	22	55	6.9	a			-11.4 ±0.7	***	0.021 ±0.016	NS
	710	22	7	1.0	a			-19.2 ±0.7	***	0.192 ±0.099	.
	860	4	70	7.0	a	b		-20.9 ±0.7	***	0.039 ±0.013	**
	860	10	63	6.3	a	b	c	-20.9 ±0.8	***	0.233 ±0.017	***
	860	22	15	5.0	a		c	-21.9 ±0.9	***	0.810 ±0.096	***
	860	30	15	5.0			c	-21.6 ±0.9	***	0.997 ±0.096	***
	990	4	28	5.6	a	b		-21.5 ±0.7	***	-0.003 ±0.029	NS
	990	22	28	5.6	a			-20.5 ±0.7	***	0.116 ±0.031	***
	1020	22	12	1.1	a			-24.5 ±0.6	***	1.561 ±0.074	***
	1030	4	29	1.2	a	b		-22.5 ±0.6	***	0.219 ±0.022	***
	1030	13	19	1.0				-22.2 ±0.7	***	0.895 ±0.037	***

V. vinifera 'Cabernet Sauvignon' (*cont.*)	1030	22	9	1.0	a		c	-22.9 ± 0.7	***	1.440 ± 0.091	***
	1440	2	100	14.3		b		-21.4 ± 0.8	***	0.099 ± 0.010	***
	1440	4	92	7.1	a	b		-21.5 ± 0.7	***	0.168 ± 0.008	***
	1440	7	49	3.5	a	b		-21.0 ± 0.7	***	0.301 ± 0.016	***
	1440	11	27	2.1	a	b	c	-22.5 ± 0.7	***	0.592 ± 0.029	***
	1440	22	10	2.0	a		c	-23.1 ± 0.9	***	1.406 ± 0.108	***
	1580	2	162	11.6		b		-18.6 ± 0.8	***	0.072 ± 0.005	***
	1580	4	79	4.9	a	b		-20.0 ± 0.7	***	0.156 ± 0.010	***
	1580	8	40	2.7		b		-20.9 ± 0.8	***	0.399 ± 0.022	***
	1580	10	20	2.0	a	b	c	-20.4 ± 0.8	***	0.539 ± 0.048	***
	1580	22	8	1.1	a		c	-20.6 ± 1.1	***	1.401 ± 0.234	***
V. vinifera 'Riesling' (R^2 = 0.921, P<0.001)	360	2	94	8.5				-12.9 ± 0.7	***	0.043 ± 0.007	***
	360	4	94	8.5	a			-12.2 ± 0.7	***	0.015 ± 0.007	*
	360	7	94	8.5	a			-12.2 ± 0.7	***	0.027 ± 0.007	***
	360	11	94	10.4	a			-12.7 ± 0.8	***	0.035 ± 0.010	***
	360	22	41	6.8	a			-13.4 ± 0.8	***	0.067 ± 0.023	**
	710	22	7	1.0	a			-21.3 ± 0.7	***	0.292 ± 0.092	**
	860	4	85	6.5	a	b		-22.1 ± 0.7	***	0.030 ± 0.008	***
	860	10	42	6.0	a	b	c	-23.6 ± 0.8	***	0.320 ± 0.021	***
	860	22	29	6.5	a		c	-21.9 ± 0.8	***	0.533 ± 0.038	***
	860	30	15	5.0			c	-21.5 ± 0.9	***	0.890 ± 0.080	***
	990	4	28	5.6	a	b		-23.4 ± 0.7	***	0.072 ± 0.025	**
	990	22	28	5.6	a			-23.3 ± 0.7	***	0.416 ± 0.026	***
	1020	22	10	1.0	a			-27.1 ± 0.6	***	1.844 ± 0.097	***
	1030	4	100	3.2	a	b		-24.0 ± 0.7	***	0.135 ± 0.005	***
	1030	13	19	1.0				-24.8 ± 0.7	***	1.089 ± 0.032	***
	1030	22	14	1.0	a		c	-22.8 ± 0.7	***	1.228 ± 0.048	***
	1440	2	100	14.3		b		-20.3 ± 0.8	***	0.102 ± 0.008	***
	1440	4	92	7.1	a	b		-20.3 ± 0.7	***	0.174 ± 0.007	***
	1440	7	49	3.5	a	b		-20.4 ± 0.7	***	0.359 ± 0.013	***
	1440	11	18	2.0	a	b	c	-22.2 ± 0.8	***	0.809 ± 0.041	***
	1440	22	10	2.5	a		c	-21.8 ± 0.8	***	1.677 ± 0.088	***
	1580	2	162	10.8		b		-20.7 ± 0.7	***	0.086 ± 0.004	***
	1580	4	79	4.9	a	b		-21.8 ± 0.7	***	0.179 ± 0.008	***
	1580	8	40	2.7		b		-21.6 ± 0.8	***	0.370 ± 0.017	***
	1580	10	20	2.0	a	b	c	-22.2 ± 0.8	***	0.618 ± 0.037	***
	1580	22	8	1.1	a		c	-22.7 ± 0.8	***	2.159 ± 0.113	***
V. vinifera 'Sauvignon blanc' (R^2 = 0.826, P<0.001)	360	2	94	8.5	a			-11.1 ± 0.5	***	-0.012 ± 0.006	.
	360	4	94	8.5	a			-11.6 ± 0.5	***	-0.026 ± 0.006	***
	360	7	94	8.5	a			-11.6 ± 0.5	***	-0.010 ± 0.006	NS
	360	11	69	7.7	a			-11.5 ± 0.5	***	0.005 ± 0.010	NS
	360	22	41	5.9	a			-11.8 ± 0.6	***	0.004 ± 0.018	NS

V. vinifera 'Sauvignon blanc' (*cont.*)	860	4	84	6.5	a	b		-19.8 ± 0.5	***	0.027 ± 0.007	***
	860	10	42	6.0	a	b	c	-20.7 ± 0.5	***	0.273 ± 0.016	***
	860	22	15	5.0	a		c	-21.4 ± 0.7	***	0.740 ± 0.092	***
	860	30	15	5.0			c	-21.5 ± 0.7	***	0.847 ± 0.092	***
	1440	2	100	14.3	a	b		-19.3 ± 0.6	***	0.081 ± 0.007	***
	1440	4	85	7.1	a	b		-20.2 ± 0.5	***	0.170 ± 0.007	***
	1440	7	35	3.5	a	b		-20.4 ± 0.5	***	0.324 ± 0.019	***
	1440	11	22	2.0	a	b	c	-20.1 ± 0.4	***	0.577 ± 0.035	***
	1440	22	10	2.0	a		c	-21.0 ± 0.7	***	1.334 ± 0.106	***
	1580	2	128	10.7	a	b		-18.9 ± 0.6	***	0.075 ± 0.006	***
	1580	4	79	5.3	a	b		-18.3 ± 0.5	***	0.122 ± 0.008	***
	1580	8	30	2.7		b		-18.8 ± 0.6	***	0.306 ± 0.026	***
	1580	10	16	2.0	a	b	c	-20.5 ± 0.6	***	0.718 ± 0.052	***
	1580	22	9	1.3	a		c	-19.2 ± 0.6	***	1.586 ± 0.111	***
V. aestivalis (R^2 = 0.844, P<0.001)	360	2	94	8.5				-13.9 ± 0.7	***	-0.007 ± 0.009	NS
	360	4	94	8.5	a			-13.8 ± 0.7	***	-0.042 ± 0.008	***
	360	7	94	8.5	a			-14.0 ± 0.7	***	-0.041 ± 0.009	***
	360	11	94	8.5				-14.9 ± 0.7	***	-0.028 ± 0.009	**
	360	22	41	6.8	a			-15.1 ± 1.0	***	-0.055 ± 0.033	.
	860	4	84	6.5	a	b		-22.7 ± 0.8	***	0.002 ± 0.009	NS
	860	10	84	6.5	a	b	c	-23.0 ± 0.8	***	0.027 ± 0.011	*
	860	22	23	5.8	a		c	-24.3 ± 0.9	***	0.525 ± 0.049	***
	860	30	23	5.8			c	-24.1 ± 0.9	***	0.676 ± 0.058	***
	1020	22	11	1.2	a		c	-28.9 ± 0.6	***	1.728 ± 0.090	***
	1440	2	100	12.7		b		-18.0 ± 1.0	***	0.068 ± 0.012	***
	1440	7	31	3.4	a	b		-22.6 ± 0.8	***	0.482 ± 0.029	***
	1580	2	89	12.7		b		-23.9 ± 0.9	***	0.154 ± 0.011	***
	1580	4	67	6.7	a	b		-24.5 ± 0.8	***	0.277 ± 0.014	***
	1580	8	37	2.8		b		-22.4 ± 0.8	***	0.338 ± 0.026	***
	1580	10	22	2.2	a	b	c	-24.8 ± 0.8	***	0.656 ± 0.039	***
	1580	22	9	1.0	a		c	-27.1 ± 0.9	***	2.116 ± 0.114	***
V. amurensis (R^2 = 0.837, P<0.001)	360	4	20	20.0	a			-8.8 ± 1.6	***	-0.150 ± 0.086	.
	710	22	7	1.0	a			-22.3 ± 1.1	***	0.377 ± 0.151	*
	860	4	84	6.5	a	b		-24.9 ± 1.0	***	0.185 ± 0.009	***
	860	10	29	5.8	a	b	c	-24.6 ± 1.1	***	0.491 ± 0.037	***
	860	22	35	7.0	a		c	-22.8 ± 1.1	***	0.601 ± 0.062	***
	860	30	15	5.0			c	-23.2 ± 1.1	***	0.715 ± 0.075	***
	990	4	28	5.6	a	b		-26.3 ± 1.1	***	0.248 ± 0.039	***
	990	22	14	4.7	a			-27.3 ± 1.1	***	1.101 ± 0.100	***
	1020	22	9	1.1	a			-26.1 ± 0.9	***	2.090 ± 0.154	***
	1030	4	20	1.0	a	b		-26.2 ± 1.0	***	0.770 ± 0.041	***
	1030	13	17	1.0				-21.0 ± 1.0	***	0.834 ± 0.054	***
	1030	22	7	1.0	a		c	-24.6 ± 1.1	***	2.152 ± 0.169	***

V. amurensis (*cont.*)	1580	2	70	10.0		b		-17.8±1.2	***	0.176±0.018	***
	1580	4	20	5.0	a	b		-22.0±1.4	***	0.614±0.090	***
	1580	8	20	2.9		b		-19.2±1.3	***	0.668±0.074	***
	1580	10	10	2.0	a	b	c	-20.4±1.2	***	1.465±0.141	***
	1580	22	4	1.0	a		c	-18.3±1.4	***	2.787±0.429	***
V. riparia (R^2 = 0.834, P<0.001)	360	2	94	8.5				-14.4±0.8	***	0.041±0.009	***
	360	4	94	8.5	a			-13.9±0.8	***	0.012±0.008	NS
	360	7	85	8.5	a			-15.0±0.8	***	0.046±0.010	***
	360	11	85	8.5	a			-15.1±0.8	***	0.106±0.010	***
	360	22	34	5.7	a			-14.1±0.9	***	0.146±0.030	***
	710	22	7	1.0	a			-24.0±0.9	***	0.150±0.150	NS
	860	4	84	6.5	a	b		-27.5±0.8	***	0.101±0.009	***
	860	10	56	6.2	a	b	c	-28.0±0.9	***	0.378±0.016	***
	860	22	23	5.8	a		c	-28.8±1.0	***	0.889±0.058	***
	860	30	15	5.0			c	-29.5±1.0	***	0.952±0.087	***
	1020	22	11	1.1	a			-27.0±0.7	***	2.079±0.111	***
	1030	4	16	1.0		b		-26.4±0.9	***	0.657±0.062	***
	1030	13	14	1.0				-22.5±1.0	***	1.129±0.082	***
	1030	22	5	1.0	a		c	-23.4±1.1	***	2.521±0.279	***
	1440	2	100	14.3		b		-15.9±1.3	***	0.063±0.016	***
	1440	4	57	8.1	a	b		-20.8±1.0	***	0.270±0.021	***
	1440	7	24	3.4	a	b		-21.2±1.0	***	0.614±0.051	***
	1440	11	14	2.0	a	b	c	-21.4±1.0	***	1.151±0.091	***
	1440	22	6	2.0	a		c	-21.4±1.2	***	2.386±0.260	***
	1580	2	148	10.6		b		-20.9±0.9	***	0.105±0.006	***
	1580	4	50	5.6	a	b		-23.6±0.9	***	0.328±0.019	***
	1580	8	27	3.0		b		-24.2±0.9	***	0.573±0.036	***
	1580	10	16	2.0	a	b	c	-24.4±0.9	***	0.844±0.054	***
	1580	22	7	1.0	a		c	-25.5±1.0	***	2.960±0.162	***

[1]Chill accumulation calculated according to North Carolina model (Shaltout and Unrath, 1983)

[2]T = temperature (°C)

[3]Total length of the experiment (days)

[4]Average interval between collections for differential thermal analysis (days)

[5]Indicates use for a given estimation: a) used for estimation of deacclimation potential; b) used for low temperature effect estimation; c) used for high temperature effect estimation.

[6]Intercept (°C) and slope (°C day^{-1}), and associated standard errors from linear models of deacclimation for each temperature at any given chill accumulation.

[7] NS- Not significant; . – significant at α = 0.05; ** - significant at α = 0.01; *** - significant at α = 0.001.